Human-Machine Interaction Studies of Occupants in Level 3 Autonomous Vehicles Using Virtual and Dynamic Environments

Ali Olayan

ECOLE DOCTORALE SCIENCES ET METIERS DE L'INGENIEUR

Institut de Biomécanique Humaine Georges Charpak – Campus de Paris
Laboratoire d'Ingénierie des Systèmes Physiques et Numériques (LISPEN) - Institut Arts et Métiers de Chalon-sur-Saône
Campus de Cluny

THÈSE

présentée par : **Ali OLAYAN**

soutenue le : **06 Novembre 2024**

Pour obtenir le diplôme de **Doctorat**

délivré par **École Nationale Supérieure d'Arts et Métiers**

Spécialité : **Virtual and Augmented Reality**

Human-Machine Interaction Studies of Occupants in Level 3 Autonomous Vehicles Using Virtual and Dynamic Environments

Thèse co-dirigée par :
CHARDONNET Jean-Rémy
et SANDOZ Baptiste

		Jury:
Mme Laure LEROY	Maîtresse de Conférences - HDR, Université Paris 8 Vincennes-Saint-Denis	Rapportrice
M. Jean-Christophe POPIEUL	Professeur, Université Polytechnique Hauts de France	Rapporteur
M. Xuguang WANG	Directeur de Recherche, Université Gustave Eiffel, Bron, France	Président
M. Jean-Rémy CHARDONNET	Professeur, Arts et Métiers	Examinateur
M. Baptiste SANDOZ	Maître de conférences - HDR, Arts et Métiers	Examinateur

THÈSE

ABSTRACT

Occupant safety in autonomous vehicles (AVs) represents a critical concern as these vehicles progress toward SAE Level 3 autonomy, where non-driving activities become more prevalent. Despite advancements in this field, the impact of occupant activities and cognitive engagement on head-neck dynamics during emergency maneuvers remains insufficiently understood. This research hypothesizes that non-driving activities and sensory modalities significantly influence occupant physiological responses, especially in sudden braking events. To investigate this, we conducted experiments using two advanced driving simulation tools, including first a driving simulator and then a dynamic SLED system, to replicate emergency braking scenarios and evaluate occupant responses under varying cognitive and physical conditions.

The first experiment utilized the Institute of Chalon-sur-Saône SAAM simulator to investigate the influence of occupant activities and auditory alerts on head-neck kinematics and muscle activation during emergency braking events. Results indicated that auditory alerts played a pivotal role in preparing occupants for deceleration, facilitating anticipatory postural adjustments and reducing head acceleration. The second experiment, using the Institut de Biomécanique Humaine Georges Charpak SLED system synchronized with a 360° virtual AV environment, confirmed these findings, demonstrating that cognitive distractions from non-driving tasks increased head acceleration and delayed muscular responses, particularly in strong braking scenarios.

This study underscores the importance of integrating sensory alerts, such as auditory cues, to enhance occupant preparedness and safety in AVs. Moreover, the results highlight the necessity for adaptive AV systems that account for individual variability in occupant responses to ensure optimal protection. By employing immersive simulation technologies, this research provides valuable insights into the interaction between non-driving activities, cognitive engagement, and occupant safety, paving the way for more effective and personalized AV design strategies that can mitigate injury risk in future autonomous transportation.

Abstract

CONTENTS TABLE

Table of Contents

LIST OF FIGURES

List of Tables

LIST OF TABLES

GENERAL INTRODUCTION

Advanced driver assistance systems (ADAS) are gradually being integrated into modern vehicles. Some of the crucial applications of ADAS center on reducing/avoiding accidents. Examples of such systems include automatic emergency braking, which detects imminent collisions and applies the brakes to prevent or mitigate accidents, and lane departure warning systems that warn occupance when they accidentally wander out of their lanes. ADAS essentially use sets of sensors that communicate information to the vehicle to give information about its surrounding environment (other vehicles, infrastructure, pedestrians). With these features, the vehicle can detect potential collisions and intervene in such ways as to warn the driver, assist them in emergency maneuvers, or even act autonomously to avoid collisions. ADAS can potentially drastically lower the consequences and severity of automotive crashes. This anticipated shift to autonomous vehicles (AV) is entering the initial stages for the automotive market in developed countries (Litman, 2014). The need for efficient, affordable, and secure societal transportation is the main drive for this progress.

In a study done by The National Highway Traffic Safety Administration in 2016 showed that more than 90% of vehicle accidents in the US in 2016 were caused by driver error (NHTSA, 2016). Similarly, according to the French National Interministerial Observatory of Road Safety (ONISR), human error is also a leading cause of road accidents in France. ONISR reports from recent years indicate that factors such as speeding, alcohol consumption, and failure to comply with traffic regulations contribute to a significant percentage of road accidents in the country (ONISR, 2020). According to Holmes et al., 2018, future and existing AV technologies are predicted to significantly lower accidents and injury rates. Moreover, advances in sensor technologies will increase AV technology capabilities; hence, the adoption of AV technologies in the future of transport will greatly benefit passengers and pedestrian safety (Wood et al., 2019).

The only AV systems available in the present vehicles on the roads are driver assistance systems, which support the driver while allowing them to maintain control of the vehicle. Nevertheless, the industry is heading towards full AV, able to safely navigate the network of roads without the intervention of a human driver (Filatov et al., 2019). The Society of Automotive Engineers (SAE) describes different levels of vehicle automation, ranging from L0, which has no automation at all, to L5, which has full automation (SAE J3016). Figure 1 shows the different levels of SAE Levels. Presently, all vehicles on the roads operate between SAE levels 0 and 3, with the majority of them at L0 or L1.

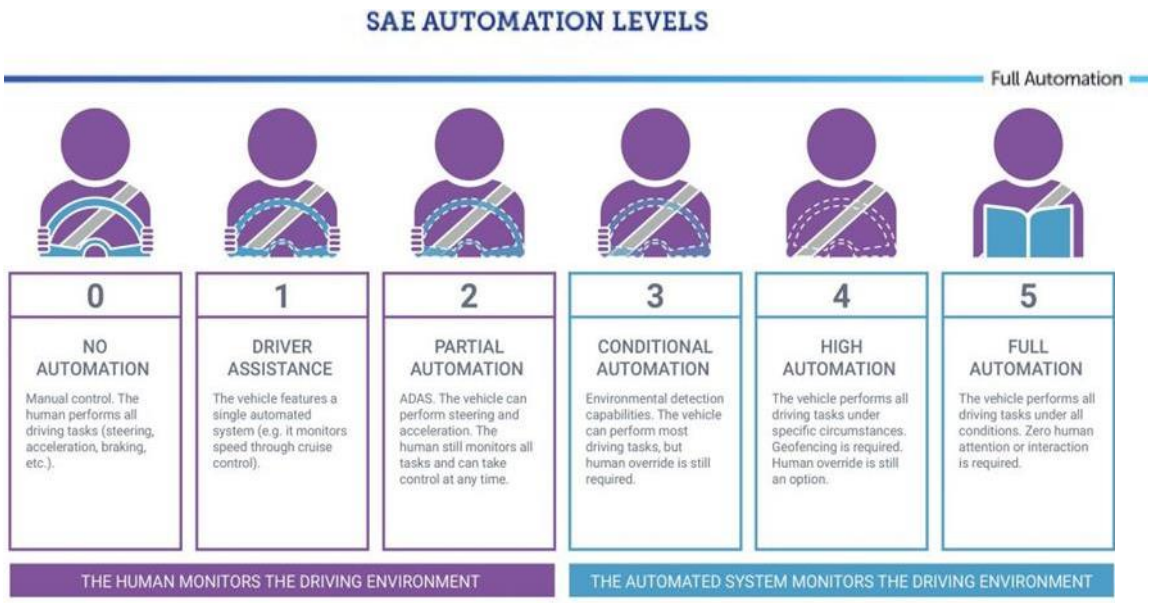

Figure 1: SAE Levels of Automation (SAE J3016)

While AVs will minimize and avert accidents, they will still happen occasionally; it is also projected that the interiors of vehicles will undergo major modification, which would make it difficult for designers and regulators to maintain occupant protection in case of collisions (Filatov et al., 2019). Given that AV occupants will not have the burden of driving, it will provide them with the time to do other activities (e.g. working, reading, using the phone) leading to Out Of Position (Östling et al., 2017). However, this still leaves the possibility of automated emergency maneuvers being initiated. The behavior of occupants and their interaction with the Human-Machine Interface (HMI) can vary in response to the type of sensory feedback received (visual, auditory, or tactile/haptic) during an emergency, subsequently affecting the outcomes of the hazardous situation (Zhang et al., 2019). In such scenarios, the security systems may be less effective in protecting the occupants. In addition, problems exist around alerting the occupants, particularly the driver, through the driving assistance systems, for example. Furthermore, there are issues with how to alert the occupants, especially the driver, using tools like driving assistance systems (Zhang et al., 2019).

This thesis is part of a major evolution linked to the increasing automation of vehicles, with crucial road safety issues with the associated risks, costs, and acceptance of autonomous technologies. Considering it from a scientific standpoint, it will be a question of understanding, through simulation and virtual reality, the cognitive mechanisms at play in response to interactions between a Level 3 AV and its driver/occupant, as well as determining their influence on the strategies adopted to stabilize the human body in potentially critical situations (such as an emergency brake). With this in mind, it is then a question of determining the most suitable human-machine interactions (HMI) that could adapt in real-time to the occupant, the environment, and the situation in order to provide optimum safety and prevent/minimize injuries. It will be essential to ensure that simulation studies are valid in comparison to reality since driving simulation and virtual reality might lead to perceptual biases.

This thesis falls under the framework of the evolution of road safety in Level 3 autonomous driving, especially the safety of occupants. Currently, security systems are mainly evaluated by impact dummies representing average human morphologies. These dummies have drastically improved vehicle safety systems, but they cannot represent the full diversity of the vehicle occupant population. Additionally, the standardized fixed seating position of these dummies renders them unsuitable for evaluating occupant safety in Level 3 and above autonomous vehicles. This limitation arises because they do not account for behavioral factors, out-of-position (OOP) postures, occupant movements, or muscle contractions, which are critical for accurately assessing the safety of human occupants in such scenarios (Grébonval et al., 2021a). Furthermore, the HMI between the occupant and the AV is still poorly understood; thus, in order to improve occupant safety, it is crucial to study their behaviour and cognition.

For that reason, the main objective is to better understand HMI, behaviour, and the position of the occupants during an emergency scenario, pre-accident, avoidance or automatic braking to improve their safety from potential injuries. It involves the personalized cognitive exploration of occupants in a Level 3 AV by trying to understand the behaviour, the different interaction strategies, and cognition of the human body in a real dynamic environment coupled with a controlled virtual environment. The virtual environment allows great flexibility in configurations and multiple scenarios (emergency braking, the addition of multimodal alerts, etc.). To achieve the objectives of this thesis in an innovative manner, this study proposes a novel approach that combines virtual reality techniques, such as driving simulators, with biomechanical analysis. This integrated approach will enable identify key HMI features, such as warning and entertainment, that influence behaviour (e.g. Decision-making) and cognition (e.g. Reaction times), while at the same time measure changes in head acceleration, muscle activity, respiration, and heart rate during emergencies within the context of a Level 3 AV.

This research was conducted through a collaboration between two laboratories of Arts et Métiers: the Georges Charpak Institute of Human Biomechanics (IBHGC) and the Laboratory of Physical and Digital Systems Engineering (LISPEN) at the Arts et Métiers Institute of Chalon-sur-Saône (previously known as Institute Image). This partnership enabled a comprehensive approach by combining expertise in human biomechanics and advanced virtual simulation technologies.

LISPEN at the Arts et Métiers Institute of Chalon-sur-Saône is one of the three entities comprising the LISPEN laboratory. Located in Chalon-sur-Saône and affiliated with the Arts et Métiers campus of Cluny, its primary objective is the development of techniques and applications for virtual immersion in engineering contexts. Over the past several years, one of LISPEN's key research areas has been driving simulation. The institute hosts several driving simulators on-site and has established a joint laboratory with Renault—the Virtual Immersion Laboratory (LiV)—to advance research in this domain.

The Georges Charpak Institute of Human Biomechanics (IBHGC) is situated on the Paris campus of Arts et Métiers and is co-accredited with Sorbonne Paris Nord University. Dedicated to human biomechanics, the IBHGC engages in a wide range of activities, including sports performance analysis, geometric modeling, quasi-static and dynamic mechanical analysis, movement analysis, and disability

studies. One of the laboratory's research focuses is on trauma and injury biomechanics, particularly the study of head-neck responses in dynamic environments. This research theme was introduced through a broader project aimed at better understanding the injury mechanisms associated with whiplash, which led to the design of a SLED-type system for studying subject dynamics (Sandoz et al., 2014).

The collaboration between LISPEN and IBHGC leverages the strengths of both laboratories to advance research in occupant behaviour and safety in dynamic environments, such as those experienced in autonomous vehicles. By integrating LISPEN's expertise in virtual immersion and driving simulation with IBHGC's specialization in human biomechanics and injury mechanisms, the research aims to develop more effective strategies for analyzing and improving occupant responses to dynamic forces. This interdisciplinary approach not only enhances the scientific rigor of the study but also contributes to the development of innovative solutions in automotive safety and human-machine interaction.

This thesis project integrates biomechanical research themes that are well-established and understood by the Georges Charpak Institute of Human Biomechanics (IBHGC)—particularly those focusing on head-neck response and, more broadly, the study of head kinematics in dynamic environments—with research issues specific to LISPEN related to the use of immersive technologies. In light of the previously stated scientific context, this project aims to explore the influence of behavioural, cognitive, safety, and human-machine interface (HMI) parameters on occupants in Level 3 autonomous vehicles (AVs) by incorporating virtual reality methods into the study. To achieve these objectives, this manuscript is organized as detailed in Figure 2.

Chapter 1 of this manuscript consists of a literature review providing a state-of-the-art overview of knowledge surrounding the head-neck biomechanics and associated experimental studies, relevant cognitive parameters in these studies, as well as research questions associated with the use of immersive simulation technologies and the different systems used.

Chapter 2 is structured around the summary of the knowledge presented by the literature review and the different obstacles. This chapter defines the objectives and formulates the research questions associated with this project. Specifically, we aim to answer the following research questions:

- *How do the activities in which occupants are engaged prior to an emergency maneuver in an autonomous vehicle influence the body's physiological response under specific pre-maneuver conditions?*

- *How can driving simulators and dynamic virtual environments help improve HMI in autonomous vehicles, especially sensory modalities?*

Chapter 3 discusses an experiment conducted using a six-degree-of-freedom driving simulator as part of this project. The experiment integrates physiological data to understand the effects of behaviour, cognition, and human-machine interaction on the physiological responses of occupants in Level 3 autonomous vehicles (AVs) during a short trip scenario. To our knowledge, this is the first experiment

designed to examine biomechanical and physiological responses during a simulated drive where occupants were free to engage in non-driving activities of their choice throughout the entire experiment, while being subjected to multiple types of emergency maneuvers.

Chapter 4 investigates the contribution of virtual reality to the study of the effects of occupant activities on head-neck dynamics and physiological responses in a virtual environment using the SLED system. In this experiment, participants wore a head-mounted display that projected the virtual environment from the perspective of an occupant in an AV and were asked to perform specific non-driving activities under different conditions. This experiment also served to validate the findings from the driving simulator experiment while focusing exclusively on occupant activity during braking events.

Chapter 5 concludes the manuscript by presenting a comparison between the two experiments and discussing the general results of the thesis project in relation to the research questions. It also addresses the limitations of the work and outlines potential development perspectives that arise from the findings.

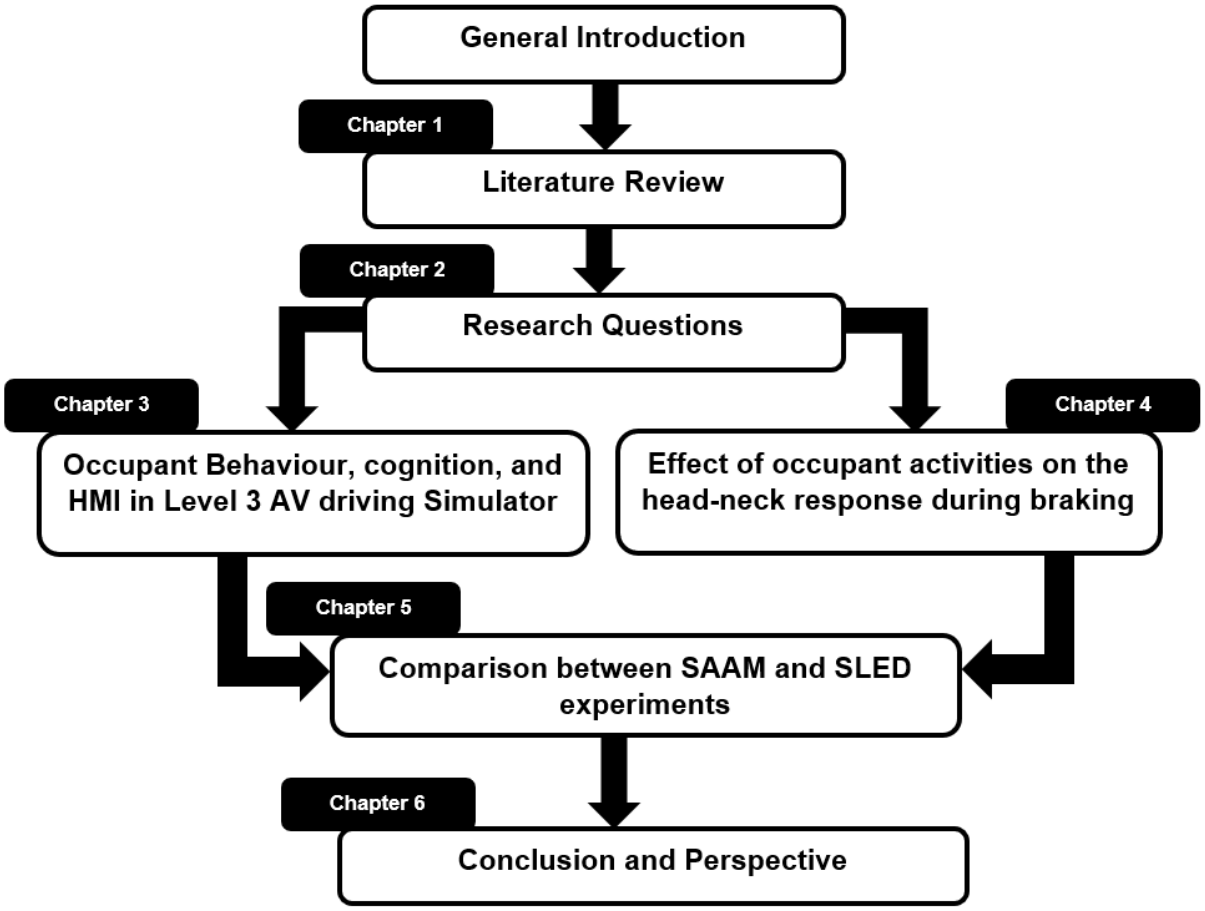

Figure 2: Organization of the manuscript

CHAPTER 1: LITERATURE REVIEW

1. Introduction

This chapter provides a comprehensive review of the current literature surrounding head-neck biomechanics, injury mechanisms, and human-machine interaction (HMI) in the context of both conventional and autonomous vehicles (AVs). As vehicle automation advances, particularly at SAE Level 3 and above, new challenges emerge in occupant safety and behaviour, necessitating a deeper understanding of the interactions between human physiology, safety systems, and the increasing complexity of vehicle dynamics.

The review commences with an analysis of the cervical spine's biomechanical characteristics, emphasizing the responses of the head and neck to various forces encountered during vehicle maneuvers such as braking, turning, and emergency actions. It highlights the current knowledge on injury mechanisms like whiplash and explores the limitations of traditional crash testing models in representing human kinematics and muscle responses. Furthermore, it investigates the efficacy of existing passive and active safety systems, such as seat belts and airbags, in mitigating injuries.

In addition to biomechanics, this chapter also addresses the critical role of HMI in AVs, particularly in managing transitions between autonomous and manual control. The literature reveals gaps in understanding the cognitive load, trust, and reaction times of occupants when faced with take-over requests in autonomous driving scenarios. Moreover, as AV designs shift towards accommodating non-driving tasks and relaxed seating postures, there is an urgent need to explore how these new seating configurations impact occupant safety.

The aim of this chapter is to identify and address these gaps in the literature, with the ultimate goal of contributing to the development of safer and more effective vehicle systems as the industry moves toward full automation. A comprehensive overview of key studies addressing autonomous vehicle technologies, head-neck biomechanics, and human-machine interaction (HMI) is provided in Table 1. This table summarizes the methodologies, key findings, and limitations of these studies, offering a consolidated understanding of the current research landscape in this field.

Table 1: Summary of Key Studies on Autonomous Vehicles, Head-Neck Biomechanics, and Human-Machine Interaction

Authors (Year)	Purpose/Objectives	Sample/Participants	Methodology	Key Findings	Limitations
Holmes et al. (2018)	Investigated the potential benefits of lane departure warning systems in reducing cross-centerline crashes.	Accident data from the US (National databases)	Simulation and statistical analysis of crash scenarios	Found significant potential to reduce crash severity and frequency with lane departure warning systems.	Limited to simulation data; real-world effectiveness requires further validation.
Mackenzie et al. (2022)	Analyzed human head and neck kinematics during autonomous and manual emergency braking scenarios.	10 participants	Experimental study using a real vehicle including automated braking preceded by an alarm warning or robot human braking.	Participants' initial positions significantly influence their head dynamics during emergency braking. Moreover, the auditory alarm emitted before braking may have helped mitigate mechanical stimuli and likely reduced the risk of injury.	The absence of physiological data, particularly electromyography (EMG), and the lack of conditions where subjects were completely unprepared for the braking event.
Zhang et al. (2019)	Conducted a meta-analysis to determine factors affecting driver take-over times in AVs.	Meta-analysis of 129 studies on automated driving	Statistical analysis of take-over times in various driving situations.	Engaging in non-driving tasks significantly increased take-over times, with handheld tasks having the most impact. Visual stimuli alone led to slower response times compared to auditory or haptic stimuli.	One of the limitation is that it only considered studies in simulated environments, not real-world AV take-over scenarios.
Grébonval et al. (2021)	Explored preferred seating positions and postures in reclined configurations for AV occupants.	18 participants in first test experiment 13 participants in second test experiment	Experimental study with the preferred seat pan angle and occupant posture in reclined configurations	The results showed that preferred seat pan angles increased with a reclining seatback, particularly for maximum angles. While both seat pan and seatback angles influenced the pelvic angle, changes in the pelvic angle were smaller than those in the seat pan and seatback angles.	The impact of soft cushioning remains to be studied, as rigid seating surfaces were used. Long-term sitting effects were also not evaluated, given the short-duration assessment.
Petermeijer et al. (2017)	Examined driver response times to different take-over request modalities (auditory, visual, tactile).	101 participants in a driving simulator study	Simulator-based experiment testing different TOR modalities.	Auditory and haptic alerts resulted in faster take-over times compared to visual-only alerts. Multimodal cues proved most effective.	Due to the technical limitations of the eye-tracking system, it was not possible to quantify the eyes-on-road reaction time for all participants.
Li et al. (2019)	Reviewed neck injuries and protective measures in vehicle accidents.	Analysis of existing crash data and safety system literature	Literature review and analysis of injury mechanisms in vehicular crashes.	Highlighted the importance of passive and active technologies development for neck injury prevention	Primarily based on conventional vehicles, with limited consideration of AV-specific injury mechanisms.
Morgan et al. (2019)	Investigated trust levels in autonomous vehicles using both driving simulators and real AVs.	46 participants, tested in both simulator and real AV scenarios	Comparative study measuring trust through subjective surveys and behavioural analysis.	Trust levels were generally high, with slightly higher trust in the simulator than in real AV scenarios. Context-specific factors (e.g., oncoming traffic) influenced trust perception.	The study's limitations included platform reliability, weather changes, simulator "jerkiness," participant nausea, potential bias due to self-selection, and a focus on T-junctions, excluding other maneuvers like parked vehicles, pedestrians, and cyclists.

2. Head-Neck Biomechanics

2.1. Biomechanical Properties of the Head/Neck Complex

2.1.1. The anatomy and biomechanics of the head/neck complex, including the cervical spine, musculature, and ligaments:

The focus here will be on essential aspects of the neck to clarify the head/neck connection system. The spine is composed of seven cervical vertebrae, twelve thoracic vertebrae, five lumbar vertebrae, the sacrum, and the coccyx. Specifically, the cervical spine, comprising the seven cervical vertebrae, provides both mobility and stability for the head in relation to the trunk. It is a crucial junction between the head, containing most sensory and cognitive functions, and the body. As seen in Figure 3, the cervical vertebrae are numbered C1 to C7, with C1 (atlas) and C2 (axis) forming the upper cervical spine, and C3 to C7 forming the lower part. The cervical spine's curvature, called lordosis, is significant for its function.

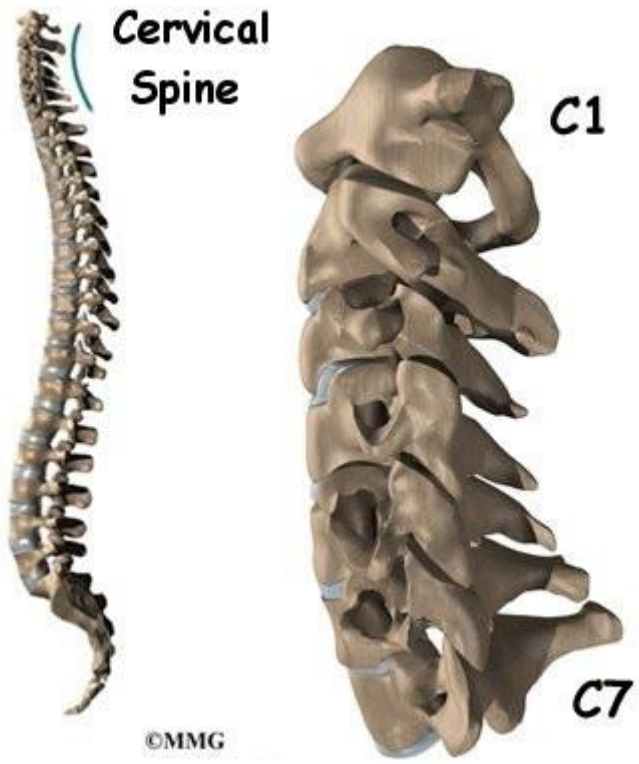

Figure 3: Schematic of the cervical spine in the cervical spine in sagittal view (images adapted from ©MMG 2000)

Numerous muscles ensure cervical spine mobility, specifically for head flexion and extension. Flexor muscles in the anterior plane, like the sternocleidomastoid (SCM), facilitate head flexion by bringing the chin to the chest. The SCM requires deep vertebral muscle activation to avoid increasing cervical lordosis. Extensor muscles in the posterior plane, including the trapezius, splenius, and SCM, enable head extension by moving the chin away from the chest.

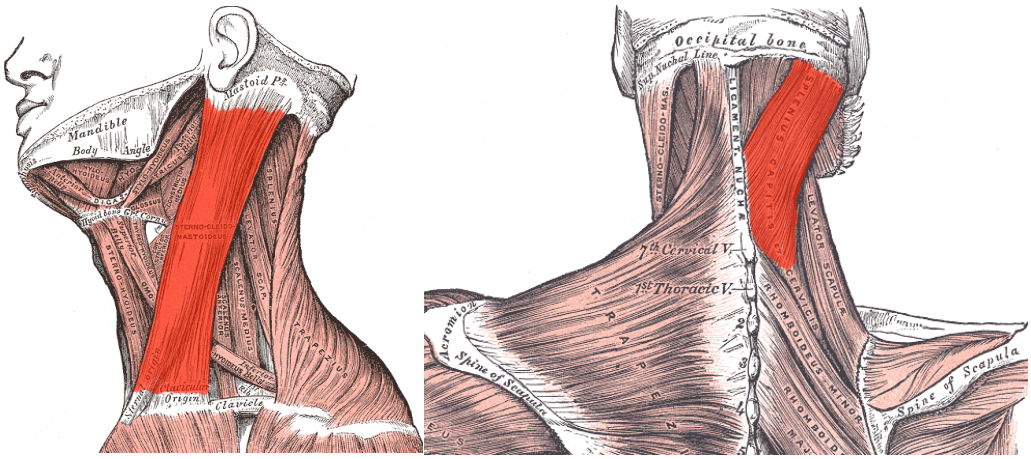

Figure 4: Right : The sternocleidomastoid (SCM) muscle; Left: The splenius capitis (SC) muscle (Standring et al., 2021)

2.1.2. Studies that have measured the range of motion

Neck movements regulated by the vestibular apparatus stabilize the head in a fixed spatial position during body movements. The neck exhibits remarkable biomechanical linkage and an extensive range of motion, attributed to the cervical spine's mobility (Dutia, 1991). Active neck movements encompass approximately up to 150° in rotation (yaw), 125° in extension/flexion (pitch), and 90° in lateral bending (roll) (Feipel et al., 1999) with translational movements spanning several centimeters along the three axes.

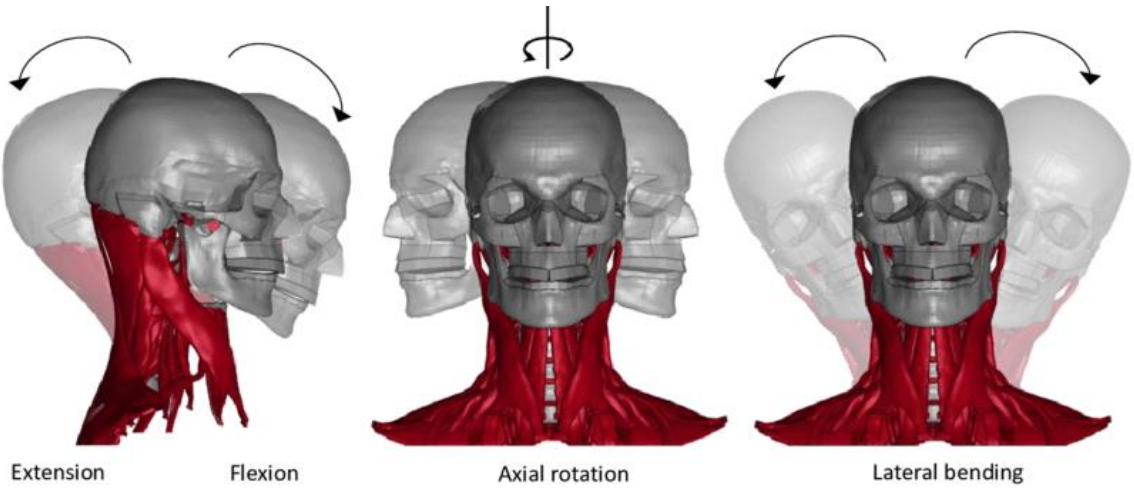

Figure 5: Head-neck range of motion (Corrales, 2021)

2.2. Impact of Braking on Head/Neck Dynamics

Non-collision incidents, such as hard braking during emergency situations, can lead to neck injuries, which are a significant health concern (Fuentes Del Toro et al., 2020). The occurrence of these injuries is expected to rise with the increased use of automatic braking systems and AV. The cervical spine is highly sensitive to sudden velocity changes. During emergency braking, forward displacement occurs, resulting in the head and torso moving with a time lag due to their differing inertial properties. This disparity in movement can potentially lead to the manifestation of a whiplash effect. This results in simultaneous vertebral flexion and hyperextension, a primary mechanism of cervical injury. Additionally, muscle response plays a crucial role in cervical injuries, especially at low speeds (Fuentes Del Toro et al., 2020).

Neck injuries encompass a diverse range of severities and classifications, varying from minor strains to severe, life-threatening, or fatal outcomes, particularly as the impact force or neck inertia increases during vehicular accidents. Whiplash injuries can result in multiple clinical diagnoses, including ligament sprains, intervertebral disc herniations, and muscle strains. In rare instances, these conditions can also affect the spinal cord itself, leading to more severe neurological symptoms (Li et al., 2019).

2.3. Head Dynamics During Turning Maneuvers

Emergency maneuvers like abrupt lane changes cause complex kinematic and kinetic responses in the head and neck. Kinematically, a significant lateral flexion and rotation of the cervical spine, could lead to high angular velocities and accelerations that strain cervical structures (Morris and Cross, 2005; Reed et al., 2018). The head may laterally displace relative to the torso depending on the maneuver's speed and severity (Kirschbichler et al., 2014; Larsson, 2023). Kinetically, these movements, if strong enough, could generate substantial shear forces and asymmetric tensile and compressive stresses within the cervical spine, affecting intervertebral discs, ligaments, and muscles (Ewing et al., 1977). Increased activation of the sternocleidomastoid and splenius capitis muscles helps stabilize the head (Di Loreto, 2019).

Research using cadaveric models has provided insights into the structural limits of the cervical spine under lateral loading. These studies help in understanding the failure thresholds of various cervical components under extreme conditions (Yoganandan et al., 1989). In vivo experiments using instrumented crash dummies and human volunteers have provided valuable data on the kinematic and kinetic responses during lateral impacts. A study on upper body behaviour of seated humans under controlled lateral accelerations found significant differences in maximum lateral head bending among various acceleration pulses (sine and plateau). Significant reductions in lateral bending were observed when muscles were braced compared to when they remained in a relaxed state (Sandoz et al., 2023).

2.4. Human Subject and Dummy Testing

Accident scenarios often involve pre-crash phases characterized by expected muscle responses. Human body kinematics are markedly influenced by both voluntary and reflexive muscle responses during perturbations. This significant effect has been extensively documented in numerous biomechanical studies, encompassing perturbations that are sudden, anticipated, or unforeseen. Research in the field of whiplash, including studies by Magnusson et al. (1999) and Siegmund (2003), has shown how muscle tone influences injury mechanisms through volunteer sled tests (Magnusson et al., 1999; Siegmund et al., 2003). Accurate injury risk assessments necessitate representing the human body such that dummies (e.g., Hybrid III, THOR) or their numerical counterparts exhibit realistic, human-like kinematics. However, a study by Muggenthaler et al. (2005) demonstrated that dummies cannot accurately predict human occupant responses all through pre-crash stages. By analyzing electromyography (EMG) data from human subjects, the researchers discovered distinct muscle activation patterns linked to vehicle acceleration, which the dummies failed to reproduce accurately (Muggenthaler et al., 2005).

Figure 6: Hybrid III crash test dummy (left); THOR crash test dummy (right) (Humanetics 2024)

2.5. Injury Mechanisms and Prevention Strategies

In passive safety, the core principle of neck protection devices is to counteract the inertia resulting from the head's movement relative to the body. Based on this principle, various protective measures have been developed, including cushioned seat backs, active and smart head restraints, energy-absorbing seat bases, seat belts, and airbags. With advancements in simulation and experimental methodologies, along with a more comprehensive understanding of neck injuries in vehicle collisions, the design of neck protection devices has evolved to become more scientifically grounded, integrated, and refined (Li et al., 2019).

While passive safety systems have advanced significantly and reached a point of maturity, the automotive industry is now shifting its focus to active safety, an area ripe with potential. Active safety

encompasses systems designed to leverage the vehicle's state to prevent or mitigate crash impacts. Utilizing sensor inputs to aid the driver, advanced driver assistance systems (ADAS) integrate various technologies, including brake assist, traction control, and electronic stability control. Sensor-based technologies, like adaptive cruise control and collision-related systems for warning, avoidance, and mitigation, form the primary focus of ongoing research in active safety. (Li et al., 2019). Studies have shown that when individuals anticipate an upcoming braking event, head movement is reduced by about 30% compared to instances where braking occurs unexpectedly (Kumar et al., 2000). This finding underscores the importance of continued development and refinement of active safety systems, particularly in autonomous vehicles.

2.6. Combined Effects of Braking and Turning

Vehicle maneuvers, such as braking or steering, occur prior to around 40–50% of automobile accidents and are directly related to the emergency events that follow (Ejima et al., 2009). These maneuvers can cause occupants to shift from their initial positions, potentially adopting postures that reduce the effectiveness of occupant protection systems during a crash (Reed et al., 2018). During combined braking and turning maneuvers, the head and neck experience a complex interplay of inertial and centripetal forces. Braking generates a forward shear force at the neck, attempting to whip the head relative to the torso. Seatbelt tension and occupant friction influence this force distribution. Conversely, turning induces lateral forces on the body, including the head, which experiences a centripetal pull inward. The head's response is not simply forward or sideways, but a combination of both, leading to excessive stretching and straining of the neck musculature, ligaments, and discs (Reed et al., 2018). Pre-existing neck conditions or weak muscles further heighten this vulnerability. This combined loading generates compressive, tensile, and shear forces within the cervical spine. Compressive forces stem from head weight and deceleration, while shear forces arise from differential head-torso movement, amplified during turning. Neck muscles activate to stabilize the head and resist these forces, with activation intensity depending on maneuver severity and individual preparedness. The rapid forward and sideways movement can lead to whiplash injuries, characterized by hyperextension and hyperflexion of the neck. Moreover, the complex loading pattern can cause strains, sprains, or even herniated discs within the vulnerable intervertebral joints and ligaments of the cervical spine.

2.7. Consequences of non-standard position (or out-of-position)

With SAE L3 and above, the occupant is not engaged in the driving task when the autopilot system is enabled, which will offer the luxury of Non-Driving-Tasks such as sleeping, using a device, or working while the vehicle operates autonomously (Östling and Larsson, 2019; Pfleging et al., 2016). Hence, the interior design of the AV should include features capable of accommodating such activities, with the most attractive feature being reclined seats and a higher range of seat manipulation (Bohrmann and Bengler, 2020). Nevertheless, the majority of the research on seating position done in the past was mainly centred on driving position; thus, it is essential to understand the occupant’s preferred seating position and the injury risks that are derived from it (Grébonval et al., 2021a; Peng et al., 2022).

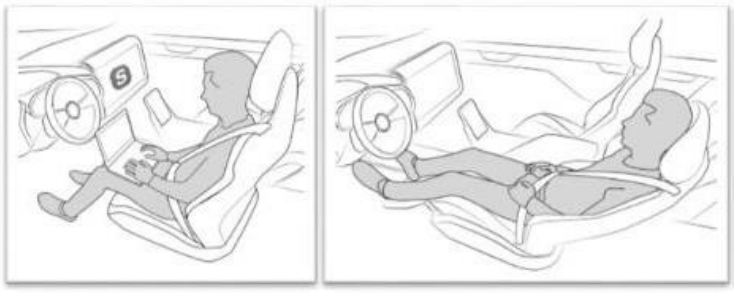

Figure 7: Working position (Left) and Relaxing position (Right). (Östling et al,. 2017)

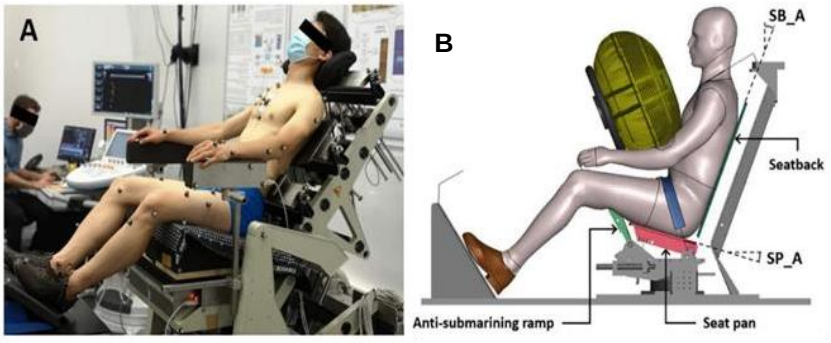

Figure 8: (A) participant sitting on the experimental seat. (B) Environment model used SB_A: Seatback angle; SP_A: Seat pan angle. (Grébonval et al., 2021)

3. Occupant Human-Machine Interaction, behaviour and cognition in SAE Level 3 AV and above

The automotive sector has seen a profound evolution in Human-Machine Interface (HMI) technology since the inception of the automobile. Early vehicles were equipped solely with interfaces featured only basic controls for steering and braking. It wasn't until the 1920s that instrument clusters were introduced, which was later followed by the integration of navigation systems in the 1980s; the the 1990s saw the integration of brought-in devices, particularly cell phones and later smartphones, which became significantly prevalent in vehicles (Akamatsu et al., 2013). When comparing HMI in vehicles from the 1950s to those from the late 2000s by the same manufacturer, the 2000s models featured 113 in-vehicle devices, nearly quadrupling the number found in the older models (Kern and Schmidt, 2009). In 2019 Wood et al., 2019, with 11 automotive and automated driving technology industry leaders, considered HMI a vital component for the safe operation of AV of Level 3 and higher in their book “Safety First for Automated Driving”. HMI offers an interface for human and machine to communicate information and actions and is developed so that occupants are able to operate the autonomous driving system in a well-defined and natural manner (Wood et al., 2019). In SAE L3 and above, HMI can use visual, haptic, and auditory cues and feedback to assist the occupant with appropriate information and data. In addition to

that, HMI can provide various forms of interfaces to gather input from the occupant. According to Wood et al., 2019, HMI has to be thoroughly developed in order to take into account various factors, such as behavioural and cognitive features, as well as the state of the occupant, to improve the occupant's interpretation of the task at hand and minimize the accidents and errors.

In 2017, the United States National Highway Transportation and safety administration (NHTSA) highlighted the minimum evaluation criteria of HMI with an AV that should be considered before achieving complete autonomy. AV must be designed in a matter that communicates their intents to the occupants efficiently and in the most comprehensive manner. Hence, a well-defined HMI design is especially of substantial significance. Therefore, the NHTSA drew attention to what have to be considered while developing HMI. They emphasized that the occupants must be aware of the existing limits of the AV (e.g. the enabled/disabled features), be notified if the AV wants them to make an action and how the AV is interacting with the surroundings, and most importantly apply universal standards method across all industries in communication of information and changing amongst the AV features. For that reason, most automotive companies follow minimalistic methods in designing HMI systems while keeping in mind the basic requirement for safe, relaxing, and efficient driving (Wood et al., 2019).

Figure 9: Mercedes S-Class SAE L3 interior (Szczesny, 2022)

4. Cognitive Load Impact on Reaction Times and Control Handover in AV

In SAE Level 3 autonomous vehicles, drivers must assume control with little notice (SAE International, 2020). These vehicles enable occupants to shift their attention to activities like working or watching movies, with the option to reassume driving responsibilities when needed. Schoettle and Sivak, 2014 reported that a significant portion of drivers— a third of drivers in the U.K. and almost half of drivers in the United States—are willing to perform cognitively demanding activities while using AVs. Similarly, Cunningham and Regan, 2018 highlighted that drivers commonly allocate their freed attention to non-driving tasks when not actively engaged in driving. However, the NHTSA warns that drivers may significantly delay or fail to re-engage in manual driving when deeply absorbed in secondary activities (Campbell et al., 2018).

The ability of drivers to take control and drive is influenced by their cognitive and emotional states, such as arousal and stress from different workloads. High-demand secondary tasks can cause distraction (Schaap et al., 2017), while low workload may lead to fatigue (Saxby et al., 2013). Fatigue reduces engagement, focus, and response times (Saxby et al., 2013) and impairs longitudinal and lateral control (Gastaldi et al., 2014). Higher workloads also decrease driving performance (Paxion et al., 2014). Müller et al., 2021 support this, showing that tasks with higher cognitive demands, such as texting and reading, significantly increase response times during automated driving. Figure 10 from their study illustrates that texting resulted in the longest reaction times, followed by reading, while simpler tasks like listening had much quicker responses. This demonstrates how increased cognitive load negatively affects drivers' ability to regain control promptly in automated vehicles.

In their meta-analysis of 129 studies on determinants of take-over time from automated driving, Zhang et al., 2019 found that reaction times are shorter in high-urgency situations, as defined by hand-coded urgency level, time budget to collision (TBTC), and time budget to boundaries (TBTB). This observation aligns with the notion that drivers' motivation to intervene increases with perceived necessity, leading to faster take-over times (Gold et al., 2018; Green, 2000). Furthermore, the meta-analysis revealed that engaging in non-driving tasks (NDTs) significantly increases take-over times (TOT), with handheld tasks exerting the most substantial impact. Figure 11 illustrated the takeover procedure. Performing visual NDTs contributed to increased TOTs, though to a lesser extent than handheld tasks, and the physical act of switching from an NDT to driving further delayed responses. While auditory and cognitive NDTs did not significantly influence TOTs, high cognitive load tasks, such as the N-back, significantly impacted performance (e.g., maintaining lane position), especially after the transition from autonomous to manual control (Melnicuk et al., 2021). These findings underscore the critical importance of minimizing distractions to optimize reaction times.

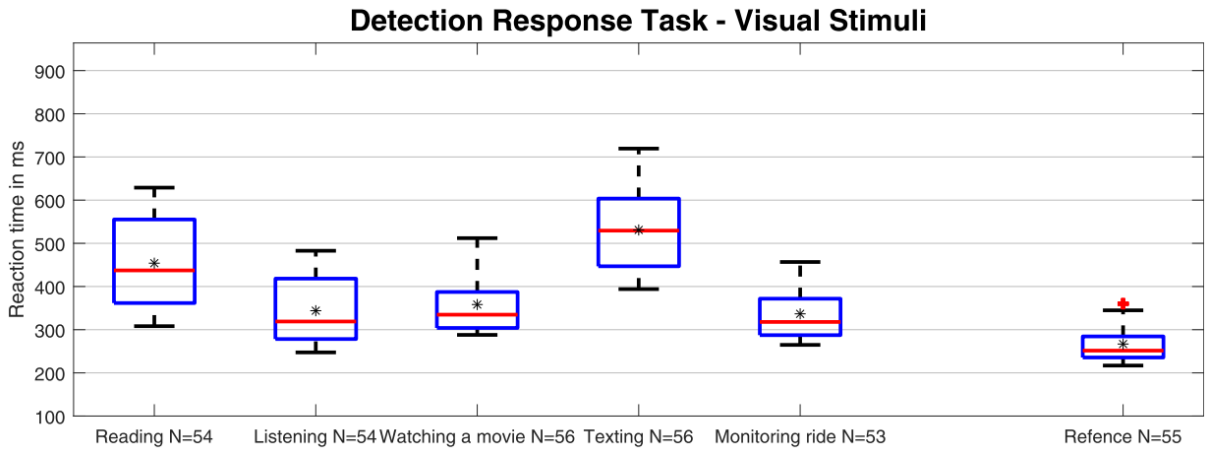

Figure 10: Boxplot representation Driving Related Task depending on the examined Non Driving Related Task in ms (Müller et al., 2021)

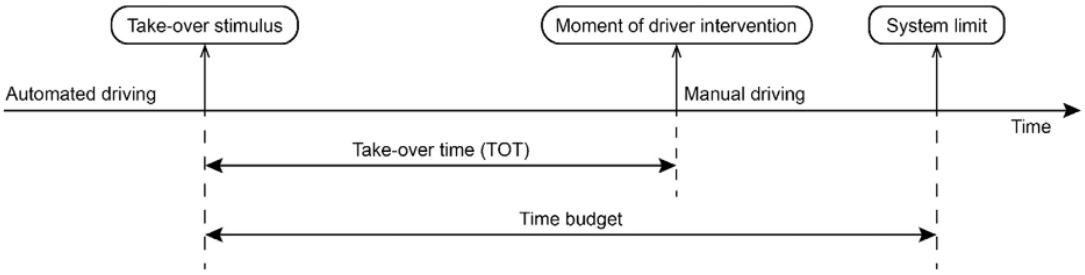

Figure 11: Illustration of the take-over procedure. The present meta-analysis focuses on the take-over time (TOT), defined as the time between the take-over stimulus (take-over request or critical event in the environment) and the intervention by the driver (Zhang et al., 2019).

5. Trust, Over-reliance, and Situational Awareness in Autonomous Driving

Automated vehicles promise to enhance road safety, reduce driver burden, and increase travel comfort through non-driving activities (Fagnant and Kockelman, 2015; Litman, 2023). However, their integration presents challenges in HMI, particularly concerning driver over-dependence and trust in automation (NHTSA, 2022; Zhang et al., 2023). Studies have identified unintended consequences, such as inappropriate trust, leading to potential risks (Mueller et al., 2024). Driver trust is influenced by subjective factors and system reliability, with over-reliance, skill degradation, and reduced vigilance being common issues (Boelhouwer et al., 2019; Walker, 2021). Trust in automated vehicles is shaped by vehicle performance, driver workload, and individual characteristics, impacting safety through diminished awareness and slower responses (Carsten and Martens, 2019). As technology advances, misconceptions about vehicle capabilities may rise, underestimating potential failures (Carsten and Martens, 2019; Holländer et al., 2019). Both overtrust and undertrust jeopardize the safe implementation of automated driving systems (Hoff and Bashir, 2015).

Studies on trust in automated vehicles highlights the growing interest in understanding how trust is conceptualized, calibrated, and measured within the context of driving automation systems (Carsten and Martens, 2019). Walker et al., 2023 findings indicate that trust calibration is highly dependent on driver experience, which should be assessed not only by distance travelled but also by the variety of driving situations encountered. The study identifies the importance of system malfunctions and recovery experiences in trust development. Trust in automated vehicles is described as a dynamic, multi-layered process influenced by dispositional factors (personal characteristics), situational factors (current context and environment), and dynamic learned trust developed through experience over time. As illustrated in Figure 12, this framework represents the development of appropriate dynamic learned trust as a cyclical process. Within this model, occupants of a vehicle interact with the AV system in diverse scenarios, they gradually learn to recognize when the vehicle's behavior is reliable and trustworthy. They adjust their reliance on its automated functions accordingly. With every interaction, occupants may dynamically adjust their trust and alter their behavior based on their enhanced understanding of the system's

capabilities. Observable factors and actions are highlighted, emphasizing that trust is continually shaped by ongoing experiences with the automated vehicle(Walker et al., 2023).

In their meta-analysis of 129 studies on determinants of take-over time from automated driving, Zhang et al., 2019 found that drivers with prior experience in take-over scenarios respond faster. Prior experience of another take-over scenario during the experiment reduced TOT by approximately 1 second. This effect underscores the value of exposure and familiarity with automated driving systems in improving take-over performance. Repeated exposure to take-over requests helps drivers become more adept at responding promptly. Furthermore, the meta-analysis revealed that higher traffic complexity and engagement in NDTs are linked to slower response times. Drivers are slower to respond when the traffic situation is complex or when they are engaged in visual-motor NDTs. This finding indicates the need for designing systems that account for situational awareness of traffic conditions and minimize non-driving distractions to ensure timely take-over responses.

Morgan et al., 2019 compared trust in autonomous vehicles (AVs) using a driving simulator and a real AV performing maneuvers at T-junctions. Both platforms demonstrated predominantly high trust levels, with the simulator platform exhibiting marginally elevated trust compared to the other. Maneuvers involving other vehicles elicited higher trust, likely due to the controlled yielding behaviour of the AVs. The level of trust exhibited variability across different scenarios. Specifically, certain events resulted in elevated trust within the simulator environment, whereas more intricate maneuvers involving oncoming traffic elicited higher trust levels in the real autonomous vehicle. Correlations indicated that trust in technology and automation positively influenced trust ratings. The study underscores the importance of context in trust assessment and suggests that both simulators and real AVs are valuable for evaluating user trust, albeit each affecting trust perceptions differently.

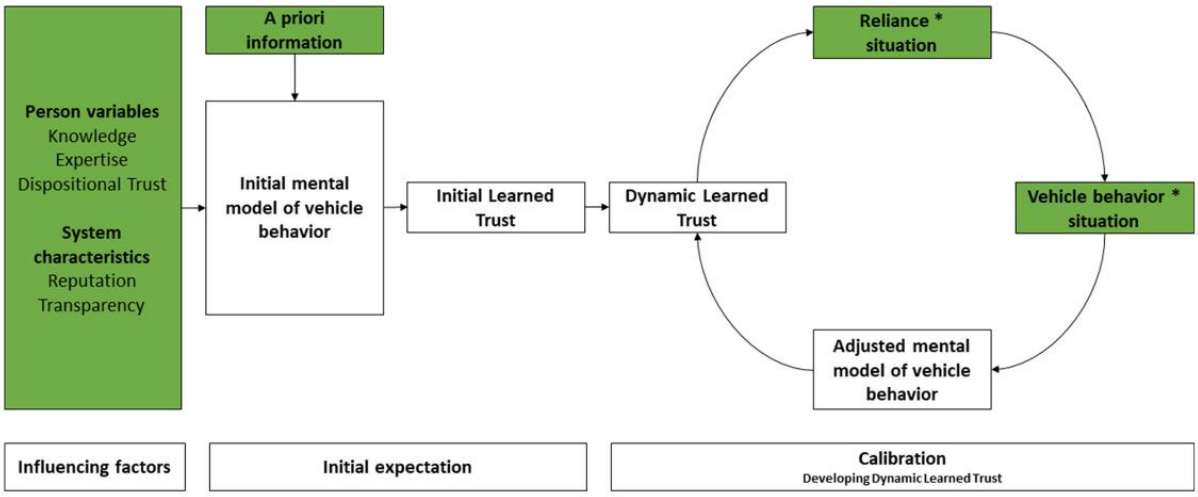

Figure 12: A conceptual framework of the development of trust toward a specific automated driving system; * = By.; (based on Lee and See, 2004; Ghazizadeh et al., 2012; Hoff and Bashir, 2015; Kraus, 2020; Walker, 2021).

6. Occupant response to sensory stimuli in AV

SAE L3 and L4 AV have to communicate a number of information with the occupant, especially in an emergency. For example, Mackenzie et al., 2022 study showed that having an auditory stimulus prior to an automatic emergency brake could play a role in reducing the injury risk (e.g. from whiplash). Studies have shown that the main stages of the occupant's information-processing start by processing the sensory stimuli (visual, haptic, auditory), then repositioning themselves and/or taking the appropriate actions if necessary (e.g., braking, taking over the vehicle, maneuvering) (Petermeijer et al., 2016; Zhang et al., 2019). In his study, Gold et al., 2013 identified four key metrics to assess occupant response time. These metrics are: the duration required for gaze adjustments, the period during which the eyes becomes focused on the roadway, the reaction times of hands and feet interacting with the steering wheel or pedals, and the time necessary to take control of the vehicle.

Zhang et al., 2019 made a statistical analysis of 129 studies to better understand the take-over time (TOT) of occupants in AV. They found an increase in the occupant's take-over time with SAE L3 and higher compared to the lower SAE levels, as well as a significantly higher take-over time with occupants engaged in non-driving related tasks while holding an object. When comparing sensory stimuli, Zhang et al., 2019 deduced that visual stimuli had the slowest mean take-over time compared to auditory or haptic stimuli. The fastest mean take-over time was achieved with a mix of all three stimuli, as seen in Figure 13. It is vital to understand the occupant's reaction time to sensory stimuli as they play a crucial role in warning the occupant in an emergency where a faster response is essential from a safety perspective (Harbluk et al., 2018). Figure 13 from Zhang et al., 2019 analysis represents 21 identified sets, where the mean difference in the average take-over time (D) for each set (square), as well as the difference in mean take-over time from each study (circles). A negative D point to a larger mean take-over time obtained by the first condition compared to the second one. "k" is the number of studies, and "p" is the p-value.

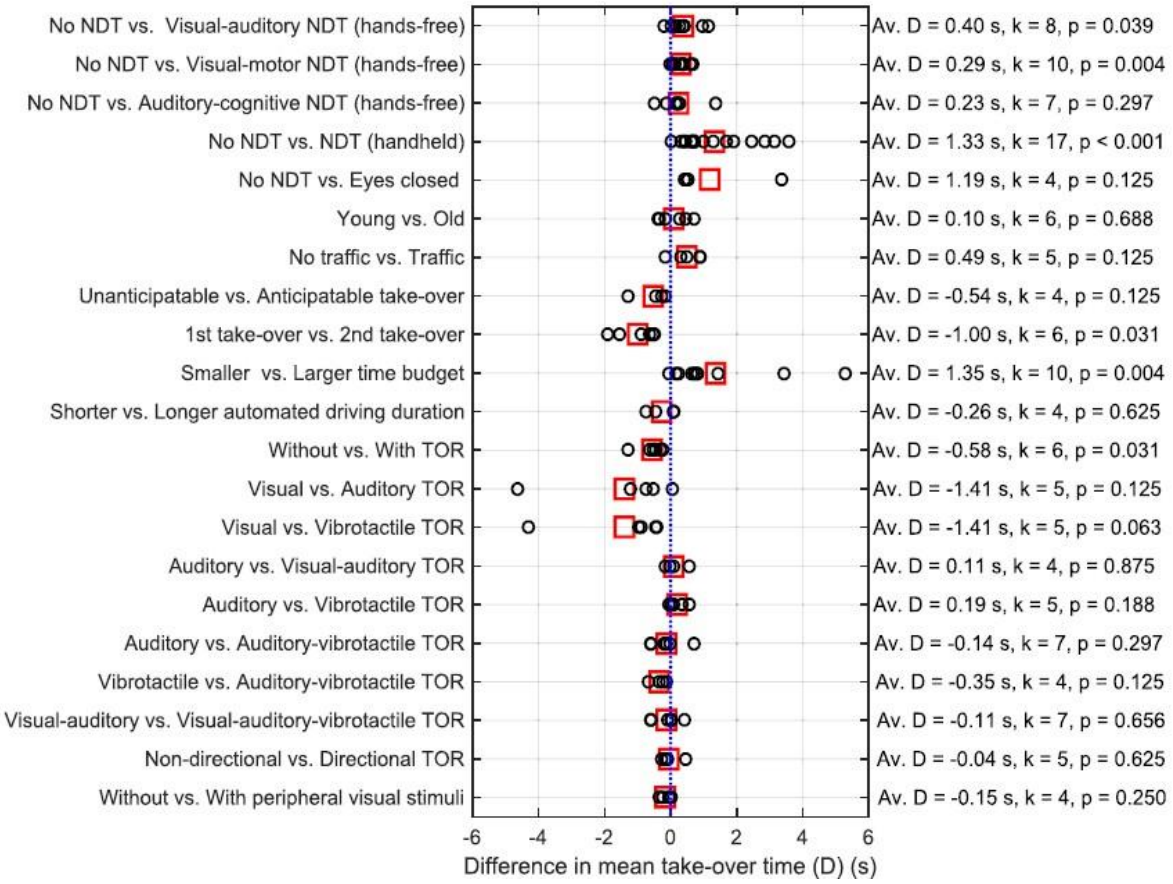

Figure 13: Analysis result of 21 within-study effects. The circles represent the difference in mean take-over time between two conditions (D) of a particular study. A positive D indicates that a larger mean TOT was obtained from the latter condition compared to the former condition. The large square markers represent the average D in the category. k represents the number of studies (D values) in the category. p is the p-value from a two-sided signed rank test for the hypothesis that the D values come from a distribution having a median of 0. TOR = Take-over request, NDT = Non-driving task. A directional TOR is a TOR that is informative about the location of the hazard. Peripheral visual stimuli are stimuli that indicate the status of the automation or the environment (e.g., using ambient LEDs) (Zhang et al., 2019).

7. HMI design and Behavioural Responses to Automated Alerts in AV

AVs can significantly change driver roles and responsibilities. Although these technologies improve safety and convenience, they also introduce risks of misuse. Studies have found that the implementation of SAE Level 2 AV systems results in a 50% increase in the likelihood of drivers taking on secondary activities compared to driving without such automated systems (Dunn et al., 2019). Drivers may find certain driver assistance systems, like forward collision warnings, irritating or distracting, leading to reduced driving performance (Biondi et al., 2014) or complete disregard of the warnings (Dijksterhuis et al., 2012). Sensor-based alert systems can reduce the risk of driver inattention by monitoring the driver and road conditions, issuing alerts when attention or manual control is needed. Request to intervene (RTI) alerts are crucial in the driver-vehicle HMI, needing to re-engage the driver without causing undue distraction, irritation, or startling to prevent the driver from ignoring or disabling the system (Mehrotra et al., 2022).

Different modalities (visual, auditory, haptic) used in HMIs affect driver cognition. Multimodal alerts, particularly those combining visual and auditory cues, are found to be effective in enhancing driver cognition by providing redundant information across multiple sensory channels, which helps drivers quickly understand and respond to emergency situations (Cohen-Lazry et al., 2019). Unimodal alerts, such as visual-only TOR, are less effective because drivers might overlook them, especially when engaged in visually demanding tasks (Petermeijer et al., 2017). The effectiveness of TORs improves when they can attract attention through multiple sensory channels. The take-over process involves multiple stages: perception of the take-over stimulus, cognitive processing, motor readiness, and action (Gold et al., 2013). Various reaction time metrics—such as the duration of gaze adjustments, the time eyes remain focused on the roadway, the response times of hands and feet interacting with the steering wheel or pedals, and the interval required to take control of the vehicle—each capture distinct facets of this process (Gold et al., 2013). Understanding these stages is crucial for designing improved systems and training programs to enhance driver response in take-over scenarios. Conversely, poorly designed alerts, particularly those that are too intrusive or complex, can hinder driver cognition by causing annoyance or distraction, which may delay response times during emergencies (Ruscio et al., 2015).

The specificity and timing of takeover requests in HMIs are crucial in supporting driver cognition. Alerts that clearly specify the reason for the takeover request and provide context about the surrounding environment help drivers to better understand the situation and make informed decisions quickly. Timing is also emphasized, with earlier and more precise alerts leading to better cognitive processing and smoother transitions/reaction during emergencies (Doubek et al., 2020). The available time budget significantly affects TOT. Short time limits or imminent collisions necessitate rapid driver take-over, while a longer time budget allows for more deliberate assessment before taking control (Radlmayr et al., 2019; Zhang et al., 2019). This underscores the importance of automated systems providing sufficient response time for effective driver intervention.

Based on a comprehensive literature review by Mehrotra et al., 2022, revised HMI design recommendations were developed, integrating past guidelines with new research insights. The recommendations are categorized into modality, information content and control, and timing and stages. Key points include designing systems to be multimodal with visual and auditory, with possible tactile elements for extra safety; presenting system status clearly and continuously; supporting driver decision-making with context-aware alerts; and ensuring alerts are timely, with intensity proportional to urgency. Multi-staged alerts should be used to enhance driver response in critical situations.

8. The Role of Virtual Reality and Driving Simulators in HMI Design, Development, and Validation in Autonomous Vehicle Studies

8.1. Virtual Reality

8.1.1. Definition

Jaron Lanier popularized the term "virtual reality" in 1987 to describe environments created by computer systems that enable users to navigate and interact within them, either individually or with others. VR specifically aims to provide users with a fully immersive sensory-motor experience within a synthetic world (Fuchs et al., 2003). Virtual reality is characterized by its capacity of full user immersion and active interaction with the virtual environment (Sherman and Craig, 2003), distinguishing it from merely viewing 360° videos in a head-mounted display which do not constitute a true VR experience.

8.1.2. The concepts of immersion and presence

Slater and Usoh, 1993 distinguish between immersion and presence in virtual environments. Immersion refers to a system's ability to replicate a real situation through sensory inputs, and it is objective and measurable. Enhancing immersion, such as by adding spatialized sound, increases the system's realism. Conversely, presence refers to the individual's subjective experience of existing physically within a simulated environment. This sense of presence is influenced by the user's sensory perceptions and cognitive representations of the surrounding environment. When presence is strong, users behave in the virtual world as they would in reality, forming memories of experiences rather than just images.

8.2. Simulator sickness

Passengers in vehicles can experience motion sickness, including symptoms like nausea and dizziness (Reason and Brand, 1975). Similar effects, known as cybersickness or Virtual Reality Induced Sickness Effects (VRISE), occur in VR and simulators environments (Mazloumi Gavgani et al., 2018). Despite different contexts, the mechanisms are likely similar, with cybersickness resulting from the mismatch between real and virtual perceived motion. This mismatch induces nausea and discomfort, which can persist for several hours following the use of VR.

Three principal theories—sensory conflict theory, ecological theory, and poison theory—are utilized to explain the phenomenon of cybersickness. The most widely accepted is the sensory conflict theory, which suggests that cybersickness results from a mismatch between sensory systems, particularly visuo-vestibular conflict (Harm, 2002). The ecological theory posits that cybersickness arises from prolonged postural instability during movement, with instability occurring before sickness (Riccio and Stoffregen, 1991). Lastly, the poison theory suggests that cybersickness symptoms are an evolutionary response to sensory hallucinations, meant to expel ingested toxins (Treisman, 1977), though this theory is debated due to the slow response time for toxins to affect the vestibular system (Harm, 2002). To

measure and assess sickness effects in simulated environments, Robert Kennedy developed the widely recognized Simulator Sickness Questionnaire (SSQ) (Kennedy et al., 1993).

In simulator studies, cybersickness—initially studied in aeronautical simulator research (Kennedy and Frank, 1985)—also significantly impacts the automotive industry's simulation field, where motion sickness has widespread societal implications (Kemeny and Panerai, 2003). Recent studies indicate that motion sickness could become more prevalent among autonomous vehicle users (Diels et al., 2016; Iskander et al., 2018; Sivak and Schoettle, 2015). In response, researchers and industries may develop motion or virtual reality systems to alleviate these effects, helping users better anticipate vehicle movements and build trust in autonomous vehicles (Oliver, 2018; Sawabe et al., 2016; Wintersberger et al., 2018).

8.2.1. Applications of VR in HMI Design for Level 3 Avs

VR offers a unique advantage over real-world testing by enabling controlled, repeatable experiments across diverse driving scenarios, which is particularly valuable for studying driver responses in Level 3 AVs. In their study on the feasibility and effectiveness of using head-mounted display (HMD) virtual reality (VR) in autonomous vehicle (AV) simulations, Zou et al., 2021 found that participants experienced a high level of immersion and presence, indicating that VR systems can effectively replicate realistic driving experiences for AV research. This finding highlights the potential of VR as a cost-effective and versatile tool for studying human-automation interaction. Moreover, VR simulations have proven invaluable in evaluating the effectiveness of HMI components, such as visual and auditory alerts, in Level 3 AVs. Various studies have used VR to simulate critical handover scenarios, demonstrating that drivers respond more effectively to multi-sensory alerts than single-modal alerts, thereby suggesting the importance of multimodal HMI systems in AV design (Huang et al., 2024; Yun et al., 2018). For instance, Sportillo et al., 2018 employed VR to assess driver attention and responsiveness during transitions from automated to manual control in Level 3 AVs. Their study showed that immersive VR environments enabled the simulation of complex driving scenarios and allowed researchers to effectively evaluate drivers' response times and decision-making under varying levels of automation. Together, these studies demonstrate the significant role of VR in advancing HMI design for Level 3 AVs, providing valuable insights into driver behaviour and enhancing the development of safe and effective autonomous vehicle systems.

8.3. Immersive Reality Devices: Commonly Used Systems

8.3.1. Head-Mounted Display (HMD)

The VR headset is a widely recognized system among the general public, worn on the user's head and secured with straps. It includes a tracking system that monitors the headset's position in real time, enabling the display of a coherent image on the internal screens. Typically, these devices offer a limited field of vision (e.g., 110 degrees for the HTC Vive), a refresh rate of at least 90 Hz, and relatively low resolution (1080x1200 pixels per eye for the HTC Vive). HMD systems are not inherently dynamic but

can be integrated with dynamic systems, such as SLED systems (Figure 14), due to their lightweight design.

Figure 14: HTC Vive (STEAM VR. 2024)

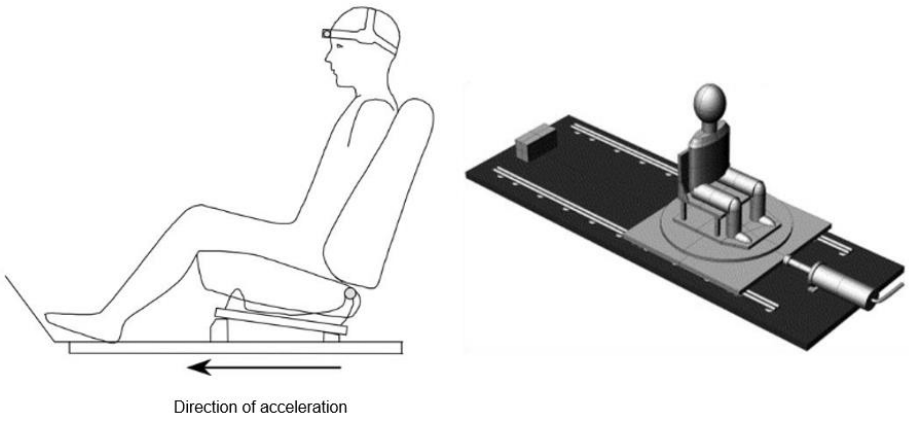

Figure 15: System called "Sled", adapted from Siegmund et al. 2003 (left) and from Kumar et al. 2005 (right)

8.3.2. Driving Simulators

Driving simulation is widely used for studying and validating features, as well as for training and designing HMI and ADAS (Bertollini et al., 2010; Kemeny and Panerai, 2003; Langlois, 2013; Reymond and Kemeny, 2000). The rise of AVs has further increased the need for driving simulation, particularly to ensure drivers can smoothly transition from autonomous to manual control, and during emergencies (Zhang et al., 2019, 2023). Given safety concerns and the extensive scenarios requiring validation, autonomous vehicle testing cannot rely solely on field tests (Kalra and Paddock, 2016; Sovani, 2017). However, driving simulation also presents challenges, including the risk of motion and cybersickness (Kemeny et al., 2020; Kemeny and Panerai, 2003). According to a review by Riegler et al., 2021, it is possible to achieve behaviour and cognition closer to reality and reduce the effects of motion sickness.

This is achieved when subjects are more immersed in the VE, feel secure and familiar with the setting, and clearly understand the task at hand.

In order to study HMI in SAE L3 and above, driving simulators are commonly used to provide a low-risk and low-cost environment with great control over the environment and vehicle conditions to validate real live scenarios (Kemeny et al., 2020). When designing an AV experiment with a driving simulator, the subject must become accustomed to the system being tested, especially with respect to HMI (Schöner and Morys, 2016). Thus, in order to achieve behaviour close to real-life scenarios, the driving simulator HMI must offer security with instructive and entrainment features whilst decreasing stress; during the experiment, the subject must be aware of the AV abilities, get well-timed warnings, and be capable to oversee the conditions around them in the virtual environment (Schöner and Morys, 2016). Furthermore, simulator/motion sickness should be taken into account as it can influence the behaviour and cognition of occupants (Kemeny et al., 2020; Rangelova and Andre, 2018). Simulator/motion sickness may take place through sensory conflict; when the visual system sees the virtual content in VR but does not match the vestibular system detection of the vehicle movements (Chardonnet et al., 2015). Studies have shown that once subjects are more immersed in the VE, feel secure and familiar with the setting, and clearly understand the task at hand; it is possible to achieve behaviour and cognition closer to reality while at the same time significantly reducing the effects of Simulator/motion sickness (Chardonnet et al., 2021; Kemeny et al., 2020; Lucas et al., 2020; Riegler et al., 2021; Williams et al., 2020). A comparative overview of different dynamic driving simulators used in research, highlighting their structural components, screen configurations, and acceleration capabilities, is provided in Table 2. This table offers valuable insights into the diverse range of driving simulators and their specifications.

Table 2: Comparative table of different dynamic driving simulators used for research (Di Loreto, 2019)

System	illustration	Structure	Screen	Displacement	Acceleration	Reference
SAAM		Hexapod	180° Screen	Longitudinal: ± 0.25 m Lateral: ± 0.25 m Vertical: ± 0.18 m	Longitudinal: ± 0.6 g Lateral: ± 0.6 g Vertical: ± 0.5 g	Aykent et al. 2014
DLR		Inverted Hexapod	270° Screen	Longitudinal: ± 1.5 m Lateral: ± 1.4 m Vertical: ± 1.4 m	Longitudinal: ± 10 m/s² Lateral: ± 10 m/s² Vertical: ± 10 m/s²	Suikat 2005
NADS		Hexapod + XY Platform	360° Screen	Longitudinal: ± 9.75 m Lateral: ± 9.75 m Vertical: ± 0.61 m	Longitudinal: ± 0.6 g Lateral: ± 0.6 g Vertical: ± 1.0 g	Chen et Papelis 2001
Daimler-Benz	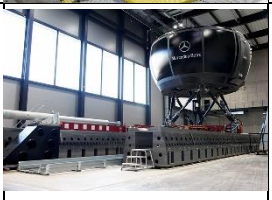	Rail X + Hexapod	360° Screen	Longitudinal: ± 16.8 m Lateral: ± 1.3 m Vertical: ± 1.0 m	Longitudinal: ± 2.0 g Lateral: ± 1.0 g Vertical: ± 1.0 g	Zeeb 2012
VIRTTEX		Hexapod	360° Screen	Longitudinal: ± 1.6 m Lateral: ± 1.6 m Vertical: ± 1.0 m	Longitudinal: ± 0.6 g Lateral: ± 0.6 g Vertical: ± 1.0 g	Blommer 2018
PSA		Hexapod + XY Platform	160° Screen	Longitudinal: ± 5.0 m Lateral: ± 2.8 m Vertical: ± 0.2 m	Longitudinal: ± 5.0 m/s² Lateral: ± 5.0 m/s² Vertical: ± 5.0 m/s²	Chapron et Colinot 2007
ROADS Renault		Hexapod + XY Platform	360° Screen	Longitudinal: ± 25 m Lateral: ± 25 m Vertical: ± 1.0 m	Longitudinal: ± 1.0 g Lateral: ± 1.0 g Vertical: ± 1.0 g	Renault Group 2024
ETH Zürich		Hexapod	3 PC Screens or HMD	Longitudinal: ± 5.0 cm Lateral: ± 5.0 cm Vertical: ± 5.0 cm	Longitudinal: ± 0.3 g Lateral: ± 0.3 g Vertical: ± 0.3 g	Ropelato et al. 2018

9. Conclusion

This chapter has provided a comprehensive review of the existing literature on head-neck biomechanics, injury mechanisms, and human-machine interaction (HMI) in the context of both conventional and autonomous vehicles. The findings emphasize the increasing complexity of ensuring occupant safety as vehicle automation advances, particularly at SAE Level 3 and beyond. The review of the biomechanical properties of the cervical spine has highlighted the intricate relationship between the head and neck during various vehicular maneuvers, such as braking, turning, and emergency actions. It has become clear that traditional crash test models may fall short in replicating the dynamic kinematics and muscle responses of real occupants, which necessitates a reassessment of current safety measures, including seat belts and airbags.

Furthermore, as vehicles evolve to accommodate more relaxed seating postures and non-driving activities, the literature points to significant gaps in understanding how these changes will impact occupant safety. Studies on HMI in autonomous vehicles reveal that transitions between manual and autonomous control, and anticipating emergency scenarios are critical, with cognitive load, reaction times, and trust in automation playing central roles in determining occupant behaviour and safety outcomes during emergencies.

Despite advances in crash test models and safety systems, the emerging challenges presented by the advent of autonomous vehicles, particularly regarding occupant behaviour and cognitive engagement, necessitate further research. The insights gained from the studies discussed in this chapter suggest that both biomechanical and cognitive factors must be carefully integrated into future safety designs for AVs. Notably, there is a lack of studies investigating the effects of occupant activity on the head-neck physiological response, particularly in short-drive scenarios within SAE Level 3 AVs, where the occupants may engage in non-driving tasks. This gap highlights the need for more comprehensive research into how different occupant activities during short-duration trips influence musculoskeletal responses and injury risk in dynamic driving conditions. Future research should focus on these interaction dynamics, as well as how new technologies such as virtual reality can be used to simulate and study human responses to critical driving scenarios.

The next chapter will delve into the specific methodologies and experimental setups designed to address these identified gaps, particularly focusing on the integration of virtual reality and biomechanical analysis in studying human-machine interactions and occupant safety in Level 3 autonomous vehicles.

CHAPTER 2: RESEACH QUESTIONS

1. Research Orientation

The literature review provided a comprehensive overview of the biomechanical and cognitive challenges associated with occupant safety in autonomous vehicles, particularly focusing on head-neck dynamics during emergency maneuvers in SAE Level 3 vehicles. Through this review, we identified key gaps in the understanding of human-machine interactions (HMI) in automated vehicles, especially in scenarios involving non-driving activities. Existing research has laid a strong foundation by exploring the occupants responses and the potential injuries mechanics such as whiplash. However, it has become evident that traditional safety models, largely based on passive occupant postures and crash simulations, does not account for the diverse range of occupant activities enabled by vehicle automation.

As vehicle technology advances, with increasing focus on SAE Level 3 autonomy, where drivers may disengage from the driving task, it is crucial to delve deeper into the interaction between occupant activities and physiological responses, especially under emergency conditions. The literature suggests that, although studies have explored the influence of biomechanical factors and certain aspects of occupant cognition, a significant gap remains regarding the impact of non-driving activities on head-neck dynamics during short-duration drives, particularly in the context of sudden vehicle maneuvers. This gap poses a crucial challenge, as these activities, ranging from looking at the road to using devices, are expected to significantly alter the way occupants experience acceleration forces, thus influencing injury risk.

Building on the insights from the literature, we will employ virtual reality (VR) and driving simulator experiments with biomechanical sensors to explore the effects of various non-driving activities in a controlled environment. The use of both VR and driving simulator will allow us to simulate complex driving conditions while monitoring real-time occupant responses, offering a unique approach to understanding the interplay between occupant cognition, activity, and safety. Specifically, one of the key research questions guiding this work is: *How can driving simulators and dynamic virtual environments help improve HMI in autonomous vehicles, especially sensory modalities?* By integrating these sensory modalities, we aim to achieve a more accurate representation of occupant behaviour under emergency conditions, bridging the gap between simulated and real-world responses.

Furthermore, the research will address another critical question: *How do the activities in which occupants are engaged prior to an emergency maneuver in an autonomous vehicle (AV) influence the body's physiological response under specific pre-maneuver conditions?* This inquiry will explore how different non-driving tasks, such as reading or reclining, alter the physiological responses of the head and neck during sudden braking events, providing crucial insights into the biomechanical implications of occupant activity in SAE Level 3 vehicles. By answering these questions, this research aims to contribute to the development of safer, more adaptable vehicle designs, enhancing both human-machine interaction and occupant protection in future autonomous vehicles.

2. Research Axes

2.1. The Impact of Occupant Activities on Head-Neck Dynamics in AVs

The central research question guiding this axis is: *How do the activities in which occupants are engaged prior to an emergency maneuver in an autonomous vehicle influence the body's physiological response under specific pre-maneuver conditions?*

As discussed in the literature review, the increasing automation of vehicles, particularly at SAE Level 3, is transforming the role of occupants by allowing them to engage in non-driving tasks during their journey. This shift creates new possibilities, such as reading, or working, but also introduces critical uncertainties regarding how these activities influence occupant safety in emergency situations. Specifically, changes in occupant cognition and body positioning due to non-driving activities are expected to affect their biomechanical response during sudden maneuvers, such as emergency braking. However, current safety models and crash test dummies fail to account for this variability, leading to a significant gap in understanding the true dynamics of human physiological responses under these conditions. This research axis focuses on investigating how the activities occupants engage in before an emergency brake affects their body's response, with an emphasis on head-neck dynamics and potential injury risk during short-drive scenarios.

2.2. Enhancing HMI in Virtual Environments for Realistic Occupant Behaviour and cognition

The central research question guiding this axis is: *How can driving simulators and dynamic virtual environments help improve HMI in autonomous vehicles, especially sensory modalities?*

As outlined in the review, the development of human-machine interfaces (HMI) in autonomous vehicles, especially within virtual environments and driving simulators, has introduced new challenges in reproducing realistic occupant behaviours during emergencies. The incorporation of sensory modalities, such as auditory feedback, plays a pivotal role in enabling occupants to anticipate dangerous situations. However, the current state of HMI in simulators does not fully replicate the complex interaction between occupants and an SAE Level 3 AV systems during an actual drive (e.g. a 15 min drive) since the interaction is made only for one specific event, leading to a disconnect between simulated and real-world responses. This research axis is dedicated to improving HMI by integrating advanced sensory modalities to create more immersive and realistic simulation environments.

3. Proposed Approach

The research presented in this manuscript is organized around the two primary research axes previously outlined. In the first experiment, we investigate occupant activity during short driving scenarios to elucidate the effects of Human-Machine Interface (HMI) interactions and occupant behaviorus on the physiological responses of head-neck dynamics. Specifically, vertical acceleration forces, matched in intensity to the horizontal acceleration forces typically experienced by occupants in normal driving conditions, were applied. This experiment was conducted using the SAAM driving simulator at the Institut Arts et Métiers in Chalon-sur-Saône.

Following this, a second experiment was undertaken to gain a more comprehensive understanding of how braking maneuvers affect the physiological responses of the head and neck, depending on the activities in which occupants are engaged. This second study also serves to validate the findings of the initial experiment. The second experiment employed a SLED system at the Institut de Biomécanique Humaine Georges Charpak in Paris. Unlike the driving simulator, the SLED system can replicate the horizontal acceleration forces experienced by drivers during real-world braking scenarios.

4. Issues faced

At the beginning of the second year of this thesis, the lab in Chalon-sur-Saône relocated to a new building. However, due to technical problems at the new site, the driving simulator, which was critical for conducting the first experiment, remained in the old facility. These technical issues prevented the transport of the simulator, resulting in a six-month delay. This translated in a significantly limited access to the simulator, particularly for conducting pre-tests necessary for developing the experimental protocol and, more specifically, for refining the motion cueing algorithm. These pre-tests were essential to enhance the realism of the simulator's motion and to synchronize adjustments in the virtual environment, ensuring the experiment was as immersive and realistic as possible. To illustrate the impact of this delay, we initially planned to conduct 2 to 3 pre-tests per day; however, due to restricted access, we were only able to complete 2 to 3 pre-tests per week. Despite these setbacks, we successfully conducted the two planned experiments, although our ability to recruit a larger number of participants was affected.

CHAPTER 3: OCCUPANT BEHAVIOUR, COGNITION, AND HMI IN LEVEL 3 AV DRIVING SIMULATOR

1. Introduction

As seen from the previous chapters, to study HMI in SAE Level 3 and above, driving simulators are often used for their low-risk, cost-effective, and controlled environments (Kemeny et al., 2020). These simulators allow for the personalized cognitive exploration of occupants in a Level 3 AV, aiming to understand their behaviour, interaction strategies, and cognitive responses in a simulated dynamic environment. The flexibility of the virtual environment enables the testing of various configurations and scenarios, such as emergency braking or the addition of audible alerts, which are crucial for evaluating the effectiveness of HMI (Schöner and Morys, 2016). When designing AV experiments, it is essential that subjects become accustomed to the system, particularly the HMI. The driving simulator HMI should ensure security with instructive and entertaining features, reduce stress, provide timely alerts, and allow subjects to monitor their surroundings in the virtual environment. Additionally, the potential for simulator/motion sickness, caused by sensory conflict between visual and vestibular systems, should be considered as it can affect behaviour and cognition (Kemeny et al., 2020; Rangelova and Andre, 2018). Studies indicate that once subjects feel secure, familiar, and understand the task, behaviour and cognition align more closely with reality, enhancing the validity of the simulation outcomes (Kemeny et al., 2020; Lucas et al., 2020; Riegler et al., 2021; Williams et al., 2020).

This research is part of a major evolution towards increased vehicle automation, addressing crucial road safety issues and the associated risks, costs, and acceptance of autonomous technologies. It focuses on understanding, through simulation and virtual reality, the cognitive mechanisms at play in interactions between a Level 3 AV and its driver/occupant. This includes determining the influence on strategies to stabilize the human body in critical situations, such as emergency braking, and identifying the most suitable human-machine interactions (HMI) that can adapt in real-time to ensure optimum safety and minimize injuries. It is essential to validate simulation studies against real-world conditions to avoid perceptual biases. Currently, safety systems are evaluated using impact dummies representing average human morphologies, which have improved vehicle safety but do not reflect the diversity of occupants (Grébonval et al., 2021a). These dummies, seated in standardized positions, fail to account for behavioural aspects, out-of-position (OOP) movements, and muscle contractions in Level 3+ AVs (Grébonval et al., 2021b; Subit et al., 2017). Understanding the HMI between the occupant and the AV is crucial for improving occupant safety by studying their behaviour and cognition. We expect that occupant activity during AV maneuvers will significantly influence physiological responses, such as head acceleration, head movement, and muscle activation, particularly during strong and emergency scenarios. Additionally, we hypothesize that HMI systems providing timely and clear auditory alerts will affect occupant head-neck dynamics during maneuvers.

The main objective of the presented chapter is to better understand HMI, behaviour, and cognition of occupants in a Level 3 AV driving simulator during emergency scenarios, avoidance, or automatic braking. To achieve the objectives, we examined the impact of AV maneuvers on various physiological parameters, including head movement, muscle activation, respiration, heart rate, as well as occupant activity. We expect that individual participants will exhibit significantly different physiological responses, despite being subjected to uniform experimental conditions. Moreover, we predict that the occupant activities performed by participants during the experiment will align with those documented in the literature for short duration drives in SAE Level 3 autonomous vehicles.

2. Materials and Methods

2.1. Participants

The experiment involved 12 participants (8 women and 4 men) with a mean age of 33.5 years (SD = 12.2 years), a mean weight of 66.2 kg (SD = 10.7 kg), a mean height of 1.69 m (SD = 0.07 m), and a mean body mass index (BMI) of 23 kg/m² (SD = 2.2 kg/m²). All participants possessed a valid driver's license for over 5 years, except for one participant who held it for less than 5 years. Visual acuity was either normal or corrected-to-normal, and participants reported no vestibular or ocular abnormalities. Regarding weekly driving habits, one participant did not drive, three drove for up to one hour, five drove between one and three hours, and three drove between three and five hours. Nine participants had no prior experience with a driving simulator, while the remainder had not encountered the specific setup employed in the experiment. All participants were instructed to abstain from excessive caffeine absorption, recreational drug use, including alcohol, for a minimum of 24 hours prior to the commencement of the experiment. All Experimental procedure were performed in accordance with the ethical guidelines of the Declaration of Helsinki. All participants gave their written informed consent prior to participation in the study.

2.2. Apparatus : Driving Simulator (SAAM)

The experiment was conducted utilizing the SAAM dynamic driving simulator (Figure 16), which comprises a cockpit modeled after a standard Renault Twingo II vehicle (ref is needed here, from a previous article that used the SAAM). The cockpit has been equipped with instrumentation while maintaining its visual fidelity to the authentic vehicle. The vehicle is affixed to a MOOG 6DOF 2000E platform boasting six degrees of freedom, employing electric cylinders with a communication rate ranging from 30 to 60 Hz. Visual stimuli are projected onto a hemicylindrical screen (height: 1.20m; field angle: 150°) by three Digital Light Processing (DLP) "Projection Design F10SX+" video projectors (resolution: 1400 x 1050 pixels at 60Hz). Real-time graphic processing, generation of the driving environment, and interface metaphors for interaction with the driving station (visual, auditory, and haptic) are managed by a cluster of six computers. Table 3 delineates the platform's constraints in terms of Degrees of Freedom. A classical motion cueing algorithm (Stewart, 1965) is employed to transform horizontal acceleration forces into vertical forces, constrained by the capabilities of the driving simulator.

This transformation process is based on pre-recorded data extracted from the simulation engine, allowing for the accurate representation of g-forces within the vertical plane. Please refer to the appendix for more details

Table 3: SAAM mouvements limits

Degree Of Freedom	Displacement	Velocity	Acceleration
Pitch	±22 deg	±30 deg/s	±500 deg/s²
Roll	±21 deg	±30 deg/s	±500 deg/s²
Yaw	±22 deg	±40 deg/s	±400 deg/s²
Heave	±0.178 m	±0.30 m/s	±0.5 g
Surge	+0.259, -0.241 m	±0.5 m/s	±0.6 g
Sway	±0.259 m	±0.5 m/s	±0.6 g

Figure 16: Renault Twingo skeleton mounted on the Moog 6DOF200E motion system platform (Also known as SAAM)

2.3. Apparatus: Instrumentation

Participants were outfitted with two inertial measurement units (IMUs, Xsens MTx): one affixed to the head and another to the first thoracic vertebra (T1). Additionally, a reference IMU was securely mounted at the center of the vehicle's floor. Orientation and acceleration data were sampled at a frequency of 100 Hz. The head IMU was firmly fastened using cable ties and tape to an adjustable rigid head strap, while the T1 IMU was adhered with double-sided tape and hypoallergenic adhesive strips. Furthermore, right sternocleidomastoid (SCM) muscle activity was captured at a rate of 2000 Hz employing a wireless electromyography (EMG) sensor (BioNomadix). Additionally, a wireless Respiration Transducer sensor belt (BIOPAC Systems BioNomadix), encircling the abdomen, recorded respiratory profile at 2000 Hz.

Heart rate was monitored at 1 Hz using a wireless optical heart rate sensor (Polar OH1+), positioned on the forearm. A Go-Pro Hero3+ Camera was used to record participants activities thought the experiment at 720p and 30 fps.

2.4. Simulator Scenario and Protocols

To assess occupant behaviour and physiology, a 13-minute ride in a Level 3 autonomous vehicle (AV) simulator was conducted. The virtual environment was built using Unreal Engine and CARLA, an open-source autonomous driving simulator (Dosovitskiy et al., 2017). The simulated environment comprises a compact urban area nestled amidst lacs and mountainous terrain. The road layout encompasses a simple network of small streets and intersections scattered among commercial buildings and residential houses. A ring road, resembling a "shape of 8," encircles the small town, with a mountain nearby. The central intersection incorporates both underpass and overpass elements, along with circular access roads (Figure 17). Telemetry data from CARLA were recoded and transformed into motion queues to transfer forces applied to the occupant from horizontal to vertical forces, enhancing immersion and reducing cybersickness. The simulated AV journey begun within the town and traversed along the highway back to the same urban area. Nevertheless, due to the environmental configuration and the chosen route, it conveyed the impression of entering a different town upon return. The AV operated at Level 3 autonomy, allowing it to perceive its surroundings and make independent decisions, such as overtaking slower vehicles. Human intervention was not necessary during the whole experiment, and participants had no control over the vehicle. However, the AV provided audible alerts to maintain awareness in potential hazard situations, such as pedestrian crossings. Participants were free to engage in various activities, including using their phones, tablet in the simulator, or listening to the radio, as they would typically do as occupants. The radio was maintained at a constant volume throughout the ride. Table 4 provides detailed information on the recorded events during the experiment, including 17 braking events (8 normal, 8 strong, and 1 emergency), 5 ninety-degree turns (4 normal and 1 strong), and 6 lane changes (5 normal and 1 strong), with some braking events accompanied by audible alerts.

Before the experiment, participants were equipped with the previously described physiological sensors (Figure 18). Upon completing the experiment, participants exited the driving simulator and proceeded to a desk to complete a Simulator Sickness Questionnaire (Kennedy et al., 1993), which was used to assess their levels of motion sickness following the simulation.

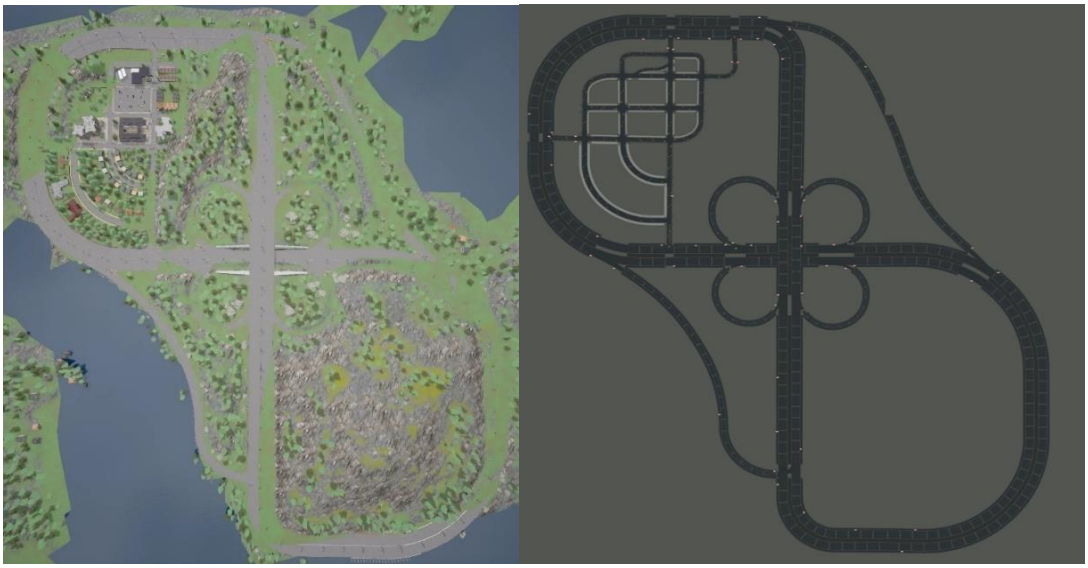

Figure 17: Top-down view of the virtual road network in the CARLA Town Map using Unreal Engine.

Table 4: Detailed Summary of Braking Events, Ninety-Degree Turns, and Lane Changes Recorded During the Experiment

Total count per event	Event Type	Count	Acceleration Range (g)	Designation Type	Including Audible Alerts
17	Braking	8	0.2 - 0.4	Normal	2
		8	0.4 - 0.6	Strong	1
		1	0.6 - 0.8	Emergency	1
5	90-Degree Turning	4	0.2 - 0.4	Normal	0
		1	0.6 - 0.8	Strong	0
6	Lane Change	5	0.2 - 0.4	Normal	0
		1	0.4 - 0.6	Strong	0

Figure 18: Participant outfitted with physiological sensors

2.5. Studied Parameters and data Processing

The studied parameters include the normal head acceleration, head pitch rotation, sternocleidomastoid (SCM) muscle activation, event-specific activities, respiration rate, and heart rate. The acceleration and pitch rotation data from the IMU sensor remained unfiltered. The orthogonal reference frames of the IMU sensors were numerically aligned with the orientation of the driving simulator (Figure 16): +X pointed towards the front of the participant, +Y was oriented to the right of the participant, and +Z was directed towards the floor.

In frontal braking scenarios, the focus lies on understanding the combined effects of braking intensity and audible alerts on various metrics such as head acceleration, pitch rotation, participant activity, SCM muscle activation, heart rate, and breathing frequency, with specific attention to the interactions between participant activity and other parameters. Similarly, during lane changes and 90-degree turns, the emphasis is placed on identifying the impact of lane-changing/turning intensity on head acceleration, pitch rotation, participant activity, SCM muscle activation, heart rate, and breathing frequency, with a particular emphasis on the interaction between participant activity and the other variables.

Table 5 provides detailed information concerning data processing, including calculations of head acceleration, head pitch rotation, SCM muscle contraction, heart rate data, respiration frequency, participant activities, and braking intensity during various driving events, including frontal braking, ninety-degree turns, and lane changes.

Table 5: Detailed Summary of data processing parameters and classification criteria during the experiment

Parameter	Description
Head Acceleration	Difference between highest and lowest values during each event
Head Pitch Rotation	Difference between highest and lowest pitch values of the head movement
SCM Muscle Contraction	1 for activation, 0 for no activation, 2 for double activation (once after hearing the alert and again during the braking event), and NaN for excessive noise.
Heart Rate Data	1 if above positive standard deviation (mean +sd) during rest, 0 if within two standard deviations, -1 if below negative standard deviation (mean -sd)
Respiration frequency Data	1 indicating a significant change and 0 indicating no significant change, when analyzed for significant changes within the intervals of 5 to 10 seconds before and 10 to 15 seconds after each event
Participant Activities	A: observing the road, B: using devices, C: device use before event and observation during event
Braking Intensity	Normal, Strong, or Emergency with indication of audible alert (yes/no)
90-Degree Turns Intensity	Normal or Strong
Lane Change Intensity	Normal or Strong

2.6. Statistics

N-way ANOVA tests were used to analyze various categorical independent variables. These tests were performed for the following parameters within each of the three categories (Frontal braking, 90-degree turn, and Lane change): head acceleration, head pitch rotation, SCM muscle activation, heart rate, and respiration frequency. In each N-way ANOVA test, one of the earlier mentioned parameters served as the sample data (e.g. head acceleration), while the grouping variables included participant number, audible alert activation (relevant only for Frontal braking), braking/turning/lane-changing intensity, and participant activity. The significance threshold was set to 0.05. A post-hoc test was not conducted, as the objective was solely to investigate the existence of significant differences between three or more groups.

3. Results

For all categories, three types of non-driving activities were identified: looking at the road ahead (A), using devices such as a phone or tablet (B), and using devices before the event and then looking at the road when event starts or when audible alert is activated (C). In the following parts, a number appended to the activity letter signifies the observed physiological change. For braking, lane changing, and turning more than 50% of the EMG data exhibited excessive noise, leading to its exclusion from detailed analysis. However, for the purpose of calculating the percentage of event occurrences, the total event count still included these instances to ensure an accurate representation of the overall event distribution, despite the exclusion of noisy data from further analysis.

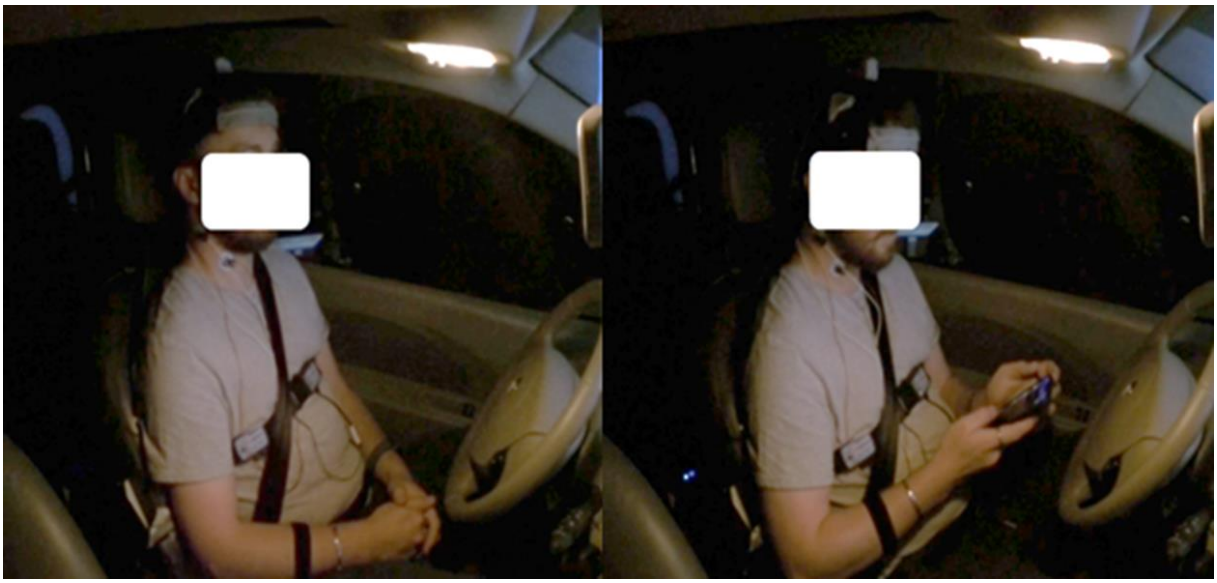

Figure 19: Occupant engaged in Activity A (left) and Activity B (right)

3.1. Frontal Braking

The audible alert was only activated in this category, all participants looked at the road when an audible alert preceded braking.

3.1.1. Head Acceleration

Table 6 presents the median and interquartile range [1st quartile; 3rd quartile] of normal head acceleration (in g) during various occupant activities under different braking intensities (Strong, Normal, Emergency). Data are compared between scenarios with and without an audible alert. "Never occurred" indicates that the specific condition was not observed during the experiment. This is because occupants were free to interact with the vehicle as they wished during the experiment, which resulted in some activities not occurring during certain braking events. For example, for Activity B (engaged with devices at the moment of braking), it “Never occurred” because all participant looked at the road when an audible alert was engaged. The highest median head acceleration was observed under emergency braking when an audible alert was present. Under strong braking intensity, head acceleration was higher when an audible alert was present compared to when it was absent. Conversely, when no alert was present, differences in head acceleration were observed. The head acceleration was slightly higher when occupants focused on the road throughout the braking event (Activity A) compared to when they engaged with devices at the moment of braking (Activity B), and the highest head acceleration in the absence of an alert was observed when occupants initially used devices but redirected their attention to the road as braking commenced or when audible alert is activated (Activity C). In normal braking, head acceleration was consistent for Activity A across both the "with alert" and "without alert" conditions, however, for Activity C the head acceleration was lower when the alert was present. In the normal braking "with alert" condition, head acceleration values for Activities A and C were similar, in contrast, under the "without alert" condition, Activity C led to higher head acceleration compared to Activity A and B.

Both Figure 20 andFigure 21 illustrate the head acceleration (in g) experienced by occupants under three different activities: Activity A, Activity B, and Activity C. The data is presented for conditions with and without an audible alert. Each panel shows the distribution of head acceleration values, with individual data points overlaid. The coloured regions represent the confidence intervals, with red indicating the "with alert" condition and yellow indicating the "without alert" condition. The black line and the asterisk within the distributions indicate the median and mean values, respectively, for each condition. Figure 20 shows these data for strong and emergency braking, while Figure 21 presents the results for normal braking.

ANOVA analysis shows that the braking intensity has a significant effect on the head acceleration ($p<10^{-5}$), and that individual participant notably influences head acceleration under uniform conditions ($p = 0.0016$). In addition, the combined effect of the audible alert and braking intensity on head acceleration is statistically significant ($p = 0.0206$). This implies that the impact of braking intensity on head acceleration is dependent upon the presence of an audible alert before the braking event.

Table 6: Median and interquartile range of normal head acceleration across different braking intensities and activities: Comparison between conditions with and without audible alert. Activity: (A) looking at the road; (B) using devices such as a phone; (C) using devices before braking and then looking at the road when braking starts or when audible alert is activated.

Braking intensity	Activity	With Alert	Without alert
		Median [1st; 3rd quartile] (g)	Median [1st; 3rd quartile] (g)
Strong	A	**0.68 [0.55 ; 0.74]**	**0.43 [0.36 ; 0.52]**
	B	**Never occurred**	**0.4 [0.32 ; 0.52]**
	C	**Never occurred**	**0.49 [0.42 ; 0.86]**
Normal	A	**0.31 [0.27 ; 0.37]**	**0.32 [0.25 ; 0.37]**
	B	**Never occurred**	**0.32 [0.29 ; 0.42]**
	C	**0.33 [0.26 ; 0.38]**	**0.43 [0.29 ; 0.47]**
Emergency	A	**0.97 [0.89 ; 1.1]**	**Never occurred**

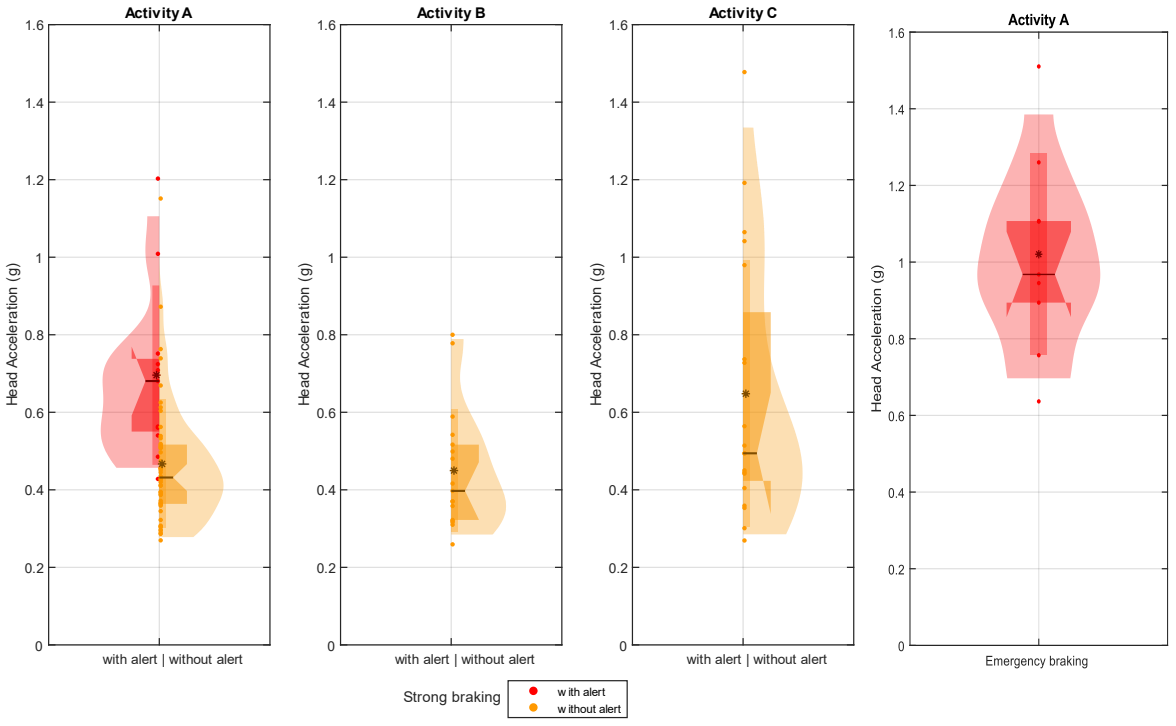

Figure 20: Head acceleration during Strong braking across different activities with and without audible alert, and Emergency braking (right) with audible alert. Activity: (A) looking at the road; (B) using devices such as a phone; (C) using devices before braking and then looking at the road when braking starts or when audible alert is activated.

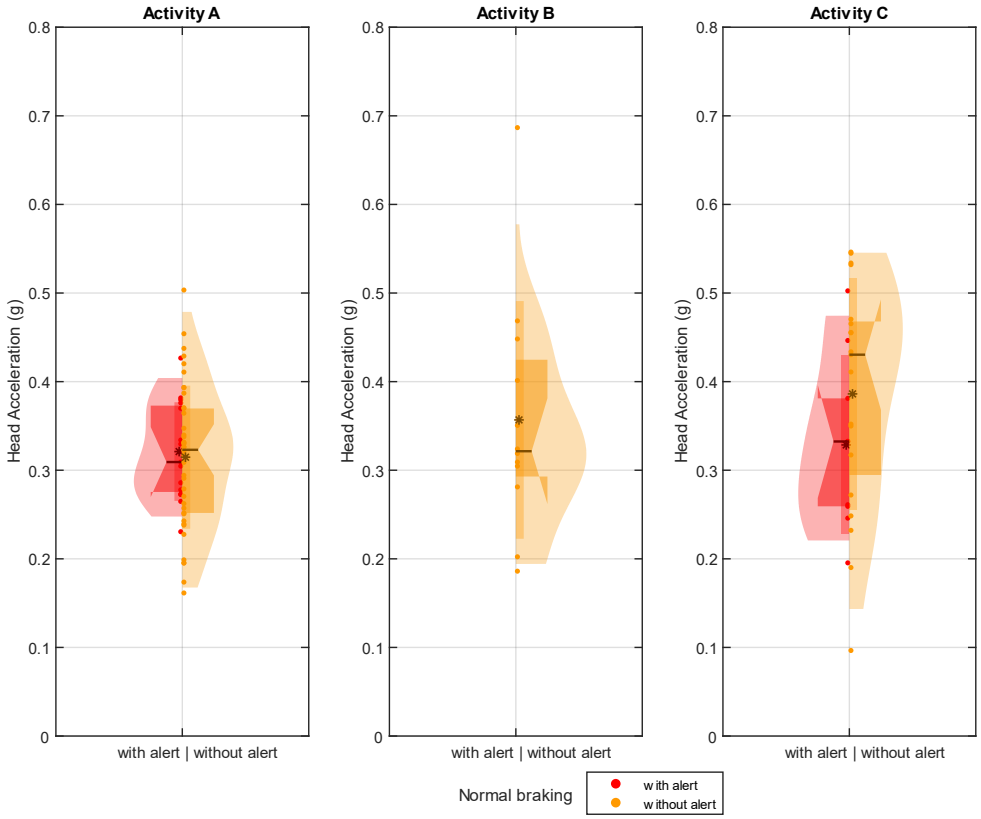

Figure 21: Head acceleration during normal braking across different activities with and without audible alert. Activity: (A) looking at the road; (B) using devices such as a phone; (C) using devices before braking and then looking at the road when braking starts or when audible alert is activated.

3.1.2. Head Pitch Rotation

Table 7 presents the median and interquartile range [1st quartile; 3rd quartile] of head rotation angles (in degrees) during various occupant activities under different braking intensities (Strong, Normal, Emergency). Data are compared between scenarios with and without an audible alert. "Never occurred" indicates that the specific condition was not observed during the experiment. This is because occupants were free to interact with the vehicle as they wished during the experiment, which resulted in some activities not occurring during certain braking events. For strong braking, head pitch rotation was greater in the "with alert" condition when the occupants focused on the road throughout braking (Activity A), compared to when no alert was given. In the absence of an alert, the head pitch rotation was almost the same for Activity B (engaging with a device) and Activity A, with the highest head pitch rotation was observed during Activity C (occupant shifted attention from using a device to focusing on the road during braking or when audible alert is activated). Under normal braking, head pitch rotation for Activity A and C was slightly lower in the "with alert" condition than without it. In the "with alert" condition, Activity C exhibited a larger head pitch rotation compared to Activity A, while in the "without alert" condition, the highest head pitch rotation was observed during Activity C, while the lowest rotation occurred in Activity B (engaging with a device).

Both Figure 22 and Figure 23 illustrate the head pitch rotation (in degrees) experienced by occupants under three different activities: Activity A, Activity B, and Activity C. The data is presented for conditions with and without an audible alert. Each panel shows the distribution of head acceleration values, with individual data points overlaid. The coloured regions represent the confidence intervals, with red indicating the "with alert" condition and yellow indicating the "without alert" condition. The black line and the asterisk within the distributions indicate the median and mean values, respectively, for each condition. Figure 22 shows these data for strong and emergency braking, while Figure 23 presents the results for normal braking.

The n-way ANOVA analysis here revealed no statistically significant differences among the groups.

Table 7: Median and interquartile range of head pitch rotation angle across different braking intensities and activities: Comparison between conditions with and without audible alert. Activity: (A) looking at the road; (B) using devices such as a phone; (C) using devices before braking and then looking at the road when braking starts or when audible alert is activated.

Braking intensity	Activity	With alert	Without alert
		Median [1st; 3rd quartile] (degrees)	Median [1st; 3rd quartile] (degrees)
Strong	A	**8.3 [4.4 ; 9.3]**	**6.4 [4.7 ; 10.6]**
	B	**Never occurred**	**6.8 [4 ; 8.5]**
	C	**Never occurred**	**14.77 [6.6 ; 17.5]**
Normal	A	**6.2 [3.8 ; 7.8]**	**7.7 [5.1 ; 10.8]**
	B	**Never occurred**	**4.6 [2.1 ; 7.6]**
	C	**10.6 [10.2 ; 13.3]**	**11.3 [6 ; 13.6]**
Emergency	A	**11.3 [9.7 ; 12.7]**	**Never occurred**

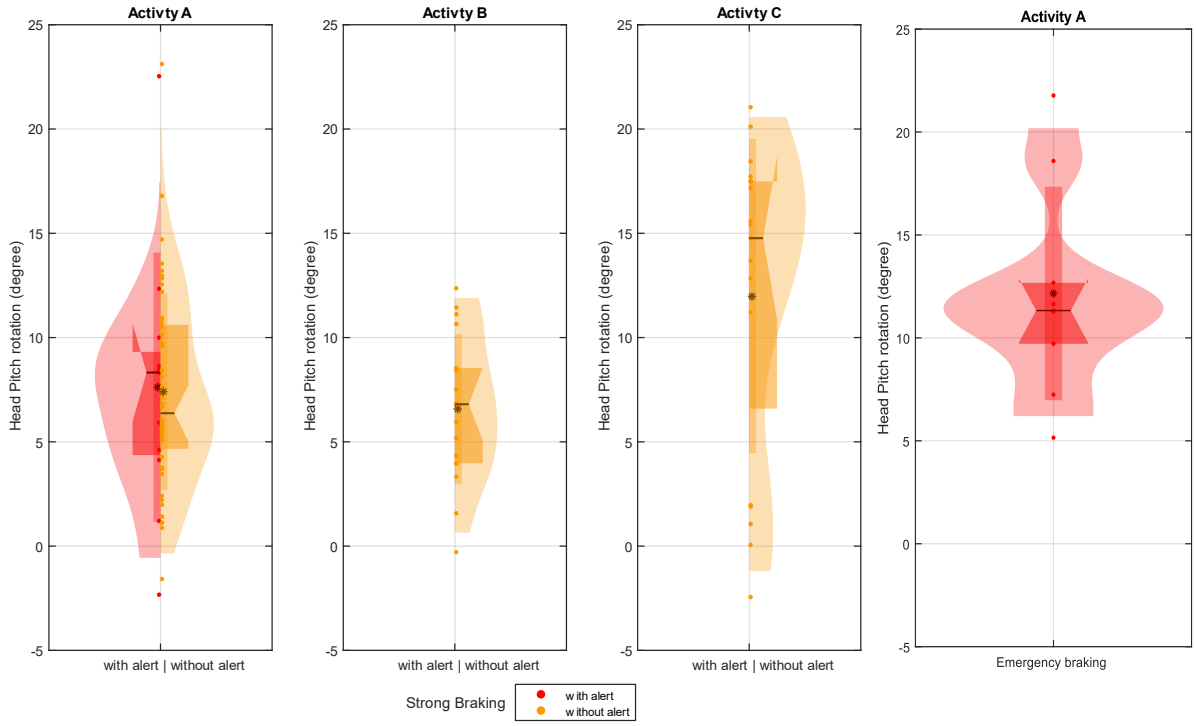

Figure 22: Head pitch rotation during Strong braking across different activities with and without audible alert, and Emergency braking (right) with activity A. Activity: (A) looking at the road; (B) using devices such as a phone; (C) using devices before braking and then looking at the road when braking starts or when audible alert is activated.

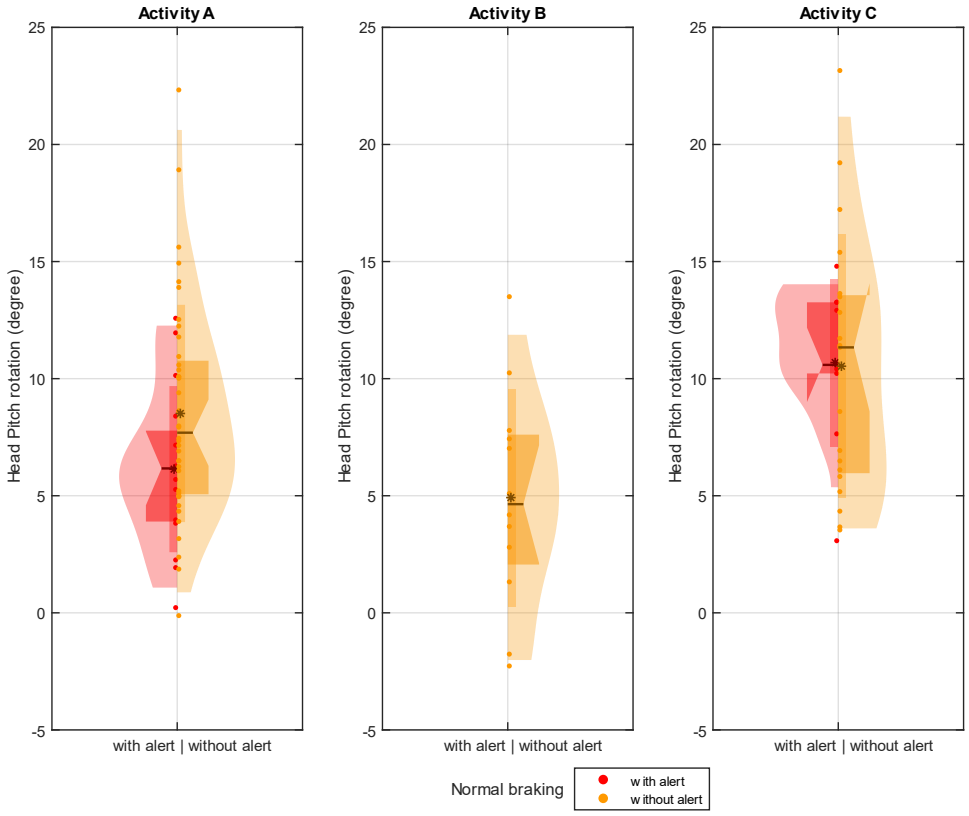

Figure 23: Head pitch rotation during normal braking across different activities with and without audible alert. Activity: (A) looking at the road; (B) using devices such as a phone; (C) using devices before braking and then looking at the road when braking starts or when audible alert is activated.

3.1.3. EMG of SCM Muscle

Table 8 systematically compares the occurrence rates of muscle activation across different braking scenarios and conditions, highlighting the relationship between occupant activity and muscle activation patterns observed through EMG recordings. On the first column, the first letter of each cell denotes the occupant's activity during the recorded event: (A) looking at the road; (B) using a device, such as a phone; (C) using a device before the event, then looking at the road when event begins or when audible alert is activated. The combination of a letter and a number following the activity letter represents the observed physiological response: M0 indicates the absence of muscle activation, M1 denotes muscle activation during or after the event, and M2 signifies muscle activation occurring twice: first, right after the audible alert, and again during or after the event. Table 8 highlights the impact of alert presence on the occurrence rates during emergency, strong, and normal braking scenarios under various experimental conditions. Figure 24 displays the percentage distribution of SCM muscle activation occurrences across different braking intensities (Emergency, Strong, Normal) and the presence or absence of an audible alert. The x-axis corresponds to the first column of Table 8, with each bar representing a specific combination of occupant activity and the associated muscle activation response. The most occurrent condition observed was A_M1, where occupant experienced a muscle activation during or after the event when looking at the road.

ANOVA analysis shows that the combined effect of participant and the presence of audible alert on SCM muscle activation is statistically significant ($p = 0.008$). This suggests that the influence of alert on muscle activation depends on individual occupants.

Table 8: *Occupant activity and muscle response in relation to braking intensity (with and without an alert): occurrence distribution of muscle activation patterns across various braking scenarios and occupant activity*. On the first column, the first letter of each cell denotes the occupant's activity during the recorded event: (A) looking at the road; (B) using a device, such as a phone; (C) using a device before the event or when audible alert is activated, then looking at the road when event begins. The combination of a letter and a number following the activity letter represents the observed physiological response: M0 indicates the absence of muscle activation, M1 denotes muscle activation during or after the event, and M2 signifies muscle activation occurring twice: first, right after the audible alert, and again during or after the event.

Occupant activity and Muscle Response over the total occurrence (204)	Occurrence	Emergency braking with alert	Strong braking with alert	Normal braking with alert	Strong braking without alert	Normal braking without alert
A_M0	24	**0**	**0**	**3**	**10**	**11**
A_M1	34	**2**	**3**	**2**	**15**	**12**
A_M2	9	**2**	**3**	**3**	**1**	**0**
B_M0	3	**0**	**0**	**0**	**2**	**1**
B_M1	3	**0**	**0**	**0**	**1**	**2**
C_M0	12	**0**	**0**	**2**	**4**	**6**
C_M1	10	**0**	**0**	**1**	**5**	**4**
C_M2	2	**2**	**0**	**0**	**0**	**0**
Noisy data	107	**N/A**	**N/A**	**N/A**	**N/A**	**N/A**

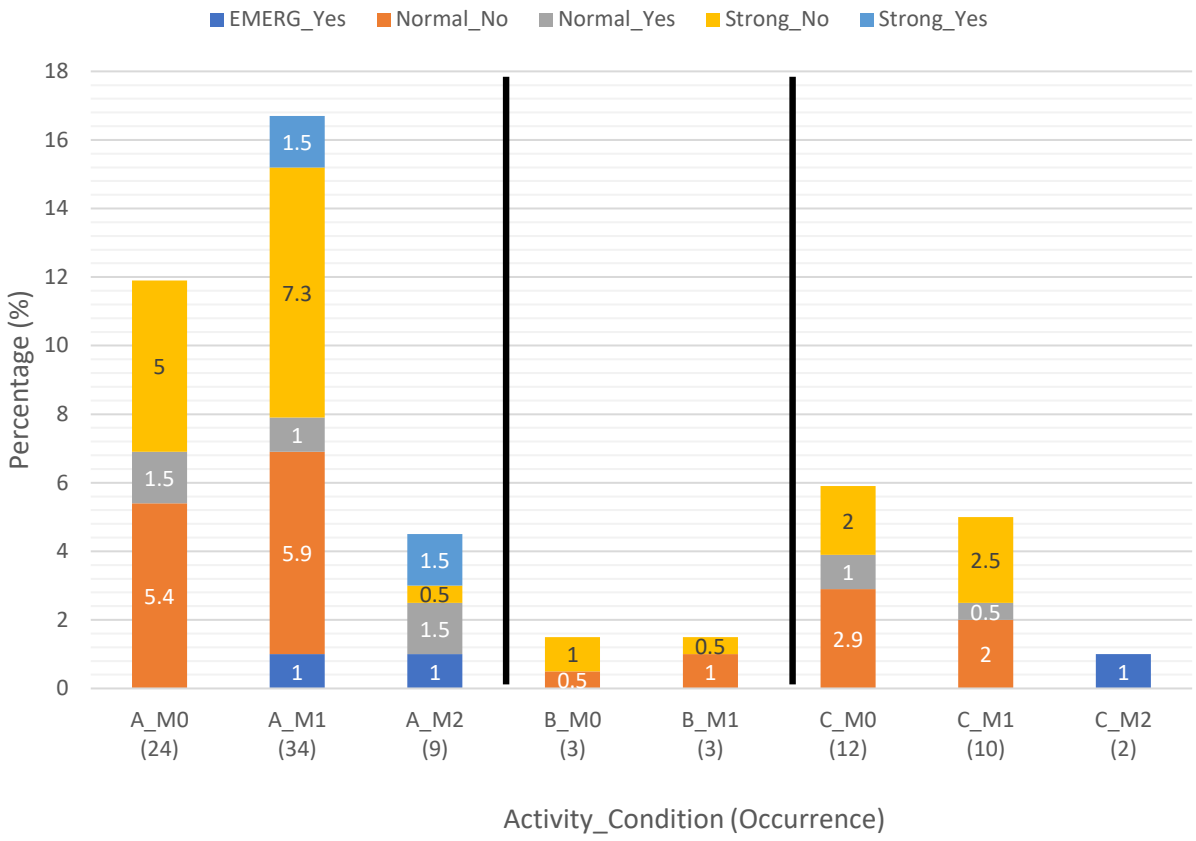

Figure 24: ***Proportion of Sternocleidomastoid (SCM) Muscle Activation Occurrences Categorized by Braking Intensity and Presence of Audible Alert.*** **The colors represent different braking intensities: Emergency, Strong, and Normal. The presence ("yes") or absence ("no") of an audible alert is indicated by labels such as Strong_yes and Strong_No. On the x-axis, the first letter of each bar denotes the occupant's activity during the recorded event: (A) looking at the road; (B) using a device, such as a phone; (C) using a device before braking, then looking at the road when braking begins or when audible alert is activated. The combination of a letter and a number following the activity letter represents the observed physiological response: M0 indicates the absence of muscle activation, M1 denotes muscle activation during or after the event, and M2 signifies muscle activation occurring twice: first, right after the audible alert, and again during or after the event. The number within parentheses indicates the frequency of occurrence for that specific condition represented by each bar.**

3.1.4. Change in Respiration Frequency

Table 9 systematically compares the occurrence rates of changes in respiration frequency across different braking scenarios and conditions, highlighting the relationship between occupant activity and respiration frequency patterns observed through respiration recordings. On the first column, the first letter of each cell denotes the occupant's activity during the recorded event: (A) looking at the road; (B) using a device, such as a phone; (C) using a device before the event, then looking at the road when event begins or when audible alert is activated. The combination of a letter and a number following the activity letter represents the observed physiological response: R0 indicates the absence of respiration frequency change after the event, and R1 denotes respiration frequency change after the event. This table highlights the impact of alert presence on the occurrence rates during emergency, strong, and normal braking scenarios under various experimental conditions. Figure 25 illustrates the percentage

distribution of changes in respiration frequency across varying braking intensities (Emergency, Strong, Normal) under conditions with and without an audible alert. The x-axis corresponds to the first column of Table 9, with each bar representing a specific combination of occupant activity and the associated change in respiration frequency response. For each activity (A, B, C), the occurrence of no change in respiration frequency consistently exceeded the occurrence of respiration frequency variability.

The n-way ANOVA analysis here revealed no statistically significant differences among the groups.

Table 9: *Occupant activity and change in respiration frequency in relation to braking intensity (with and without an alert): occurrence distribution of change in respiration frequency patterns across various braking scenarios and occupant activity*. On the first column, the first letter of each cell denotes the occupant's activity during the recorded event: (A) looking at the road; (B) using a device, such as a phone; (C) using a device before the event, then looking at the road when event begins or when audible alert is activated. The combination of a letter and a number following the activity letter represents the observed physiological response: R0 indicates the absence of respiration frequency change after the event, and R1 denotes respiration frequency change after the event.

Occupant activity and change in respiration frequency over the total occurrence (204)	Occurrence	Emergency braking Wirth alet	Strong braking with alert	Normal braking with alert	Strong braking without alert	Normal braking without alert
A_R0	77	**2**	**3**	**6**	**35**	**31**
A_R1	47	**7**	**8**	**9**	**13**	**10**
B_R0	21	**0**	**0**	**0**	**12**	**9**
B_R1	8	**0**	**0**	**0**	**5**	**3**
C_R0	38	**1**	**1**	**6**	**14**	**16**
C_R1	13	**2**	**0**	**3**	**5**	**3**

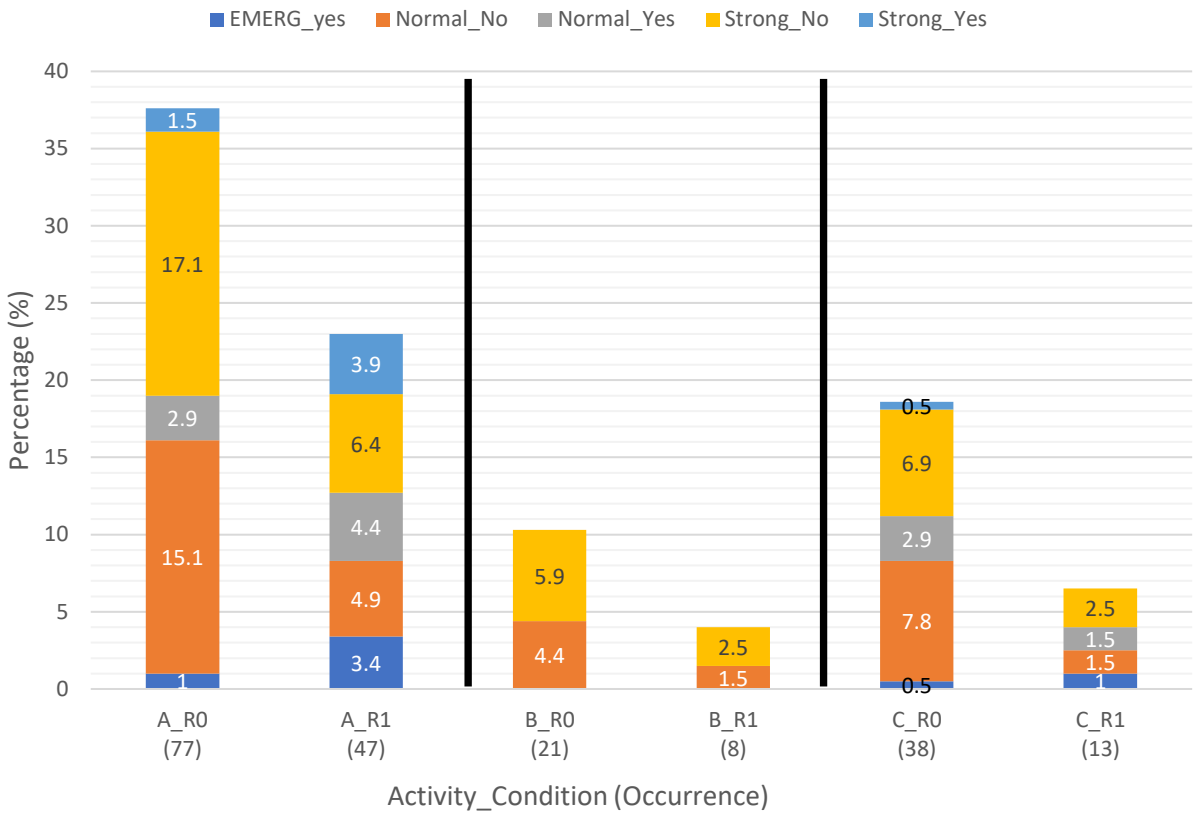

Figure 25: ***Proportion of Change in Respiration Frequency Categorized by Braking Intensity and Presence of Audible Alert.*** **The colors represent different braking intensities: Emergency, Strong, and Normal. The presence ("yes") or absence ("no") of an audible alert is indicated by labels such as Strong_yes and Strong_No. On the x-axis, the first letter of each bar denotes the occupant's activity during the recorded event: (A) looking at the road; (B) using a device, such as a phone; (C) using a device before braking, then looking at the road when braking begins or when audible alert is activated. The combination of a letter and a number following the activity letter represents the observed physiological response: R0 indicates the absence of respiration frequency change after the event, and R1 denotes respiration frequency change after the event. The number within parentheses indicates the frequency of occurrence for that specific condition represented by each bar.**

3.1.5. Heart Rate

Table 10 systematically compares the occurrence rates of heart rate changes across different braking scenarios and conditions, highlighting the relationship between occupant activity and heart rate changes observed. On the first column, the first letter of each cell denotes the occupant's activity during the recorded event: (A) looking at the road; (B) using a device, such as a phone; (C) using a device before the event, then looking at the road when event begins or when audible alert is activated. The combination of a letter and a number following the activity letter represents the observed physiological response: H-1 indicates heart rate less than (Mean at rest) -SD during/after the event, H0 denotes heart rate within (Mean at rest) +SD and (Mean at rest) -SD during and after the event, and H1 signifies heart rate is higher than the (Mean at rest) +SD during and after the event. Table 10 highlights the impact of alert presence on the occurrence rates during emergency, strong, and normal braking scenarios under various experimental conditions. Figure 26 displays the percentage distribution of heart rate changes

occurrences across different braking intensities (Emergency, Strong, Normal) and the presence or absence of an audible alert. The x-axis corresponds to the first column of Table 10, with each bar representing a specific combination of occupant activity and the associated heart rate response. For each activity (A, B, C), the occurrence of “no change in heart” rate consistently exceeded the occurrence of “heart rate variability”.

The n-way ANOVA analysis here revealed no statistically significant differences among the groups.

Table 10: ***Occupant activity and heart rate in relation to braking intensity (with and without an alert): occurrence distribution of heart rate patterns across various braking scenarios and occupant activity.*** **On the first column, the first letter of each cell denotes the occupant's activity during the recorded event: (A) looking at the road; (B) using a device, such as a phone; (C) using a device before the event or when audible alert is activated, then looking at the road when event begins. The combination of a letter and a number following the activity letter represents the observed physiological response: H-1 indicates heart rate less than (Mean at rest) -SD during/after the event, H0 denotes heart rate within (Mean at rest) +SD and (Mean at rest) -SD during and after the event, and H1 signifies heart rate is higher than the (Mean at rest) +SD during and after the event.**

Occupant activity and Heart rate over the total occurrence (204)	Occurrence	Emergency braking Wirth alet	Strong braking with alert	Normal braking with alert	Strong braking without alert	Normal braking without alert
A_H-1	14	**1**	**2**	**2**	**2**	**7**
A_H0	64	**7**	**7**	**8**	**27**	**15**
A_H1	46	**1**	**2**	**5**	**19**	**19**
B_H-1	4	**0**	**0**	**0**	**1**	**3**
B_H0	15	**0**	**0**	**0**	**9**	**6**
B_H1	10	**0**	**0**	**0**	**7**	**3**
C_H-1	11	**1**	**0**	**0**	**5**	**5**
C_H0	29	**2**	**0**	**7**	**9**	**11**
C_H1	11	**0**	**1**	**2**	**5**	**3**

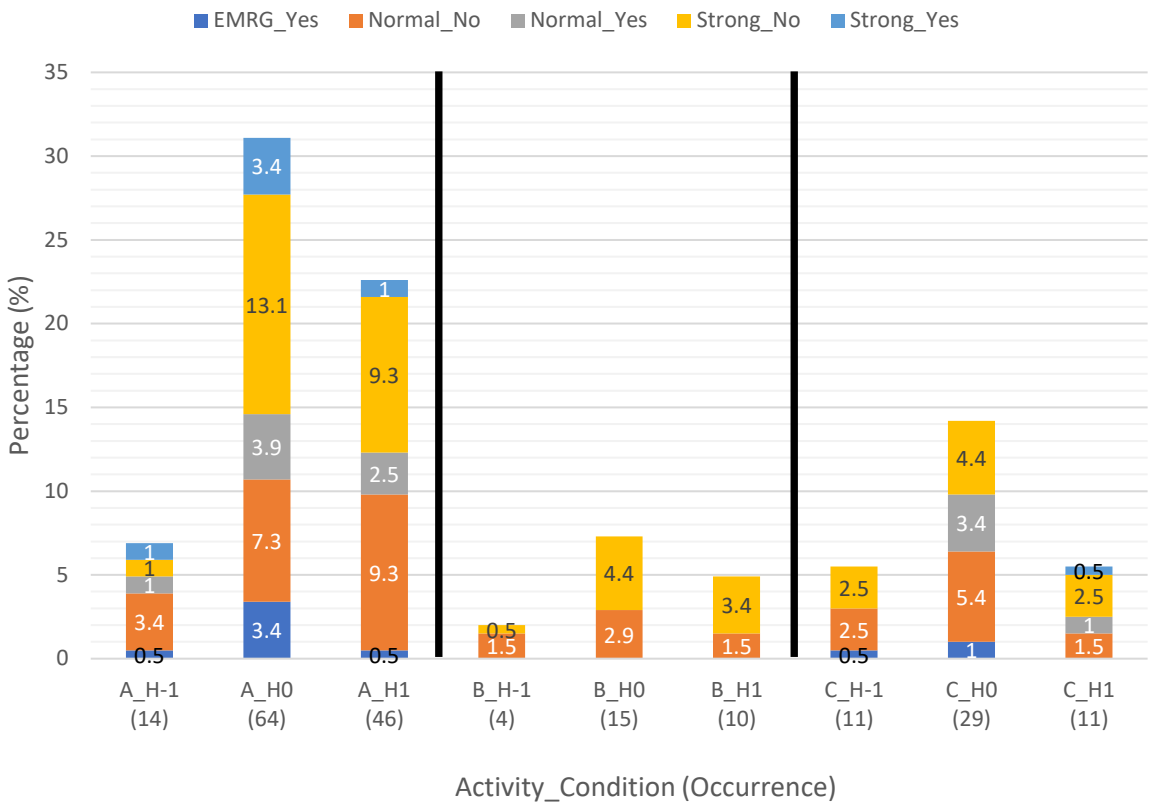

Figure 26: ***Proportion of Heart Rate Categorized by Braking Intensity and Presence of Audible Alert.*** **The colors represent different braking intensities: Emergency, Strong, and Normal. The presence ("yes") or absence ("no") of an audible alert is indicated by labels such as Strong_yes and Strong_No. On the x-axis, the first letter of each bar denotes the occupant's activity during the recorded event: (A) looking at the road; (B) using a device, such as a phone; (C) using a device before braking, then looking at the road when braking begins or when audible alert is activated. The combination of a letter and a number following the activity letter represents the observed physiological response: H-1 indicates heart rate less than (Mean at rest) -SD during/after the event, H0 denotes heart rate within (Mean at rest) +SD and (Mean at rest) -SD during and after the event, and H1 signifies heart rate is higher than the (Mean at rest) +SD during and after the event. The number within parentheses indicates the frequency of occurrence for that specific condition represented by each bar.**

3.2. Lane-Changing

During this category of events there was no audible alert.

3.2.1. Head Acceleration

Table 11 presents the median and interquartile range [1st quartile; 3rd quartile] of normal head acceleration (in g) during various occupant activities under different braking intensities (Strong, Normal). Data are presented in scenarios without an audible alert. "Never occurred" indicates that the specific condition was not observed during the experiment. This is because occupants were free to interact with the vehicle as they wished during the experiment, which resulted in some activities not occurring during certain lane changing events. Under strong lane changing conditions, the head acceleration was higher when occupants initially used devices but redirected their attention to the road as lane changing commenced (Activity C), compared to when they focused on the road throughout the event (Activity A). Under normal lane changing intensity, there was no significant difference between all three occupants' activities.

Figure 27 illustrates the head acceleration (in g) experienced by occupants under three different activities: Activity A (looking at the road), Activity B (using a device, such as a phone), and Activity C (using a device before braking, then looking at the road when braking begins). The data is presented for lane changing events without an audible alert. Each panel shows the distribution of head acceleration values, with individual data points overlaid. The colored regions represent the confidence intervals, with blue indicating the "Normal Lane changing" condition and green indicating the "Strong Lane changing" condition. The black line and the asterisk within the distributions indicate the median and mean values, respectively, for each condition.

The n-way ANOVA analysis here revealed no statistically significant differences among the groups.

Table 11: Median and interquartile range of normal head acceleration across different lane changing intensities and activities without audible alert. Activity: (A) looking at the road; (B) using devices such as a phone; (C) using devices before the maneuver and then looking at the road when the maneuver starts.

Lane changing intensity	Activity	Median [1st; 3rd quartile] (g)
Strong	A	**0.44 [0.42 ; 0.51]**
	B	**Never Occurred**
	C	**0.51 [0.49 ; 0.53]**
Normal	A	**0.26 [0.22 ; 0.3]**
	B	**0.25 [0.2 ; 0.27]**
	C	**0.28 [0.15 ; 0.37]**

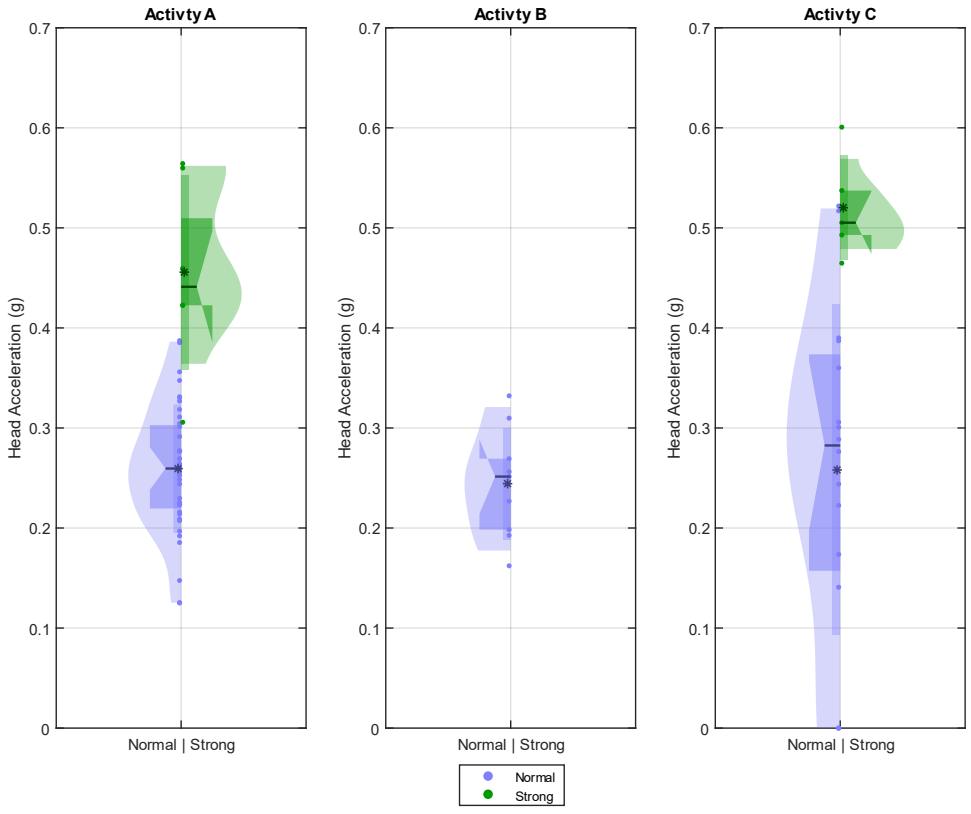

Figure 27: Head acceleration during Strong (green) and Normal (blue) lane changing across different activities without audible alert. Activity: (A) looking at the road; (B) using devices such as a phone; (C) using devices before the maneuver and then looking at the road when the maneuver starts.

3.2.2. Head Pitch Rotation

Table 12 presents the median and interquartile range [1st quartile; 3rd quartile] of head rotation angles (in degrees) during various occupant activities under different lane-changing intensities (Strong, Normal). "Never occurred" indicates that the specific condition was not observed during the experiment. Under strong lane changing, there was no significant difference in head pitch rotation between occupant activities. For normal lane changing, head pitch rotation was greater when occupants shifted their attention from using a device to focusing on the road (Activity C), compared to when they remained focused on the road throughout the maneuver (Activity A). The lowest head pitch rotation occurred when occupants were engaged with a device during the event (Activity B).

Figure 28 illustrates the head pitch rotation (in degrees) experienced by occupants under three different activities: Activity A, Activity B, and Activity C. The data is presented for lane changing events without an audible alert. Each panel shows the distribution of head pitch rotation values, with individual data points overlaid. The colored regions represent the confidence intervals, with blue indicating the "Normal Lane changing" condition and green indicating the "Strong Lane changing" condition. The black line and the asterisk within the distributions indicate the median and mean values, respectively, for each condition.

The n-way ANOVA analysis herhe revealed no statistically significant differences among the groups.

Table 12: Median and interquartile head range of pitch rotation across different lane changing intensities and activities without audible alert. Activity: (A) looking at the road; (B) using devices such as a phone; (C) using devices before the maneuver and then looking at the road when the maneuver starts.

Lane changing intensity	Activity	Median [1st; 3rd quartile] (degree)
Strong	A	**8.4 [6.5 ; 10.9]**
	B	**Never Occurred**
	C	**7.7 [1.7 ; 9.6]**
Normal	A	**5.1 [3.4 ; 6.7]**
	B	**2.6 [1.2 ; 4.2]**
	C	**8.2 [3.8 ; 13.3]**

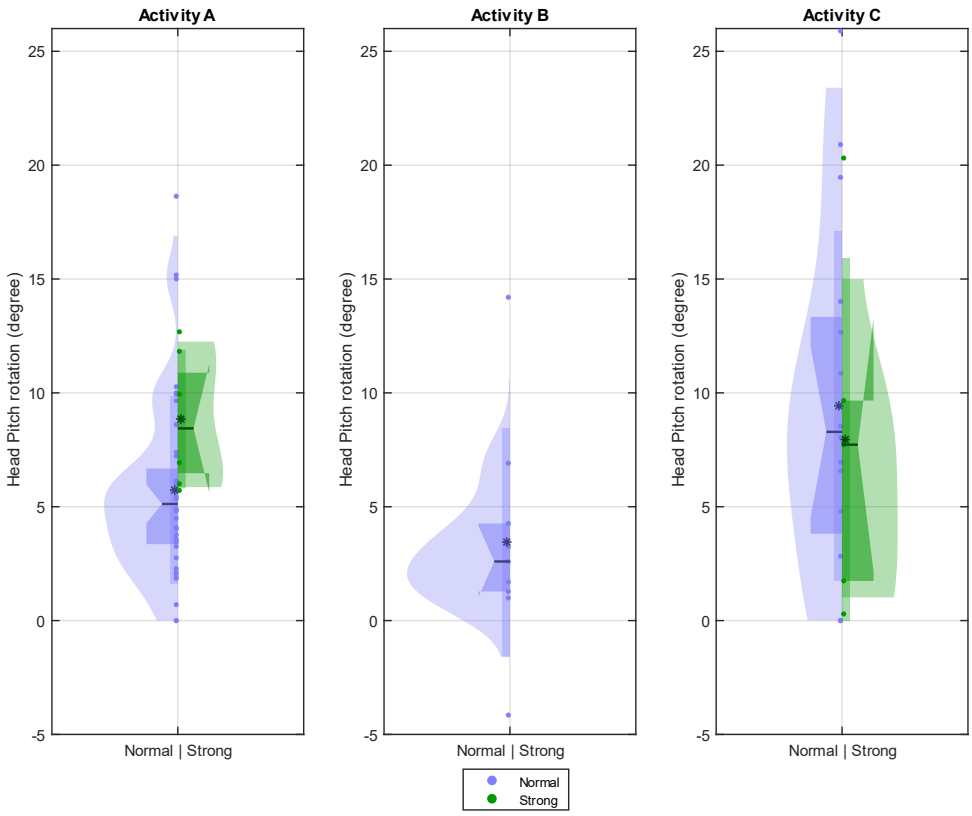

Figure 28: Head pitch rotation during Strong (green) and Normal (blue) lane changing across different activities without audible alert. Activity: (A) looking at the road; (B) using devices such as a phone; (C) using devices before the maneuver and then looking at the road when the maneuver starts.

3.2.3. EMG of SCM Muscle

Table 13 systematically compares the occurrence rates of muscle activation across different lane changing scenarios and conditions, highlighting the relationship between occupant activity and muscle activation patterns observed through EMG recordings. On the first column, the first letter of each cell denotes the occupant's activity during the recorded event: (A) looking at the road; (B) using a device, such as a phone; (C) using a device before the event, then looking at the road when event begins. The combination of a letter and a number following the activity letter represents the observed physiological response: M0 indicates the absence of muscle activation, M1 denotes muscle activation during or after the event, and M2 signifies double muscle activation occurring both before and during or after the event. Figure 29 displays the percentage distribution of SCM muscle activation occurrences across different lane changing intensities (Strong, Normal). The x-axis corresponds to the first column of Table 13, with each bar representing a specific combination of occupant activity and the associated muscle activation response. The two most frequently observed conditions were A_M0, followed by A_M1.

ANOVA analysis shows that the participant term signifies statistical significance ($p = 0.0101$). This suggests that each individual participant notably influences muscle activation under uniform conditions.

Table 13: *Occupant activity and muscle response in relation to lane changing intensity (without an alert): occurrence distribution of muscle activation patterns across various lane-changing scenarios and occupant activity.* On the first column, the first letter of each cell denotes the occupant's activity during the recorded event: (A) looking at the road; (B) using a device, such as a phone; (C) using a device before the maneuver, then looking at the road when the maneuver begins. The combination of a letter and a number following the activity letter represents the observed physiological response: M0 indicates the absence of muscle activation, M1 denotes muscle activation during or after the event, and M2 signifies double muscle activation occurring both before and during or after the event.

Occupant activity and Muscle Response over the total occurrence (72)	Occurrence	Strong Lane-changing without alert	Normal Lane-changing without alert
A_M0	13	**0**	**13**
A_M1	11	**3**	**8**
A_M2	0	**0**	**0**
B_M0	0	**0**	**0**
B_M1	0	**0**	**0**
C_M0	5	**1**	**4**
C_M1	2	**1**	**1**
C_M2	1	**1**	**0**
Noisy data	40	**N/A**	**N/A**

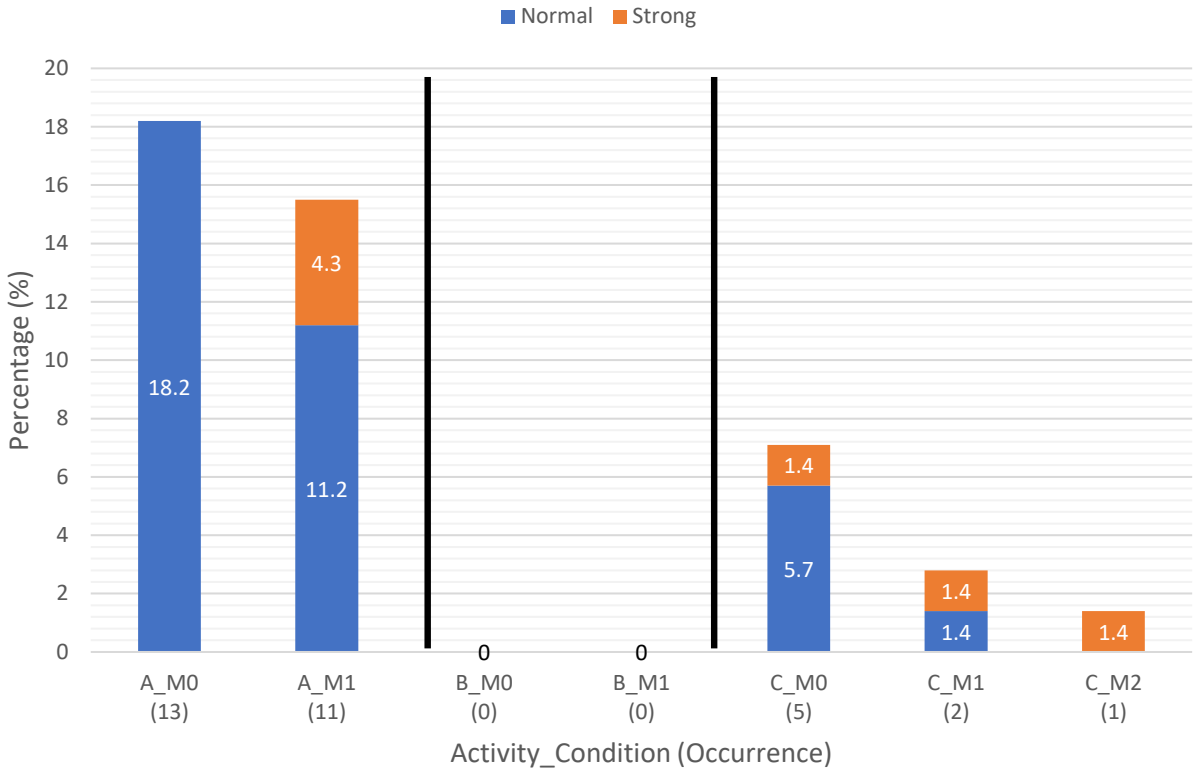

Figure 29: ***Proportion of Sternocleidomastoid (SCM) Muscle Activation Occurrences Categorized by Lane-Changing Intensity.*** **The colors represent different braking intensities: Strong, and Normal. On the x-axis, the first letter of each bar denotes the occupant's activity during the recorded event: (A) looking at the road; (B) using a device, such as a phone; (C) using a device before the maneuver, then looking at the road when the maneuver begins. The combination of a letter and a number following the activity letter represents the observed physiological response: M0 indicates the absence of muscle activation, and M1 denotes muscle activation during or after the maneuver, and M2 signifies double muscle activation occurring both before and during or after the maneuver. The number within parentheses indicates the frequency of occurrence for that specific condition represented by each bar**

3.2.4. Change in Respiration Frequency

Table 14 systematically compares the occurrence rates of changes in respiration frequency across different lane changing intensities, highlighting the relationship between occupant activity and respiration frequency patterns observed through respiration recordings. On the first column, the first letter of each cell denotes the occupant's activity during the recorded event: (A) looking at the road; (B) using a device, such as a phone; (C) using a device before the event, then looking at the road when event begins. The combination of a letter and a number following the activity letter represents the observed physiological response: R0 indicates the absence of respiration frequency change after the event, and R1 denotes respiration frequency change after the event. This table highlights the impact of strong, and normal lane changing scenarios without audible alert. Figure 30 illustrates the percentage distribution of changes in respiration frequency across varying lane changing intensities (Strong, Normal) without an audible alert. The x-axis corresponds to the first column of Table 14, with each bar representing a specific combination of occupant activity and the associated change in respiration

frequency response. For each activity (A, B, C), the occurrence of no change in respiration frequency consistently exceeded the occurrence of respiration frequency variability, though the majority of strong lane change events resulted in a change in respiration frequency.

The n-way ANOVA analysis revealed no statistically significant differences among the groups.

Table 14: *Occupant activity and change in respiration frequency in relation to lane changing intensity (without an alert): occurrence distribution of change in respiration frequency patterns across various lane-changing scenarios and occupant activity*. On the first column, the first letter of each cell denotes the occupant's activity during the recorded event: (A) looking at the road; (B) using a device, such as a phone; (C) using a device before the maneuver, then looking at the road when the maneuver begins. The combination of a letter and a number following the activity letter represents the observed physiological response: R0 indicates the absence of respiration frequency change after the event, and R1 denotes respiration frequency change after the event.

Occupant activity and change in respiration frequency over the total occurrence (72)	Occurrence	Strong Lane changing without alert	Normal Lane changing without alert
A_R0	30	**1**	**29**
A_R1	14	**5**	**9**
B_R0	9	**1**	**8**
B_R1	1	**0**	**1**
C_R0	10	**1**	**9**
C_R1	8	**4**	**4**

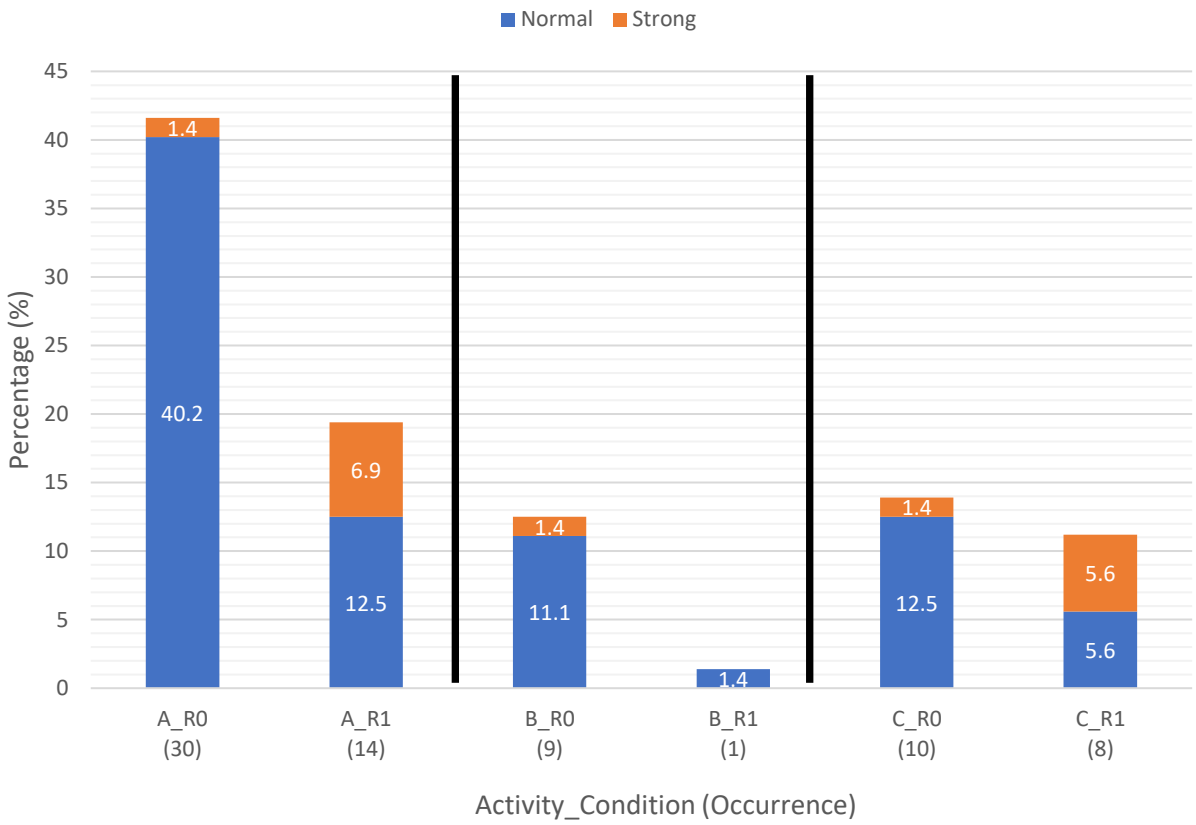

Figure 30: ***Proportion of Change in Respiration Frequency Categorized by Lane-Changing Intensity.*** **The colors represent different braking intensities: Strong, and Normal. On the x-axis, the first letter of each bar denotes the occupant's activity during the recorded event: (A) looking at the road; (B) using a device, such as a phone; (C) using a device before the maneuver, then looking at the road when the maneuver begins. The combination of a letter and a number following the activity letter represents the observed physiological response: R0 indicates the absence of respiration frequency change after the event, and R1 denotes respiration frequency change after the event. The number within parentheses indicates the frequency of occurrence for that specific condition represented by each bar.**

3.2.5. Heart Rate

Table 15 systematically compares the occurrence frequency of heart rate changes across different lane changing intensities, highlighting the relationship between occupant activity and heart rate variability. On the first column, the first letter of each cell denotes the occupant's activity during the recorded event: (A) looking at the road; (B) using a device, such as a phone; (C) using a device before the event, then looking at the road when event begins. The combination of a letter and a number following the activity letter represents the observed physiological response: H-1 indicates heart rate less than (Mean at rest) -SD during/after the event, H0 denotes heart rate within (Mean at rest) +SD and (Mean at rest) -SD during and after the event, and H1 signifies heart rate is higher than the (Mean at rest) +SD during and after the event. Figure 31 displays the percentage distribution of heart rate changes occurrences across different lane changing intensities (Strong, Normal) without audible alert. The x-axis corresponds to the first column of Table 15, with each bar representing a specific combination of occupant activity and the associated heart rate response. For activities A and B, the occurrence of no change in heart rate

consistently exceeded the occurrence of heart rate variability. However, in activity C, the occurrence of heart rate changes was slightly more frequent than those of no change.

Table 15: ***Occupant activity and heart rate in relation to lane changing intensity (without an alert): occurrence distribution of heart rate patterns across various lane-changing scenarios and occupant activity.*** **On the first column, the first letter of each cell denotes the occupant's activity during the recorded event: (A) looking at the road; (B) using a device, such as a phone; (C) using a device before the maneuver, then looking at the road when the maneuver begins. The combination of a letter and a number following the activity letter represents the observed physiological response: H-1 indicates heart rate less than (Mean at rest) -SD during/after the maneuver, H0 denotes heart rate within (Mean at rest) +SD and (Mean at rest) -SD during and after the maneuver, and H1 signifies heart rate is higher than the (Mean at rest) +SD during and after the maneuver.**

Occupant activity and Heart rate over the total occurrence (204)	Occurrence	Strong Lane-changing without alert	Normal Lane-changing without alert
A_H-1	8	**1**	**7**
A_H0	23	**3**	**20**
A_H1	13	**2**	**11**
B_H-1	1	**0**	**1**
B_H0	6	**1**	**5**
B_H1	3	**0**	**3**
C_H-1	4	**2**	**2**
C_H0	6	**1**	**5**
C_H1	8	**2**	**6**

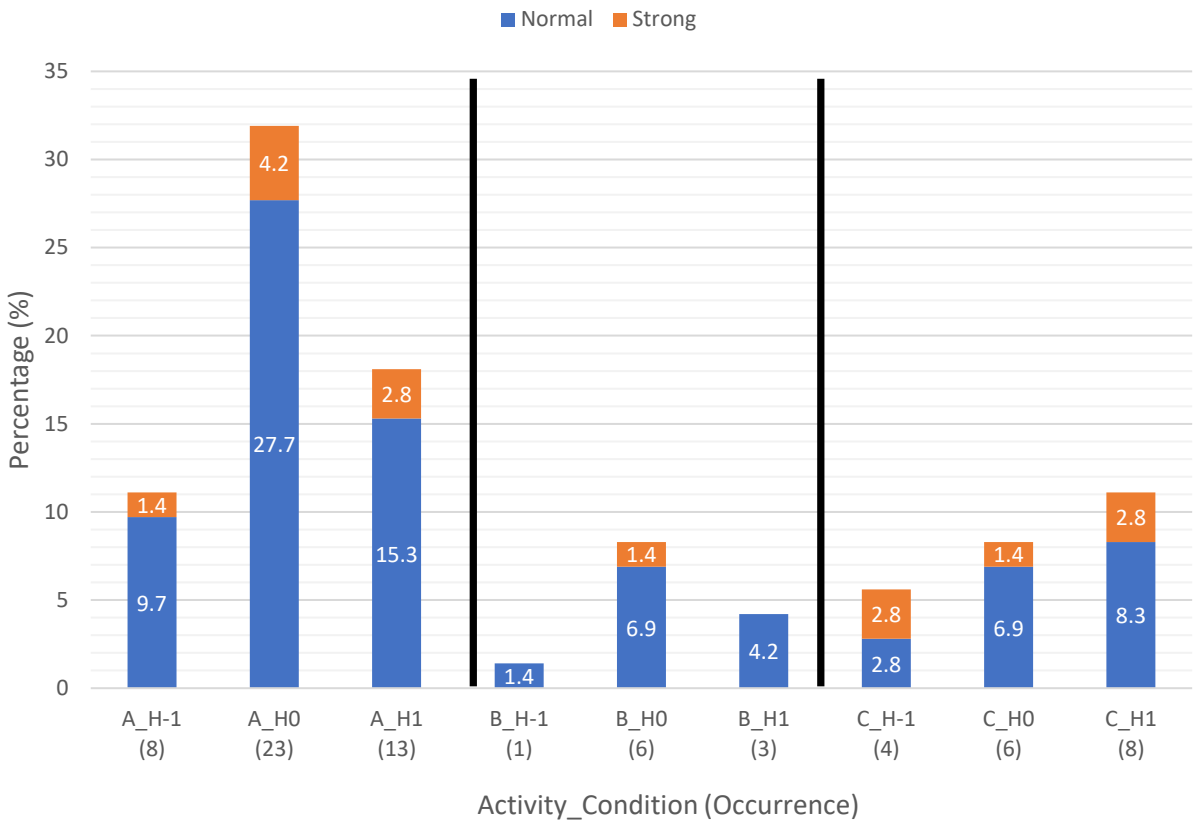

Figure 31: ***Proportion of Heart Rate Categorized by Lane-Changing Intensity.*** **The colors represent different lane-changing intensities: Strong, and Normal. On the x-axis, the first letter of each bar denotes the occupant's activity during the recorded event: (A) looking at the road; (B) using a device, such as a phone; (C) using a device before the maneuver, then looking at the road when the maneuver begins. The combination of a letter and a number following the activity letter represents the observed physiological response: H-1 indicates heart rate less than mean-SD after the maneuver, H0 denotes heart rate within mean+SD and mean-SD during and after the maneuver, and H1 signifies heart rate is higher than the mean+sd during and after the maneuver. The number within parentheses indicates the frequency of occurrence for that specific condition represented by each bar.**

3.3. Ninety Degrees Turning

During this category of events there was no audible alert.

3.3.1. Head Acceleration

Table 16 presents the median and interquartile range [1st quartile; 3rd quartile] of normal head acceleration (in g) during various occupant activities under different turning intensities (Strong, Normal). "Never occurred" indicates that the specific condition was not observed during the experiment. Under strong turning intensity, the head acceleration was lower when occupants initially used devices but redirected their attention to the road as lane changing commenced (Activity C) compared to when they focused on the road throughout the event (Activity A). Under normal turning intensity, head acceleration was greater when occupants shifted their attention from using a device to focusing on the road (Activity C), compared to when they remained focused on the road throughout the maneuver (Activity A). The

lowest head acceleration occurred when occupants were engaged with a device during the event (Activity B).

Figure 32 illustrates the head acceleration (in g) experienced by occupants under three different activities: Activity A (looking at the road), Activity B (using a device, such as a phone), and Activity C (using a device before braking, then looking at the road when braking begins). The data is presented for turning events without an audible alert. Each panel shows the distribution of head acceleration values, with individual data points overlaid. The colored regions represent the confidence intervals, with blue indicating the "Normal turning" condition and green indicating the "Strong turning" condition. The black line and the asterisk within the distributions indicate the median and mean values, respectively, for each condition.

The n-way ANOVA analysis revealed no statistically significant differences among the groups.

Table 16: Median and interquartile range of normal head acceleration across different turning intensities and activities without audible alert. Activity: (A) looking at the road; (B) using devices such as a phone; (C) using devices before the maneuver and then looking at the road when the maneuver starts.

Turning intensity	Activity	Median [1st; 3rd quartile] (g)
Strong	A	**0.82 [0.62 ; 0.9]**
	B	**Never Occurred**
	C	**0.78 [0.74 ; 1.11]**
Normal	A	**0.23 [0.17 ; 0.3]**
	B	**0.19 [0.17 ; 0.21]**
	C	**0.31 [0.28 ; 0.32]**

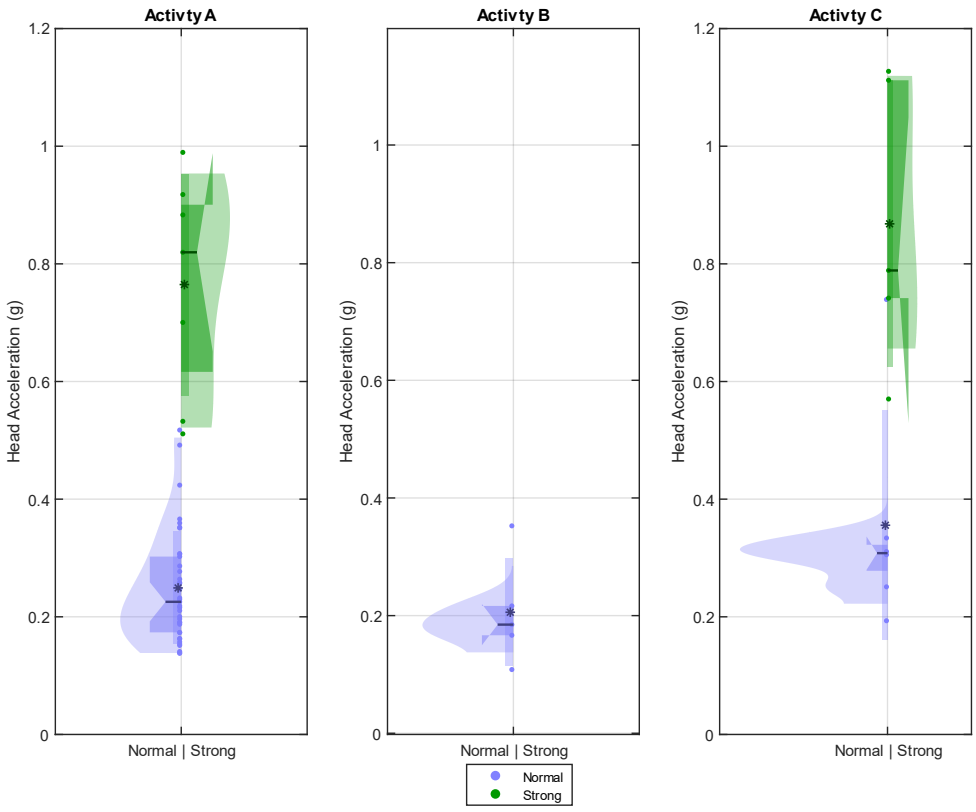

Figure 32: Head acceleration during Strong (green) and Normal (blue) turning across different activities without audible alert. Activity: (A) looking at the road; (B) using devices such as a phone; (C) using devices before the maneuver and then looking at the road when the maneuver starts.

3.3.2. Head Pitch Rotation

Table 17 presents the median and interquartile range [1st quartile; 3rd quartile] of head rotation angles (in degrees) during various occupant activities under different turning intensities (Strong, Normal). "Never occurred" indicates that the specific condition was not observed during the experiment. For strong turning intensity, the head pitch was significantly higher when occupants shifted their attention from using a device to focusing on the road (Activity C), compared to when they remained focused on the road throughout the maneuver (Activity A). Under normal turning intensity, the head pitch rotation was almost the same for Activity B (engaging with a device) and Activity A, with the highest head pitch rotation was observed during Activity C.

Figure 33 illustrates the head pitch rotation (in degrees) experienced by occupants under three different activities: Activity A (looking at the road), Activity B (using a device, such as a phone), and Activity C (using a device before braking, then looking at the road when braking begins). The data is presented for turning events without an audible alert. Each panel shows the distribution of head pitch rotation values, with individual data points overlaid. The colored regions represent the confidence intervals, with blue indicating the "Normal turning" condition and green indicating the "Strong turning" condition. The black line and the asterisk within the distributions indicate the median and mean values, respectively, for each condition.

ANOVA analysis shows that the interaction term between participant and turning intensity meets the criterion of statistical significance ($p = 0.0484$). This suggests that the influence of turning intensity on head pitch varies among participants, implying individualized responses to changes in turning intensity.

Table 17: Median and interquartile range of head pitch rotation across different turning intensities and activities without audible alert. Activity: (A) looking at the road; (B) using devices such as a phone; (C) using devices before the maneuver and then looking at the road when the maneuver starts.

Turning intensity	Activity	Median [1st; 3rd quartile] (degrees)
Strong	A	**1.7 [0.6 ; 5.9]**
	B	**Never Occurred**
	C	**6.3 [0.47 ; 12.3]**
Normal	A	**5.1 [2.5; 8.2]**
	B	**5.3 [3.7 ; 8.2]**
	C	**14.4 [9.9 ; 15.6]**

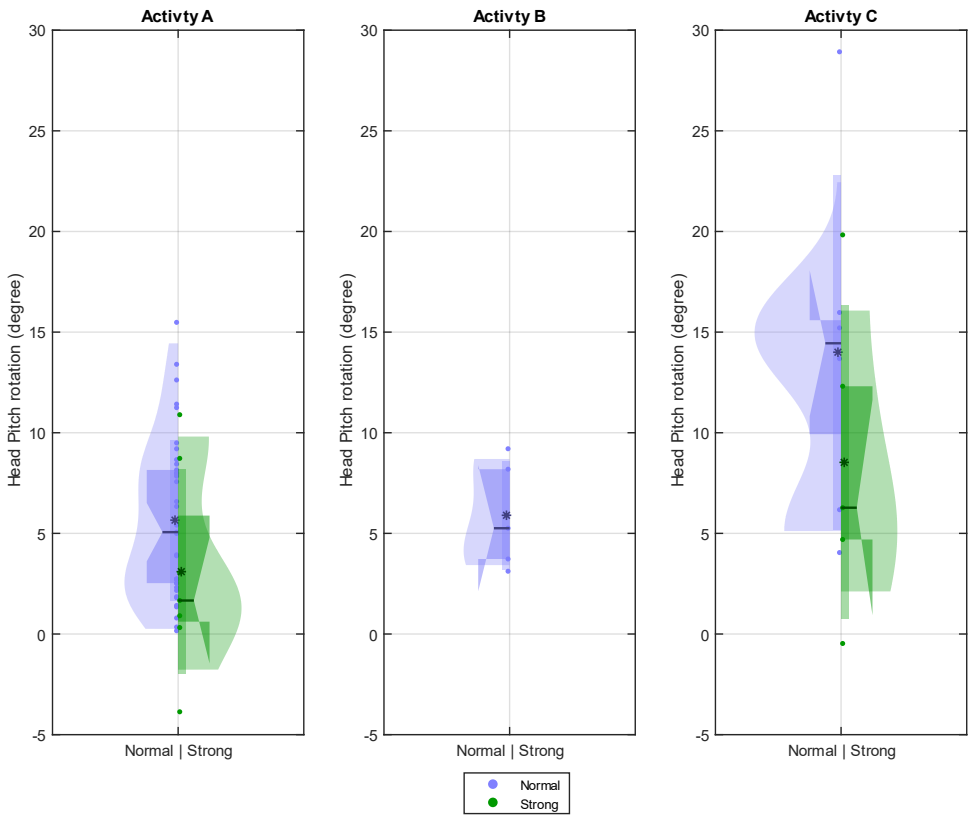

Figure 33: Head pitch rotation during Strong (green) and Normal (blue) turning across different activities without audible alert. Activity: (A) looking at the road; (B) using devices such as a phone; (C) using devices before the maneuver and then looking at the road when the maneuver starts.

3.3.3. EMG of SCM Muscle

Table 18 systematically compares the occurrence rates of muscle activation across different turning scenarios and conditions, highlighting the relationship between occupant activity and muscle activation patterns observed through EMG recordings. On the first column, the first letter of each cell denotes the occupant's activity during the recorded event: (A) looking at the road; (B) using a device, such as a phone; (C) using a device before the event, then looking at the road when event begins. The combination of a letter and a number following the activity letter represents the observed physiological response: M0 indicates the absence of muscle activation, M1 denotes muscle activation during or after the event, and M2 signifies double muscle activation occurring both before and during or after the event. Figure 34 displays the percentage distribution of SCM muscle activation occurrences across different turning intensities (Strong, Normal). The x-axis corresponds to the first column of Table 18, with each bar representing a specific combination of occupant activity and the associated muscle activation response. The most frequently observed condition was A_M1, where occupant experienced a muscle activation during or after the event when looking at the road.

The n-way ANOVA analysis revealed no statistically significant differences among the groups.

Table 18: ***Occupant activity and muscle response in relation to turning intensity (without an alert): occurrence distribution of muscle activation patterns across various turning scenarios and occupant activity.*** **On the first column, the first letter of each cell denotes the occupant's activity during the recorded event: (A) looking at the road; (B) using a device, such as a phone; (C) using a device before the maneuver, then looking at the road when the maneuver begins. The combination of a letter and a number following the activity letter represents the observed physiological response: M0 indicates the absence of muscle activation, M1 denotes muscle activation during or after the event, and M2 signifies double muscle activation occurring both before and during or after the event.**

Occupant activity and Muscle Response over the total occurrence (60)	Occurrence	Strong Turning without alert	Normal Turning without alert
A_M0	9	**0**	**9**
A_M1	18	**5**	**13**
A_M2	0	**0**	**0**
B_M0	0	**0**	**0**
B_M1	1	**0**	**1**
C_M0	0	**0**	**0**
C_M1	2	**2**	**1**
C_M2	0	**0**	**0**
Noisy data	30	**N/A**	**N/A**

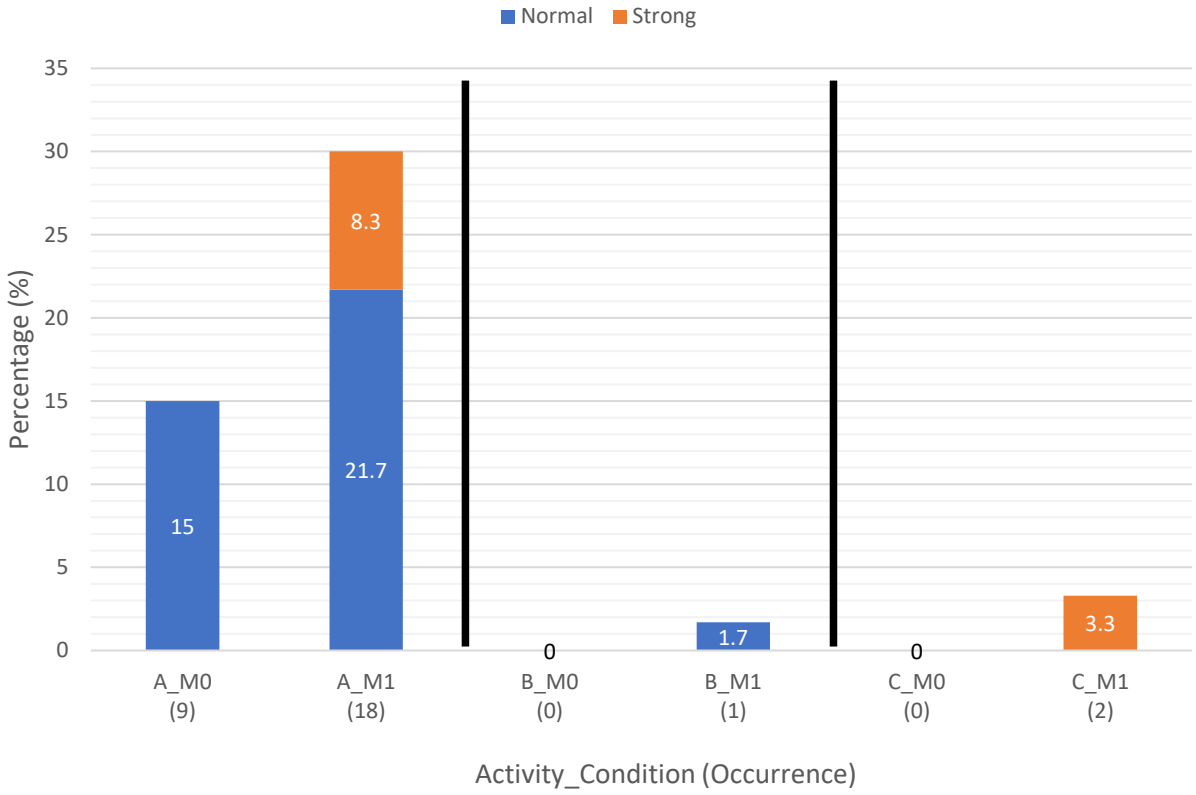

Figure 34: ***Proportion of Sternocleidomastoid (SCM) Muscle Activation Occurrences Categorized by Turning Intensity.*** **The colors represent different turning intensities: Strong, and Normal. On the x-axis, the first letter of each bar denotes the occupant's activity during the recorded event: (A) looking at the road; (B) using a device, such as a phone; (C) using a device before the maneuver, then looking at the road when the maneuver begins. The combination of a letter and a number following the activity letter represents the observed physiological response: M0 indicates the absence of muscle activation, M1 denotes muscle activation during or after the event, and M2 signifies double muscle activation occurring both before and during or after the event. The number within parentheses indicates the frequency of occurrence for that specific condition represented by each bar.**

3.3.4. Change in Respiration Frequency

Table 19 systematically compares the occurrence rates of changes in respiration frequency across different turning intensities, highlighting the relationship between occupant activity and respiration frequency patterns observed through respiration recordings. On the first column, the first letter of each cell denotes the occupant's activity during the recorded event: (A) looking at the road; (B) using a device, such as a phone; (C) using a device before the event, then looking at the road when event begins. The combination of a letter and a number following the activity letter represents the observed physiological response: R0 indicates the absence of respiration frequency change after the event, and R1 denotes respiration frequency change after the event. Figure 35 illustrates the percentage distribution of changes in respiration frequency across varying lane changing intensities (Strong, Normal) without an audible alert. The x-axis corresponds to the first column of Table 19, with each bar representing a specific combination of occupant activity and the associated change in respiration frequency response. For each activity (A, B, C), the occurrence of no change in respiration frequency consistently exceeded the

occurrence of respiration frequency variability, though the majority of strong turning events resulted in a change in respiration frequency.

The n-way ANOVA analysis revealed no statistically significant differences among the groups.

Table 19: *Occupant activity and change in respiration frequency in relation to turning intensity (without an alert): occurrence distribution of change in respiration frequency patterns across various turning scenarios and occupant activity.* On the first column, the first letter of each cell denotes the occupant's activity during the recorded event: (A) looking at the road; (B) using a device, such as a phone; (C) using a device before the maneuver, then looking at the road when the maneuver begins. The combination of a letter and a number following the activity letter represents the observed physiological response: R0 indicates the absence of respiration frequency change after the event, and R1 denotes respiration frequency change after the event.

Occupant activity and change in respiration frequency over the total occurrence (60)	Occurrence	Strong Turning without alert	Normal Turning without alert
A_R0	25	**0**	**25**
A_R1	19	**7**	**12**
B_R0	3	**0**	**3**
B_R1	2	**0**	**2**
C_R0	7	**1**	**6**
C_R1	4	**4**	**0**

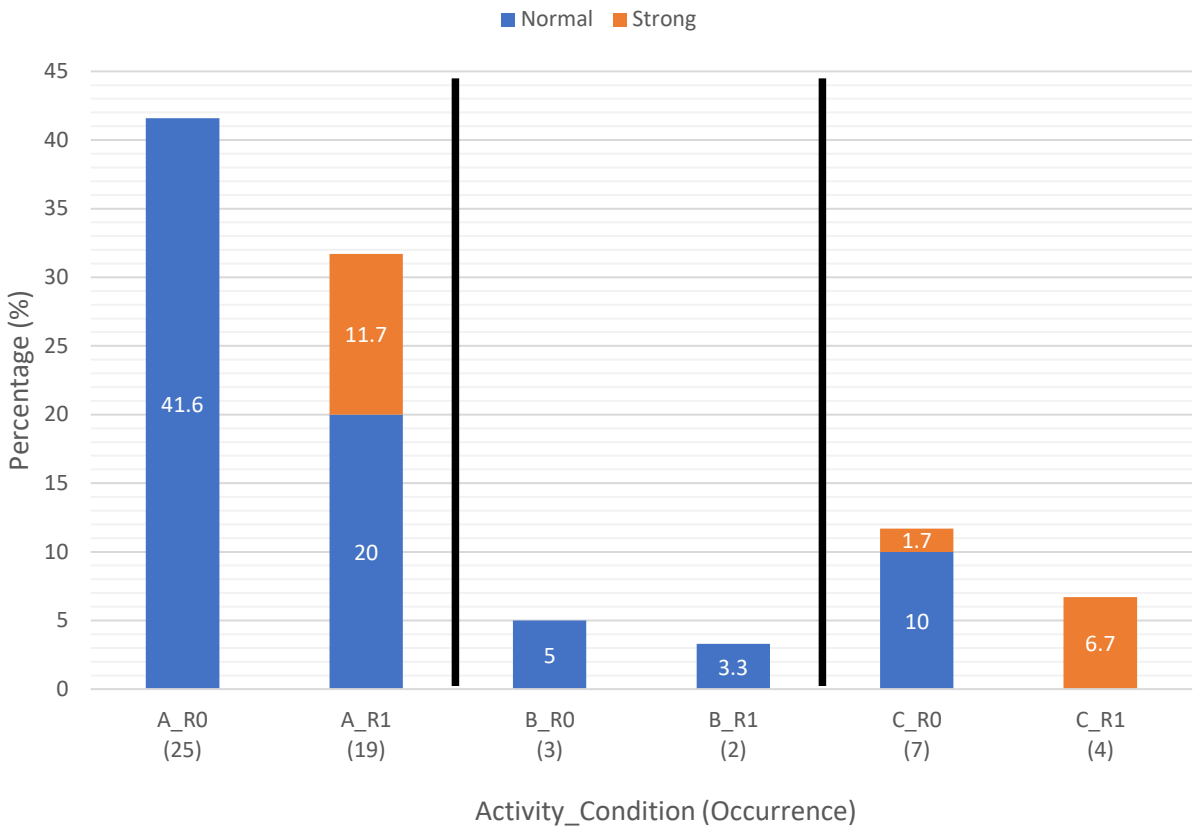

Figure 35: ***Proportion of Change in Respiration Frequency Categorized by Turning Intensity.*** **The colors represent different turning intensities: Strong, and Normal. On the x-axis, the first letter of each bar denotes the occupant's activity during the recorded event: (A) looking at the road; (B) using a device, such as a phone; (C) using a device before the maneuver, then looking at the road when the maneuver begins. The combination of a letter and a number following the activity letter represents the observed physiological response: R0 indicates the absence of respiration frequency change after the event, and R1 denotes respiration frequency change after the event. The number within parentheses indicates the frequency of occurrence for that specific condition represented by each bar.**

3.3.5. Heart Rate

Table 20 systematically compares the occurrence frequency of heart rate changes across different turning intensities, highlighting the relationship between occupant activity and heart rate variability. On the first column, the first letter of each cell denotes the occupant's activity during the recorded event: (A) looking at the road; (B) using a device, such as a phone; (C) using a device before the event, then looking at the road when event begins. The combination of a letter and a number following the activity letter represents the observed physiological response: H-1 indicates heart rate less than (Mean at rest) -SD during/after the event, H0 denotes heart rate within (Mean at rest) +SD and (Mean at rest) -SD during and after the event, and H1 signifies heart rate is higher than the (Mean at rest) +SD during and after the event. Figure 36 displays the percentage distribution of heart rate changes occurrences across different turning intensities (Strong, Normal) without audible alert. The x-axis corresponds to the first column of Table 20, with each bar representing a specific combination of occupant activity and the associated heart rate response. For activity C, the occurrence of no change in heart rate slightly

exceeded the occurrence of heart rate variability. However, in activities A and B, the occurrence of heart rate changes was slightly more frequent than those of no change.

The n-way ANOVA analysis revealed no statistically significant differences among the groups.

Table 20: *Occupant activity and heart rate in relation to turning intensity (without an alert): occurrence distribution of heart rate patterns across various turning scenarios and occupant activity.* On the first column, the first letter of each cell denotes the occupant's activity during the recorded event: (A) looking at the road; (B) using a device, such as a phone; (C) using a device before the maneuver, then looking at the road when the maneuver begins. The combination of a letter and a number following the activity letter represents the observed physiological response: H-1 indicates heart rate less than (Mean at rest) -SD during/after the maneuver, H0 denotes heart rate within (Mean at rest) +SD and (Mean at rest) -SD during and after the maneuver, and H1 signifies heart rate is higher than the (Mean at rest) +SD during and after the maneuver.

Occupant activity and Heart rate over the total occurrence (204)	Occurrence	Strong Turning without alert	Normal Turning without alert
A_H-1	4	**0**	**4**
A_H0	19	**3**	**16**
A_H1	21	**4**	**17**
B_H-1	1	**0**	**1**
B_H0	1	**0**	**1**
B_H1	3	**0**	**3**
C_H-1	1	**1**	**0**
C_H0	7	**4**	**3**
C_H1	3	**0**	**3**

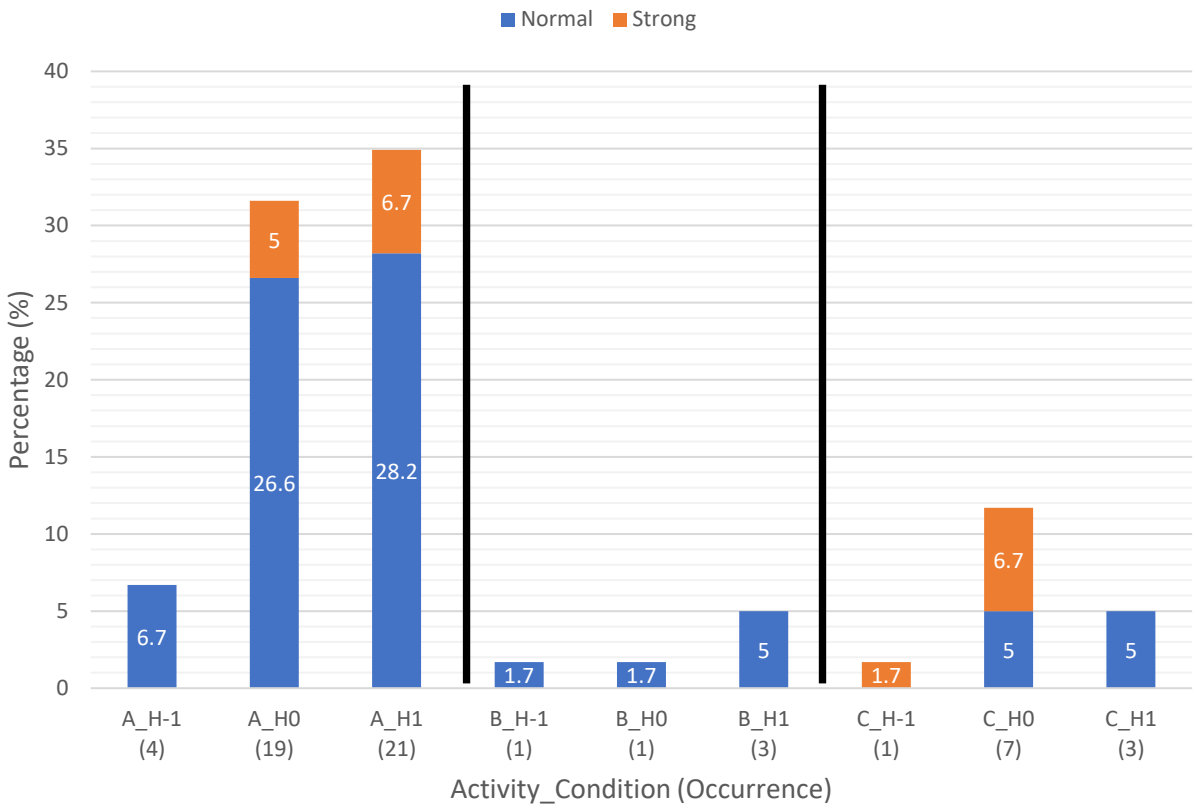

Figure 36: ***Proportion of Heart Rate Categorized by Turning Intensity.*** **The colors represent different turning intensities: Strong, and Normal. On the x-axis, the first letter of each bar denotes the occupant's activity during the recorded event: (A) looking at the road; (B) using a device, such as a phone; (C) using a device before the maneuver, then looking at the road when the maneuver begins. The combination of a letter and a number following the activity letter represents the observed physiological response: H-1 indicates heart rate less than (Mean at rest) -SD during/after the maneuver, H0 denotes heart rate within (Mean at rest) +SD and (Mean at rest) -SD during and after the maneuver, and H1 signifies heart rate is higher than the (Mean at rest) +SD during and after the maneuver. The number within parentheses indicates the frequency of occurrence for that specific condition represented by each bar.**

3.4. Motion Sickness

Upon completing the experiment, participants exited the driving simulator and proceeded to complete a Simulator Sickness Questionnaire (Kennedy et al., 1993), which was used to assess their levels of motion sickness following the simulation. Out of the 12 participants, 11 experienced minimal or no simulator sickness. Only 1 participant reported mild simulator sickness, indicating the presence of symptoms, though mild, which did not significantly impair performance or results (Stewart, 1965).

4. Discussion

This study investigates the multi-layered nature of occupant responses within Level 3 AV simulator. Physiological measures, in conjunction with observed occupant behaviour, provide valuable insights into how individuals respond to various driving events. A multi-faceted approach, incorporating IMU measurements, SCM muscle activity, respiration monitoring, and heart rate analysis, provides a nuanced picture of occupant physiological responses during various braking, lane-changing, and turning events. A complex interplay emerges between external cues, such as audible alerts, the intensity of AV maneuvres, occupant's activity, and occupant's physiological state. Individual variations in these responses underscore the importance of understanding the degrees of occupant experiences. The occupants own activities during this short drive were similar to what was observed in a previous study by Östling and Larsson, 2019. To the best of our knowledge, this is the first study where it simultaneously examines the impact of AV maneuvres on a comprehensive range of physiological parameters, including head movement, muscle activation, respiration, and heart rate, while also considering individual variability and occupant activity.

This multi-dimensional approach is crucial for gaining a general understanding of occupant human-machine interaction, behaviour, cognition, and safety within AVs, while answering the research questions: How do pre-brake conditions and occupant activities in an autonomous vehicle (AV) influence the body's response to emergency braking events?

4.1. Frontal Braking

Our results demonstrated that the effect of braking intensity on the head acceleration is significantly affected by the presence of an audible alert. Specifically, during instances of strong intensity braking events where alert s preceded the braking events, participants exhibited an increased head acceleration compared to the events without a preceding alert. However, during instances of normal braking intensity, an inverse effect was observed, which is more in line with previous studies performed in a real car and level 3 environment (Mackenzie et al., 2022). When looking at the road, head acceleration remained unchanged, whereas when looking at a device then returning attention to the road, it was 0.1 g lower when an alert proceeded the braking event. This suggests that in the event of strong braking either the preparatory effect triggered by audible alerts might lead to anticipatory postural changes potentially influencing head movement, that participants were unprepared for intense braking due to an expectation of normal braking, or a combination of both factors. This is in accordance with Liang et al., 2020, where they demonstrated that through repetitive exposure to external perturbations, participant were able to rely solely on auditory cues to generate adequate anticipatory postural adjustments. Conversely, the absence of alerts before braking resulted in similar head acceleration levels when looking at the road and looking at a device across both braking intensities, while looking at a device then returning attention to the road exhibited higher head acceleration. This implies that occupants engaged in this latter activity may exhibit a more passive response, indicating lesser preparedness for the force of the braking maneuver.

The effect of alerts on SCM muscle activation was significantly influenced by individual differences. This further supports the finding by Santos-Cuadros et al., 2021, where they showed that during emergency braking with a warning, there was a notable difference observed in the SCM muscle response according to gender and age. Some occupatns exhibited double SCM activation when alerts were present, regardless of braking intensity. This may represent a heightened startle response or anticipatory bracing. This double muscle activation was similarly observed in a study by Krašna and Đorđević, 2020, which measured upper trapezius muscle activity during a SLED low-severity impact experiment. The study found that in trials where participants were aware of the impending impact, a startle reflex or anticipatory bracing response was evident. Nevertheless, most occupants in our experiement demonstrated SCM activation primarily in response to high-intensity events, even without alerts. These findings highlight the importance of understanding individual variability in physiological responses to AV events, especially with regards to potential comfort and safety implications. That being said, the high degree of noise in our EMG data, unfortunately, limited robust conclusions about muscle activation patterns. This could be attributed to factors such as sensor placement, individual differences in skin conductivity, or movement artifacts. Future research must prioritize optimizing EMG signal quality to gain clearer insights into the muscular responses of AV occupants. Possible strategies include refined sensor placement techniques less prone to motion artifacts and reducing electrical noise.

Our N-way ANOVA identified a statistically significant effect of the 'participant' variable on head acceleration. This emphasizes the inherent variability among individuals in their responses to identical AV events. Understanding this variability is crucial for developing AV systems that adapt to diverse occupant needs and preferences. Factors such as prior driving experience, simulator susceptibility, and baseline physiological differences could all contribute to the observed variability. Our findings suggest that the design of auditory alert systems in AV may greatly impact occupant experience and could have safety implications. The interplay between alerts, braking intensity, and individual responses warrants further investigation to develop adaptive systems that cater to diverse occupant preferences and sensitivities. Additionally, the observed variations in head movement raise questions about potential risk factors in different AV scenarios.

While our analysis did not reveal statistically significant patterns in respiration changes and heart rate variability across different braking conditions, certain trends warrant further exploration. For instance, without audible alerts, a slightly higher percentage of participants exhibited altered respiration frequencies during strong braking events compared to normal braking. This could potentially hint at increased anxiety or stress in response to unexpected maneuvers. Heart rate variability also showed subtle shifts during these events. A larger sample size, more refined heart rate analysis techniques, or monitoring Electrodermal activity might clarify if these observed trends reflect physiologically meaningful responses that could contribute to occupant comfort and perceived safety in AV.

4.2. Lane-Changing and Ninety Degrees Turning

This study found a statistically measurable impact of individual participants on both SCM muscle activity and heart rate variability during lane changes. This highlights a critical point: occupant responses to AV maneuvers (even standardized ones) are likely to exhibit a degree of individual variability. Several factors might contribute to this variability, such as pre-existing differences in baseline muscle tone or autonomic nervous system reactivity could play a role. Additionally, occupants' prior experience with driving simulators, their expectations about AV behaviour, or psychological factors like anxiety could potentially influence these results. It's important to consider that individual variability might also influence responses to other maneuvers beyond lane changes. While the high levels of noise in the EMG data limit strong conclusions in this study, future work with refined EMG techniques could explore whether participants exhibit distinct muscle activation patterns during AV braking events or other AV maneuvers.

Furthermore, the statistically significant interaction effect between participant and turning intensity for head pitch during 90-degree turns provides further evidence of individual variability in occupant responses. This suggests that some participants might be more sensitive to changes in turning intensity and exhibit larger head pitch rotations compared to others. Acknowledging these individual differences is essential for designing inclusive AV systems, since it suggests that a "one-size-fits-all" approach might not be optimal. Ideally, AVs should incorporate personalization or adaptive features that can tailor the driving environment and motion profiles to optimize comfort and minimize adverse physiological responses for diverse occupants (Ataya et al., 2021; Bellem et al., 2017; Manawadu et al., 2015). While the high levels of noise in the EMG data limit strong conclusions in this study, future work with refined EMG techniques is necessary to fully explore the influence of individual factors on muscle activation patterns.

While our analysis did not reveal statistically significant results for head acceleration, and respiration frequency for both lane-change condition, certain trends warrant further investigation. For instance, the change in respiration frequency under the strong condition, compared to normal maneuvers. This could potentially hint at increased stress in response to unexpected maneuvers. Additionally, the SCM muscles activity during the strong turning events always had a muscle activation, compared to no muscle activation during normal turning. A larger sample size might clarify if these observed trends reflect physiologically meaningful responses that could contribute to occupant comfort and perceived safety in AV.

Expanding the range of physiological measurements, such as electrodermal activity or eye-tracking, could provide a more nuanced understanding of both overt and subtle occupant responses, potentially revealing additional ways in which audible alerts shape anticipation and comfort in AVs.

4.3. Limitations

Several limitations were encountered during this study, which should be addressed in future experiments. First, electrical noise from the driving simulator affected the accuracy of EMG data acquisition. To mitigate this, future experiments should utilize more advanced EMG sensors with improved noise reduction capabilities. Additionally, the need to cover the side windows of the simulator to maintain a sense of immersion limited the realism of the environment. This issue could be resolved by employing a modern mixed-reality headset, such as the Apple Vision Pro or VARJO XR-4, or using a more advanced driving simulator with a 360-degree screen. Another limitation was the uneven distribution of activity data, which hindered the ability to determine the significant effect of occupant activity on physiological responses using ANOVA. A potential solution is to conduct a follow-up experiment with the same participants, providing specific instructions on which activities to engage in during each scenario. Lastly, although a higher number of participants would have been ideal for more robust statistical analysis, only 12 experiments were conducted due to time constraints and logistical challenges. Expanding the sample size in future studies would enhance the reliability and generalizability of the findings.

The validity of driving simulators as a research tool in this study is critical to ensure that the physiological and behavioural responses observed accurately reflect real-world driving scenarios. While driving simulators provide a controlled, low-risk environment that allows for repeated exposure to specific events, some challenges exist in replicating real-world conditions. For instance, the fidelity of motion cues, visual immersion, and the presence of simulator/motion sickness can influence how participants respond. Previous research suggests that simulators can closely mimic real-world responses in areas such as braking, lane changes, and turning, but individual variability, sensory mismatches, and the artificiality of the environment might introduce perceptual biases. In this study, efforts were made to align the simulator environment with reality, including the use of pre-recorded braking maneuvers and standardized alerts. However, full validation against real-world driving requires further refinement of the simulator's visual and haptic feedback mechanisms. Future studies should continue to address these limitations by enhancing the realism of the simulator, potentially through the use of 360-degree displays or mixed-reality headsets, and validating simulator findings with real-world trials to ensure the applicability of results to actual autonomous vehicle behaviour and occupant safety.

4.4. Contrasting Emergency and Normal Maneuvers

A key finding is the distinct physiological signature of emergency maneuvers versus their normal counterparts. Emergency events appear to trigger a stronger, more immediate response across head movement and muscle activation parameters. This is likely due to a combination of factors, including:

- **Sudden and Unexpected Force:** Emergency-level maneuvers often involve greater acceleration and sharper changes in direction, leading to higher inertial forces acting upon the occupant's body.

- **Lack of Anticipatory Cues:** Without the gradual buildup experienced in normal maneuvers, there's less opportunity for anticipatory postural adjustments, potentially contributing to more reactive muscle activation patterns.

4.5. Recommendations for the design of HMIs in Avs

Level 3 Autonomous Vehicles

(Level 3 vehicles can handle all driving tasks in certain conditions but may require human intervention)

1. **Clear Handover Process:**
    - **Visual Alerts:** Use prominent visual signals on the dashboard or heads-up display (HUD) to alert the driver when control needs to be taken over.
    - **Auditory Alerts:** Incorporate distinct auditory cues that are easily distinguishable and escalate in urgency if the driver does not respond promptly.
    - **Haptic Feedback:** Utilize vibrations in the steering wheel or seat to provide an additional layer of alert.
2. **Redundant Systems:**
    - **Multiple Alerts:** Use redundant alert systems (visual, auditory, haptic) to ensure the driver is aware of any situations requiring attention.
    - **Backup Controls:** Ensure manual controls are always available and functional for emergency situations.
3. **State Awareness**
    - **Driver Monitoring System (DMS):** Implement cameras and sensors to monitor the driver’s attention and readiness to take control. If the driver is distracted or inattentive, the system should alert them and potentially slow down the vehicle.
    - **Driving Mode Display:** Ensure the current driving mode (manual, assisted, autonomous) is always clearly displayed and easily understood by the driver.
4. **User-Friendly Interface:**
    - **Intuitive Controls:** Design simple and intuitive controls for engaging and disengaging autonomous mode. Avoid complex sequences that could confuse the driver.
    - **Information Clarity:** Provide clear and concise information about the vehicle’s actions and intentions, such as upcoming lane changes or speed adjustments.
5. **Transition Assistance:**
    - **Guided Transition:** During handover, offer guidance through visual and auditory cues to help the driver reorient to the driving environment.
    - **Buffer Time:** Ensure the system provides sufficient buffer time for the driver to take control, considering factors like reaction time and situational awareness.
    - **Interactive Features:** Consider adding interactive features like external speakers or displays that can communicate with pedestrians or cyclists in critical situations.

5. Conclusion

This study presents a comprehensive analysis of the physiological and behavioural responses of occupants in autonomous vehicles (AVs) during various driving maneuvers. Our findings underscore the significant impact of auditory alerts, maneuver intensity, and individual differences on physiological responses such as head acceleration, SCM muscle activity, respiration, and heart rate variability. The interaction between auditory alerts and braking intensity notably influences head acceleration and SCM muscle activation, suggesting that such alerts could enhance preparedness and potentially improve safety by enabling anticipatory postural adjustments. However, the variability in responses highlights the need for AV systems to account for individual occupant differences. These findings advocate for the development of adaptive auditory alert systems tailored to occupant sensitivities and preferences. Additionally, our results indicate that individual variability significantly affects physiological responses during AV maneuvers, including lane changes and turns. This variability can be attributed to factors such as prior driving experience, susceptibility to motion sickness, and baseline physiological states. Therefore, designing AV systems that can adapt to this individual variability is crucial. Implementing personalized settings or adaptive features that cater to the unique needs of each occupant could optimize comfort and safety.

The limitations encountered with EMG data noise underline the necessity for improved data acquisition methods. Future research should focus on enhancing sensor placement and signal processing techniques to obtain more reliable measures of muscle activation, which are essential for understanding the full scope of physiological responses in AV environments. In conclusion, our study contributes to the growing body of knowledge on human-machine interaction within AVs. It highlights the importance of considering both universal and individual factors in the design of AV systems to enhance occupant experience and safety. Continued research in this area is imperative to refine AV technologies, making them more adaptable and responsive to the diverse needs of occupants, thereby facilitating wider acceptance and use of autonomous transportation solutions.

The findings from Chapter 3 underscore the complexity of occupant physiological responses during autonomous vehicle (AV) maneuvers, highlighting the need for adaptive systems that can accommodate individual variability in response to auditory alerts and driving conditions. While auditory cues and braking intensity were shown to influence head acceleration and muscle activation, the variability in occupant responses calls for more personalized approaches to AV safety systems. These insights provide a strong foundation for further investigation into how specific occupant activities influence physiological and cognitive responses during critical driving scenarios, such as emergency braking.

Building on this understanding, Chapter 4 shifts focus to a more controlled experimental setup, where participants' activities were directed based on previous observations. By using a SLED system and a 360° virtual environment, the upcoming study delves deeper into the effects of occupant activities on head-neck dynamics during varying braking conditions. This transition allows for a more refined analysis of how pre-determined occupant behaviours interact with braking intensity, providing a more nuanced

understanding of the human-machine interface (HMI) and its implications for occupant safety in AVs. This chapter aims to address the gap in existing literature by focusing on the kinematic and physiological responses elicited by different braking scenarios and occupant activities.

CHAPTER 4: EFFECT OF OCCUPANT ACTIVITIES ON THE HEAD-NECK RESPONSE DURING BRAKING

1. Introduction

In the previous chapter, the SAAM experiment allowed occupants to engage freely with the AV. In this experiment, however, participants were instructed on how to interact with the AV in a virtual environment based on their behaviours during the SAAM experiment. This approach ensured a more uniform distribution of data under consistent testing conditions, enabling a focused analysis of the effects of different activities on physiological responses under varying braking intensities and conditions. Existing research, particularly studies using SLED systems, has predominantly examined the effects of frontal impacts or braking when the occupant is facing forward, both with and without prior alerts (Beeman et al., 2012; Kumar et al., 2003). However, there is a significant gap in understanding how different occupant activities influence the physiological head-neck response in autonomous vehicles (AVs). This chapter aims to address this gap by investigating the impact of various occupant activities on head-neck dynamics during emergency braking events in an AV context.

The relationship between occupant activity and its physiological effects on head-neck dynamics, particularly during emergency braking, remains inadequately understood, as discussed in the literature review. Existing studies have primarily examined the influence of braking intensity, with and without prior alerts, on head-neck responses using dynamic systems, commonly known as "SLED" systems, which expose participants to controlled acceleration and deceleration forces. These studies highlight the critical role of neck muscle engagement in mitigating head acceleration and pitch during deceleration (Beeman et al., 2011). Activation of the neck muscles has been shown to reduce head movement, thereby lowering the risk of injury (Beeman et al., 2011). Furthermore, prior alerts before braking events have been found to significantly reduce head acceleration and pitch rotation, while also triggering a neck muscle response that enhances head stabilization (Di Loreto, 2019). In light of these findings, the study of human-machine interface (HMI) effects on cognitive and physiological parameters is crucial for advancing our understanding of head-neck stabilization strategies during braking events in AVs. This knowledge could provide deeper insights into potential injury mechanisms and inform the development of warning systems aimed at preventing or reducing head-neck injuries in AVs.

A study involving five participants was conducted and is presented in this chapter, comparing the kinematics and muscle response of the head and neck using a SLED system under various braking conditions. The SLED was specifically chosen to replicate braking events with horizontal acceleration, providing a more accurate simulation of real-world braking forces than what could be achieved with a driving simulator. In previous experiments with driving simulators, horizontal acceleration forces were translated into vertical forces. By using the SLED, we were able to simulate different braking intensities more closely aligned with the real-world experience in a Level 3 autonomous vehicle (AV) context. Participants wore a Head-Mounted Display (HMD) that provided a 360° view inside a virtual

environment, simulating an AV in a high-rise urban setting. This immersive setup was designed to replicate typical occupant activities during Level 3 AV driving, with the aim of investigating the effects of these activities on participants' cognitive and physiological responses under varying braking conditions.

We hypothesize that occupant activity during/before AV braking will significantly influence physiological responses, including head acceleration, head movement, and muscle activation. Furthermore, we expect that human-machine interface (HMI) systems providing timely and clear auditory alerts will impact occupant head-neck dynamics during these braking events. Additionally, we anticipate that individual participants will exhibit significantly different physiological responses, despite being subjected to uniform experimental conditions, highlighting the importance of considering individual variability in AV safety designs.

2. Materials and Methods

2.1. Participants

The experiment involved 5 participants (2 women and 3 men) with a mean age of 25.6 years (SD = 2.3 years), a mean weight of 70.8 kg (SD = 15.9 kg), a mean height of 1.73 m (SD = 0.09 cm), and a mean body mass index (BMI) of 23.3 kg/m² (SD = 2.7 kg/m²). three participants possessed a valid driver's license for over 5 years, one participant held it for less than 5 years, and one participant did not have a driving licence. Visual acuity was either normal or corrected-to-normal, and participants reported no vestibular or ocular abnormalities. Regarding weekly driving habits, two participants did not drive, one drove for up to one hour, one drove between three and five hours, and one drove more than five hours. All participants had no prior experience with the SLED. All participants were instructed to abstain from excessive caffeine absorption, recreational drug use, including alcohol, for a minimum of 24 hours prior to the commencement of the experiment. All Experimental procedure were performed in accordance with the ethical guidelines of the Declaration of Helsinki. All participants gave their written informed consent prior to participation in the study. The protocol was approved by the French Ethics Committee CPP IDF VII number 15–018. All volunteers were fully informed and signed a consent form.

2.2. Apparatus: SLED

Participants were seated on an instrumented four-meter-long sled system (SLED) and secured by a Velcro belt across the chest (Figure 37). The SLED is a dynamic system consisting of a seat mounted on rails, allowing uniaxial translation via ball bearings, and its movement is powered by a belt system driven by a three-phase servomotor (Compumotor APEX640), controlled by Labview software. The sled pulses and acceleration profiles, reaching 0.3 g for normal braking and 0.6 g for strong braking, were precisely programmed and validated using closed-loop control, as confirmed in a previous study (Sandoz et al., 2014). An additional IMU (Xsens MTx, 100 Hz) was fixed under the seat plate to record acceleration, with all sensors synchronized to a common trigger signal. For safety reasons, only the first

three meters of the SLED were used, and the system included elastic restraint systems, and an emergency stop button to ensure the smooth operation of the sled's movement.

Table 21: SLED movement limits

Degree Of Freedom	Displacement	Velocity	Acceleration
Surge	±3 m	±3 m/s	±1 g

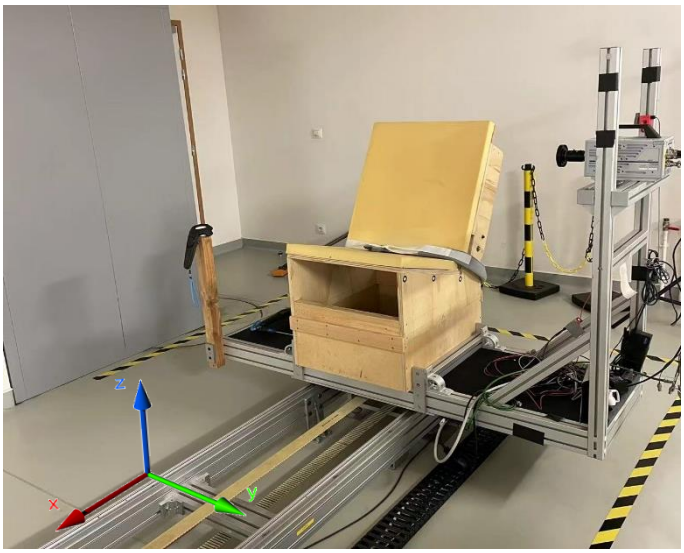

Figure 37: SLED system

2.3. Apparatus: Instrumentation

Participants were outfitted with two inertial measurement units (IMUs, Xsens MTx): one affixed to the head and another to the first thoracic vertebra (T1). Additionally, a reference IMU was securely mounted under the seat. Orientation and acceleration data were sampled at a frequency of 100 Hz. The head IMU was firmly fastened using cable ties and tape to an adjustable rigid head strap, while the T1 IMU was adhered with double-sided tape and hypoallergenic adhesive strips. Furthermore, the activity of the right sternocleidomastoid (SCM) and splenius capitis (SC) muscles was recorded using a wireless electromyography (EMG) sensor (Trigno Delsys) at a sampling rate of 2000 Hz. Additionally, a high-speed camera (Photron Ultra-High-Speed FASTCAM) was mounted on the moving section of the SLED to capture head-neck movements from the left side of the participants during braking, throughout the first 10 trials of the experiment. The camera was equipped with a wide-angle lens designed to minimize image distortion, positioned at a distance of 30 cm from the participants. The acquisition rate was set at 50 frames per second. A synchronization signal emitted by the high-speed camera ensured that all experimental sensors were synchronized with precise timing. During the experiment, the virtual environment was projected using an HTC Vive head-mounted display (HMD), which participants wore

throughout the entire procedure. Participants took short 2-minute breaks after every 10 braking events, during which they remained seated and removed the HMD.

2.4. Virtual Environment and Protocols

Prior to the experiment, participants were outfitted with the physiological sensors mentioned above to monitor their physical responses throughout the trials. Participants were seated on the SLED, secured by a Velcro belt across the chest, and wore an HTC Vive head-mounted display (HMD), which projected a virtual environment simulating the view from inside an autonomous vehicle (AV) (Figure 38). The virtual environment was developed using Unity and depicted a high-rise urban area with straight roads and two intersections per road (Figure 39 to Figure 41). To prevent participants from becoming too familiar with the environment, the buildings and lighting were altered after every few trials. The AV was programmed to operate at SAE Level 3 autonomy, where it independently made decisions, such as braking, without requiring human intervention. However, participants were given specific tasks to perform during each trial, including looking at the road (Activity A), looking down as if using their phones (Activity B), or looking down and then glancing up when the braking event started or when an audible alert was triggered (Activity C). An audible alert system was integrated to maintain participant awareness during potential hazard situations, such as pedestrian crossings. The audible alert was engaged 500 milliseconds to 1 second before braking. The radio was set to each participant's preferred station at a constant volume throughout the experiment to enhance their sense of immersion.

The synchronization between the real-world sled system (SLED) and the virtual environment was crucial for enhancing the experiment’s realism and minimizing cybersickness. The SLED, constrained to a 3-meter translation for safety, was controlled by a belt system driven by a three-phase servomotor (Compumotor APEX640). Telemetry data from the virtual vehicle was captured and converted into motion cues, which were used to simulate a relative acceleration and desired deceleration forces on the participant, creating an immersive and realistic braking experience. All sensors were synchronized through a common trigger signal to ensure precise data acquisition.

To assess the occupant behavioural effects on the head-neck physiological response in a Level 3 AV, the experiment consisted of thirty dynamic trials, conducted in a randomized, counterbalanced design. These trials were distributed across ten distinct braking and behaviour conditions, with each condition tested three times (Table 22). Please refer to the appendix for the acceleration, velocity and position profiles of each braking intensity on the SLED (Figure 50 and Figure 51). To control for potential order effects, the trials were divided into three batches of ten, with each batch containing all ten conditions. The order of conditions within each batch was randomized to ensure an unbiased distribution of participant responses. At the end of each batch of ten trials, participants completed the Simulator Sickness Questionnaire (Kennedy et al., 1993) to assess their motion sickness levels. This approach ensured that both physical and subjective data were captured to provide a comprehensive understanding of the effects of different behaviour and braking conditions on human response in a simulated AV environment.

Figure 38 : Participant outfitted with physiological sensors and HMD sitting on the SLED

Table 22: Braking and behaviour conditions

Activity	Braking Intensity	Deceleration force (g)	Alert
A	Normal	**0.3**	No
B			
C			
A	Normal	**0.3**	Yes
C			
A	Strong	**0.6**	No
B			
C			
A	Strong	**0.6**	Yes
C			

Figure 39: Exterior (right) and Interior (left) of the car in the virtual environment

Figure 40: example of emergency braking: pedestrian crossing (right); Vehicle collision Infront (left)

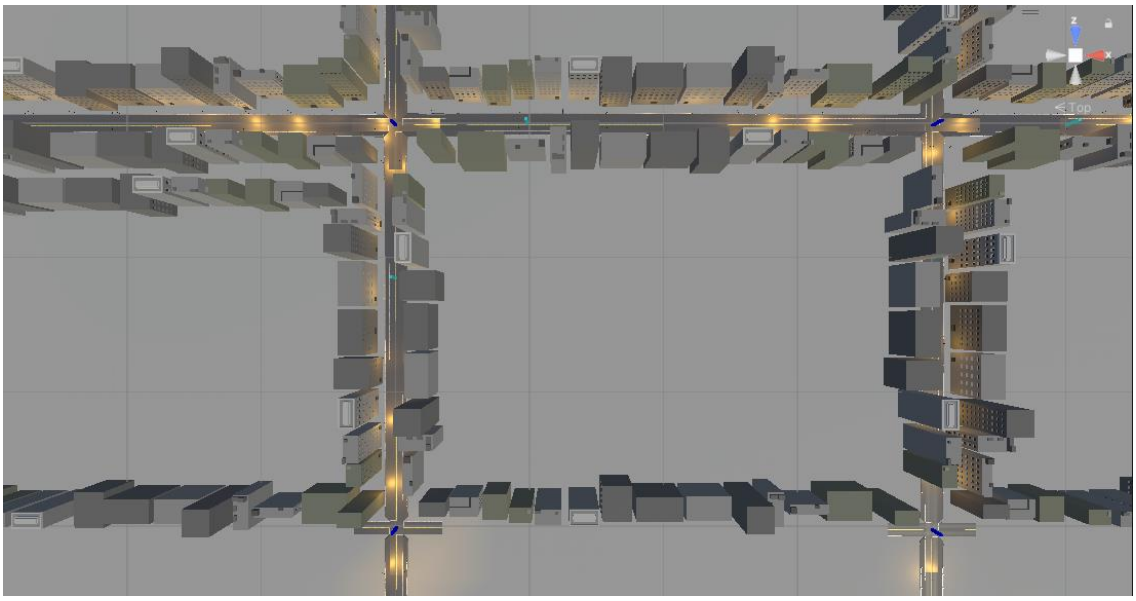

Figure 41: Top view of the virtual environment

2.5. Statistics

N-way ANOVA tests were used to analyze various categorical independent variables. These tests were performed for the following parameters within the braking categories: head acceleration, head pitch rotation, SCM muscle activation, and SC muscle activation. In each N-way ANOVA test, one of the earlier mentioned parameters served as the sample data (e.g. head acceleration), while the grouping variables included participant number, audible alert activation, braking intensity, and participant activity. For head acceleration and head pitch, the muscle activity was included as a grouping variable. The significance threshold was set to 0.05. A post-hoc test was not conducted, as the objective was solely to investigate the existence of significant differences between three or more groups.

3. Results

For all categories, three types of non-driving activities were tested: looking at the road ahead (A), using devices such as a phone or tablet (B), and using devices before the event and then looking at the road when event starts or when audible alert is activated (C).

3.1. Head Acceleration

Table 23 presents the median and interquartile range [1st quartile; 3rd quartile] of normal head acceleration (in g) during various occupant activities under different braking intensities (Strong and Normal). Data are compared between scenarios with and without an audible alert. "Never occurred" indicates that the specific condition was not studied for this experiment. Under strong braking intensity, head acceleration was higher when an audible alert was not present compared to when it was activated. There was no significant difference in head acceleration between activities when an audible alert was present. Conversely, when no alert was present, differences in head acceleration were observed. The head acceleration was slightly higher when occupants focused on the road throughout the braking event (Activity A) compared to when they engaged with devices at the moment of braking (Activity B), and the highest head acceleration in the absence of an alert was observed when occupants initially used devices but redirected their attention to the road as braking commenced or when audible alert is activated (Activity C). In normal braking, head acceleration was consistent for Activity A across both the "with alert" and "without alert" conditions, however, for Activity C the head acceleration was lower when the alert was present. In the normal braking "with alert" condition, head acceleration values for Activities A and C were almost equal, in contrast, under the "without alert" condition, Activity C led to higher head acceleration compared to Activity A and B, with activity A having the lowest head acceleration.

Both Figure 42 and Figure 43 illustrate the head acceleration (in g) experienced by occupants under three different activities: Activity A, Activity B, and Activity C. The data is presented for conditions with and without an audible alert. Each panel shows the distribution of head acceleration values, with individual data points overlaid. The colored regions represent the confidence intervals, with red indicating the "with alert" condition and yellow indicating the "without alert" condition. The black line and the asterisk within the distributions indicate the median and mean values, respectively, for each

condition. Figure 42 shows these data for normal braking, while Figure 43 presents the results for strong braking.

A multivariate analysis of variance (N-way ANOVA) was conducted to evaluate the effects of multiple factors on head acceleration, with braking intensity, audible alert activation, SCM and SC muscle activity, and occupant activity as the grouping variables. The participant number was included to account for inter-individual variability. The significance threshold was set at 0.05 for all statistical tests.

The analysis revealed several significant effects on head acceleration:

- **Braking intensity** had a highly significant effect on head acceleration ($p < 10^{-5}$), indicating that the intensity of braking is strongly associated with changes in head movement during the event.
- **Occupant activity** also showed a highly significant effect on head acceleration ($p < 10^{-5}$), suggesting that the tasks occupants were engaged in at the time of the event significantly influenced head acceleration.
- There was a **significant interaction between participant and the presence of an audible alert** ($p < 10^{-5}$), highlighting that the effect of the alert varied across individuals, influencing head acceleration differently for each participant.
- A **significant interaction between participant and occupant activity** was also observed ($p = 0.0024$), suggesting that different participants exhibited varying head acceleration responses depending on their activity at the time of the event.
- The **interaction between audible alert and braking intensity** had a significant effect on head acceleration ($p = 0.0469$), indicating that the effect of the alert on the head acceleration was influenced by different braking intensities.
- Additionally, the **interaction between audible alert and occupant activity** was highly significant ($p < 10^{-5}$), implying that the presence of an audible alert had differing effects on head acceleration based on the occupants' activities.
- Lastly, the **interaction between muscle activity and audible alert** was found to have a significant effect on head acceleration ($p = 0.0054$), suggesting that the presence of an audible alert altered the relationship between SCM and SC muscle activity and head acceleration.

Table 23: Median and interquartile range of normal head acceleration across different braking intensities and activities: Comparison between conditions with and without audible alert. Activity: (A) looking at the road; (B) using devices such as a phone; (C) using devices before braking and then looking at the road when braking starts or when audible alert is activated.

Braking intensity	Activity	With Alert	Without alert
		Median [1st; 3rd quartile] (g)	Median [1st; 3rd quartile] (g)
Strong	A	**0.36 [0.32; 0.42]**	**0.42 [0.31; 0.5]**
	B	**Never occurred**	**0.5 [0.47; 0.61]**
	C	**0.41 [0.35; 0.59]**	**1.11 [0.66; 1.25]**
Normal	A	**0.18 [0.14; 0.19]**	**0.17 [0.15; 0.22]**
	B	**Never occurred**	**0.32 [0.27; 0.34]**
	C	**0.19 [0.14; 0.22]**	**0.73 [0.51; 1.25]**

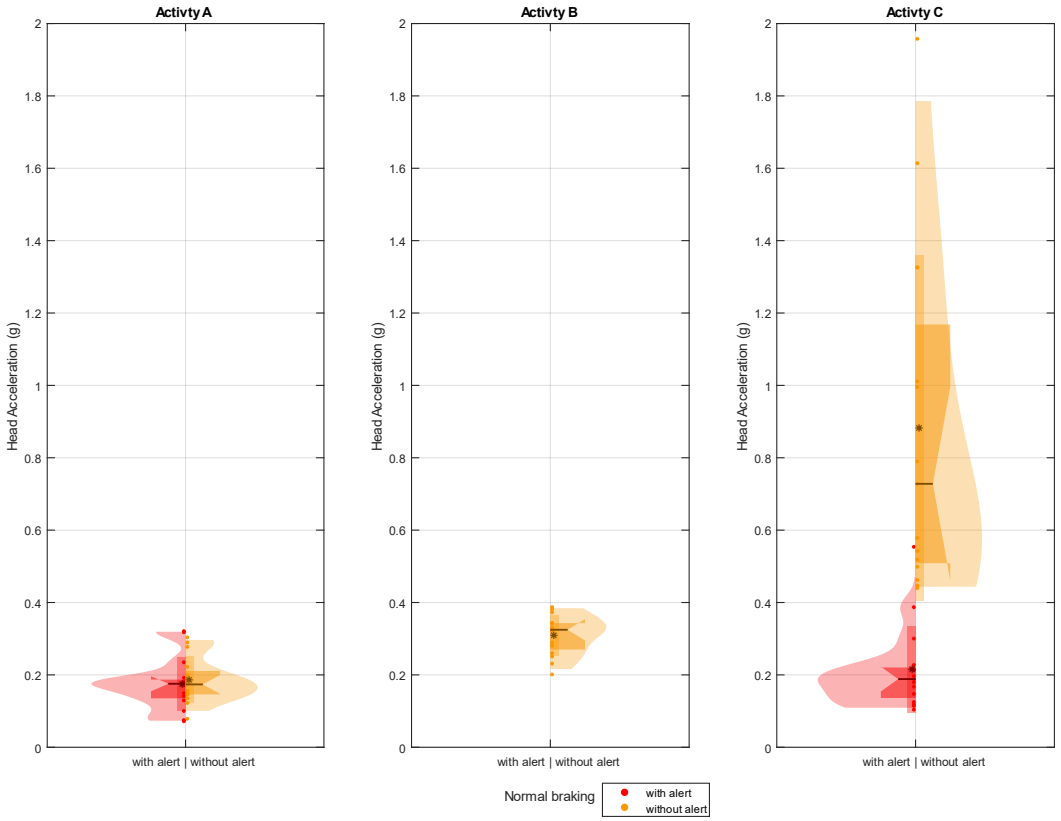

Figure 42: Head acceleration during Normal braking across different activities with and without audible alert. Activity: (A) looking at the road; (B) using devices such as a phone; (C) using devices before braking and then looking at the road when braking starts or when audible alert is activated.

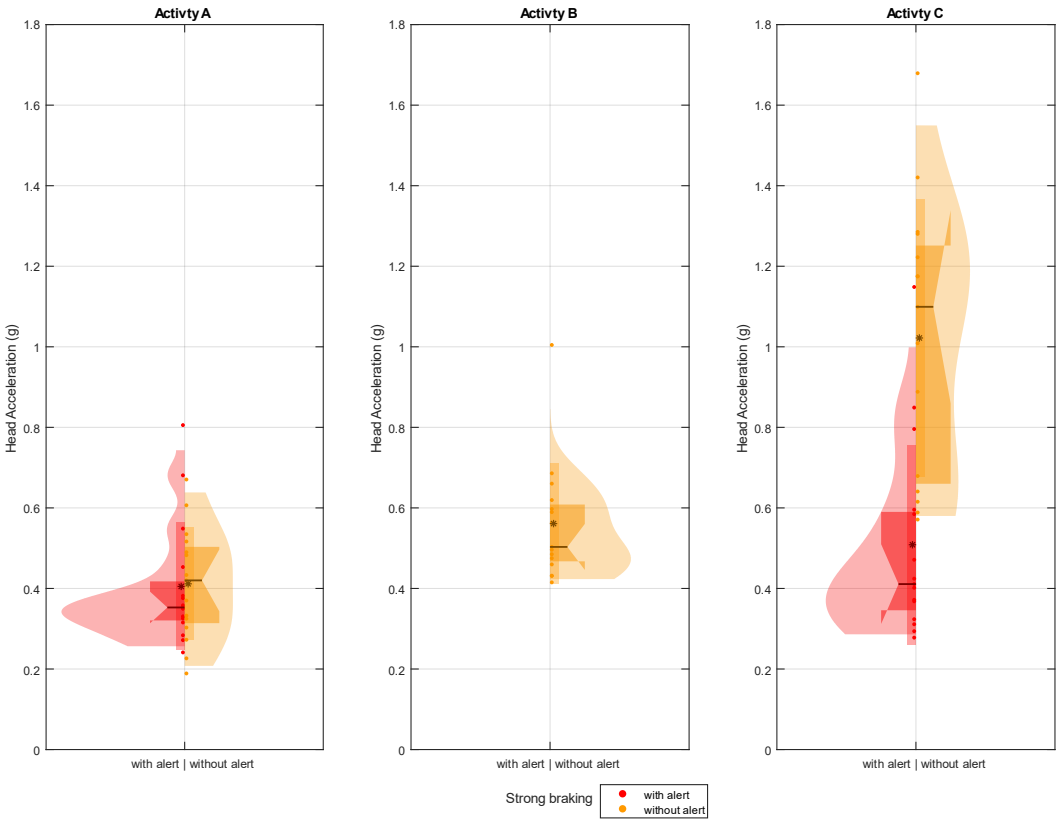

Figure 43: Head acceleration during Strong braking across different activities with and without audible alert. Activity: (A) looking at the road; (B) using devices such as a phone; (C) using devices before braking and then looking at the road when braking starts or when audible alert is activated.

3.2. Head Pitch Rotation

Table 24 presents the median and interquartile range [1st quartile; 3rd quartile] of head rotation angles (in degrees) during various occupant activities under different braking intensities (Strong and Normal). Data are compared between scenarios with and without an audible alert. "Never occurred" indicates that the specific condition was not studied for this experiment. For normal braking, head pitch rotation was almost identical in the "with alert" and “without alert “conditions when the occupants focused on the road throughout braking (Activity A). However, for the Activity C (occupant shifted attention from using a device to focusing on the road during braking or when audible alert is activated), the head pitch rotation was much higher in the absence of an alert. In the "with alert" condition, head pitch rotation is slightly greater during Activity A compared to Activity C. Additionally, in the "with alert" condition, Activities A and B (device engagement) exhibit nearly identical median head pitch rotations, whereas Activity C shows a significantly higher head pitch rotation. Under strong braking, head pitch rotation in Activity A was slightly lower in the "with alert" condition compared to the "without alert" condition, whereas in Activity C, head pitch rotation was significantly higher in the absence of an alert. In the "with alert" condition, Activity C showed greater head pitch rotation than Activity A. On the other hand, in the "without alert" condition, the highest head pitch rotation was observed in Activity C, followed by Activity B (engaging with a device), with the lowest rotation occurring in Activity A.

Both Figure 44 and Figure 45 illustrate the head pitch rotation (in degrees) experienced by occupants under three different activities: Activity A, Activity B, and Activity C. The data is presented for conditions with and without an audible alert. Each panel shows the distribution of head acceleration values, with individual data points overlaid. The colored regions represent the confidence intervals, with red indicating the "with alert" condition and yellow indicating the "without alert" condition. The black line and the asterisk within the distributions indicate the median and mean values, respectively, for each condition. Figure 44 shows these data for normal braking, while Figure 45 presents the results for strong braking.

A multivariate analysis of variance (N-way ANOVA) was performed to examine the factors affecting head pitch rotation, with participant number, audible alert activation, braking intensity, SCM and SC muscle activity, and occupant activity as the grouping variables. The significance threshold was set at 0.05 for all tests.

The analysis revealed several significant effects on head pitch rotation:

- **Participant** had a highly significant effect on head pitch rotation ($p < 10^{-5}$), indicating substantial inter-individual variability in head pitch movement during the events.
- **Braking intensity** had a significant effect on head pitch rotation ($p = 0.0456$), suggesting that different braking intensities caused measurable changes in head pitch rotation.
- **Occupant activity** was found to significantly affect head pitch rotation ($p < 10^{-5}$), demonstrating that the type of activity the occupant was engaged in influenced head pitch rotation.
- There was a **significant interaction between participant and the presence of an audible alert** ($p = 0.0101$), indicating that the effect of the audible alert on head pitch rotation varied across different participants.
- A **significant interaction between participant and braking intensity** was also observed ($p = 0.0206$), suggesting that the relationship between braking intensity and head pitch rotation differed across participants.
- A highly significant **interaction between participant and occupant activity** was found ($p < 10^{-5}$), highlighting that individual differences among participants influenced how occupant activity affected head pitch rotation.
- The **interaction between participant and muscle activity** had a significant effect on head pitch rotation ($p = 0.0007$), implying that the interaction of SCM and SC muscle activity with head pitch rotation varied among participants.
- The **interaction between audible alert and occupant activity** was highly significant ($p < 10^{-5}$), showing that the presence of an audible alert had differential effects on head pitch rotation depending on the activity of the occupant.
- Lastly, the **interaction between audible alert and muscle activity** was significant ($p = 0.0462$), indicating that the effect of muscle activity on head pitch rotation was influenced by the presence of an audible alert.

Table 24: Median and interquartile range of head pitch rotation angle across different braking intensities and activities: Comparison between conditions with and without audible alert. Activity: (A) looking at the road; (B) using devices such as a phone; (C) using devices before braking and then looking at the road when braking starts.

Braking intensity	Activity	With alert	Without alert
		Median [1st; 3rd quartile] (degrees)	Median [1st; 3rd quartile] (degrees)
Strong	A	**6.5 [4.4; 10.2]**	**9.1 [5.4; 14.7]**
	B	**Never occurred**	**13.7 [7.8; 17.1]**
	C	**13.3 [9.5; 21.9]**	**31.4 [21.4; 39.7]**
Normal	A	**10.1 [6.9; 12]**	**9.7 [6.8; 11.3]**
	B	**Never occurred**	**9.5 [5.4; 12.7]**
	C	**8.8 [6; 13.1]**	**31.5 [24.6; 35.5]**

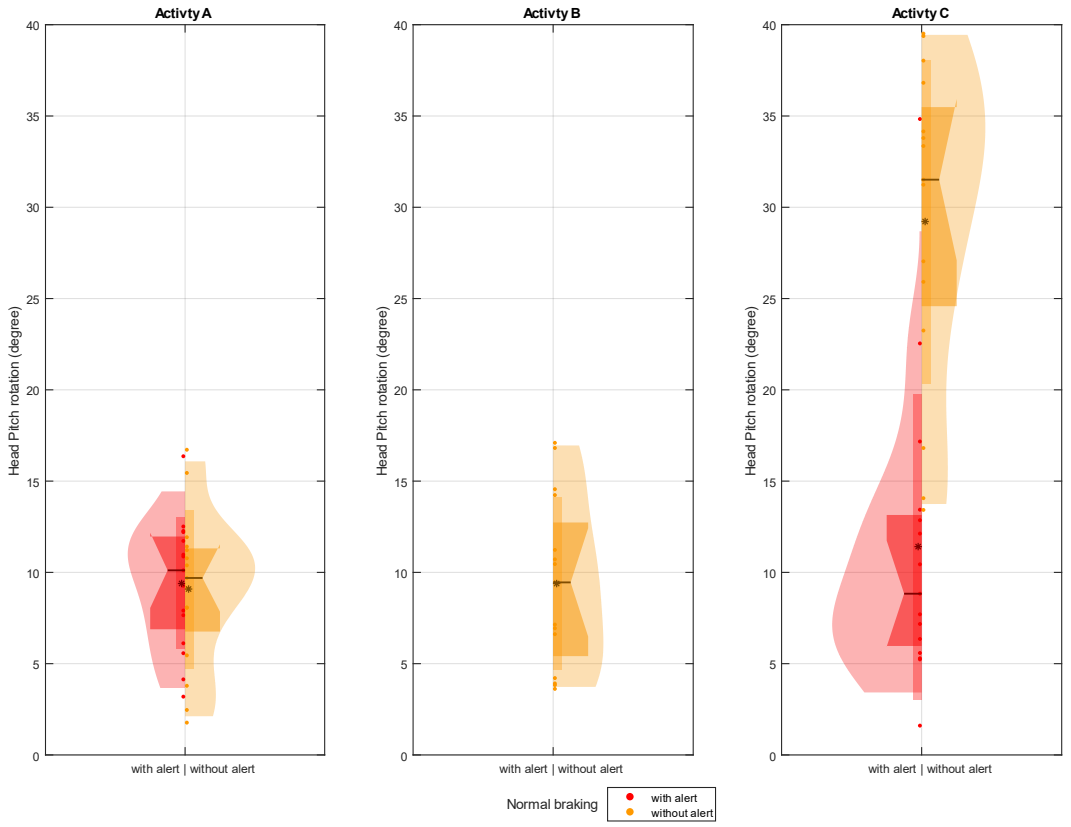

Figure 44: Head pitch rotation during normal braking across different activities with and without audible alert. Activity: (A) looking at the road; (B) using devices such as a phone; (C) using devices before braking and then looking at the road when braking starts or when audible alert is activated.

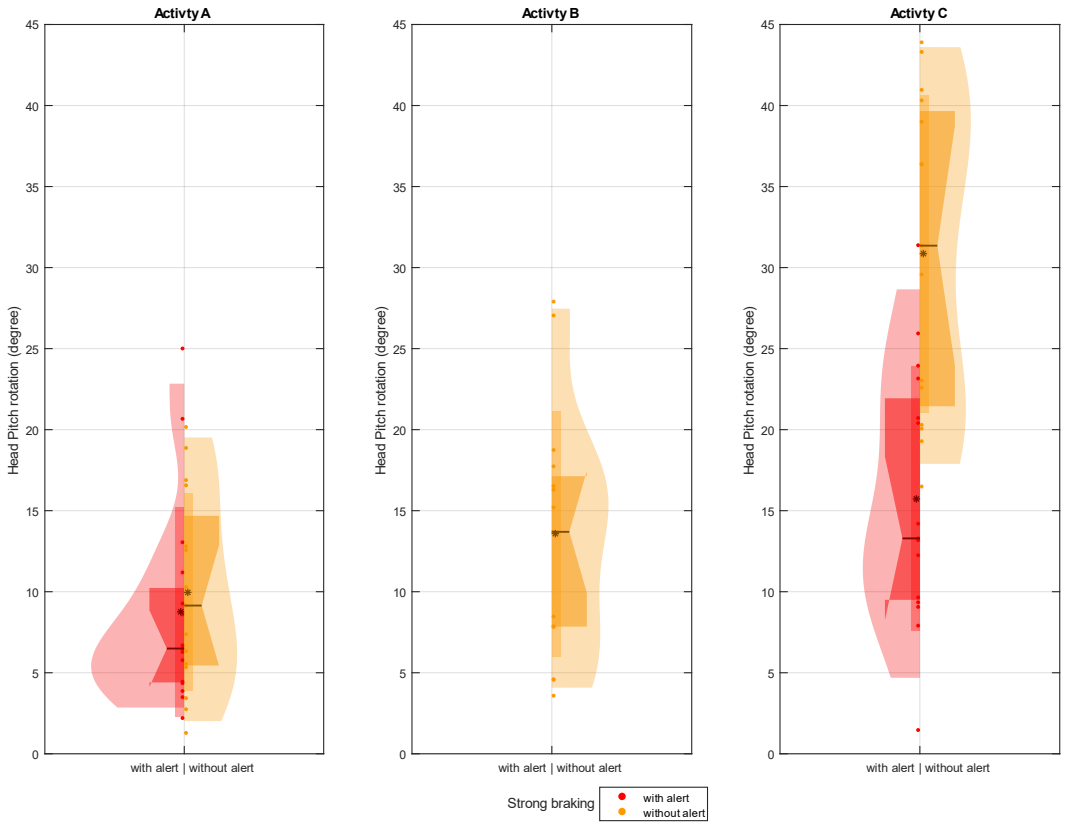

Figure 45: Head pitch rotation during strong braking across different activities with and without audible alert. Activity: (A) looking at the road; (B) using devices such as a phone; (C) using devices before braking and then looking at the road when braking starts or when audible alert is activated.

3.3. EMG of SCM and SC muscle activation

3.3.1. EMG of SCM Muscle activation

Table 25 systematically compares the occurrence rates of muscle activation across different braking scenarios and conditions, highlighting the relationship between occupant activity and muscle activation patterns observed through EMG recordings. On the first column, the first letter of each cell denotes the occupant's activity during the recorded event: (A) looking at the road; (B) using a device, such as a phone; (C) using a device before the event, then looking at the road when event begins or when audible alert is activated. The combination of a letter and a number following the activity letter represents the observed physiological response: M0 indicates the absence of muscle activation, and M1 denotes muscle activation during or after the event. Table 25 highlights the impact of alert presence on the occurrence rates during strong, and normal braking scenarios under various experimental conditions. In general, the presence of muscle activation (M1) increased under strong braking conditions compared to normal braking, particularly when an alert was provided. This trend was most pronounced for occupants who initially used a device but then looked at the road, as they demonstrated the highest rate of muscle activation (C_M1) during strong braking events both with (11 occurrences) and without (11 occurrences) an alert.

Figure 46 displays the percentage distribution of SCM muscle activation occurrences across different braking intensities (Strong, Normal) and the presence or absence of an audible alert. The x-axis corresponds to the first column of Table 25, with each bar representing a specific combination of occupant activity and the associated muscle activation response. The most occurrent condition observed was A_M1, where occupant experienced a muscle activation during or after the event when looking at the road.

Table 25: ***Occupant activity and SCM muscle response in relation to braking intensity (with and without an alert): occurrence distribution of muscle activation patterns across various braking scenarios and occupant activity*****. On the first column, the first letter of each cell denotes the occupant's activity during the recorded event: (A) looking at the road; (B) using a device, such as a phone; (C) using devices before braking and then looking at the road when braking starts or when audible alert is activated. The combination of a letter and a number following the activity letter represents the observed physiological response: M0 indicates the absence of muscle activation, and M1 denotes muscle activation `during or after the event.**

Occupant activity and SCM Muscle Response over the total occurrence (150)	Occurrence	Normal braking without alert	Normal braking with alert	Strong braking without alert	Strong braking with alert
A_M0	33	11	11	6	5
A_M1	27	4	4	9	10
B_M0	23	15	Never Occurred	8	Never Occurred
B_M1	7	0	Never Occurred	7	Never Occurred
C_M0	24	7	9	4	4
C_M1	36	8	6	11	11

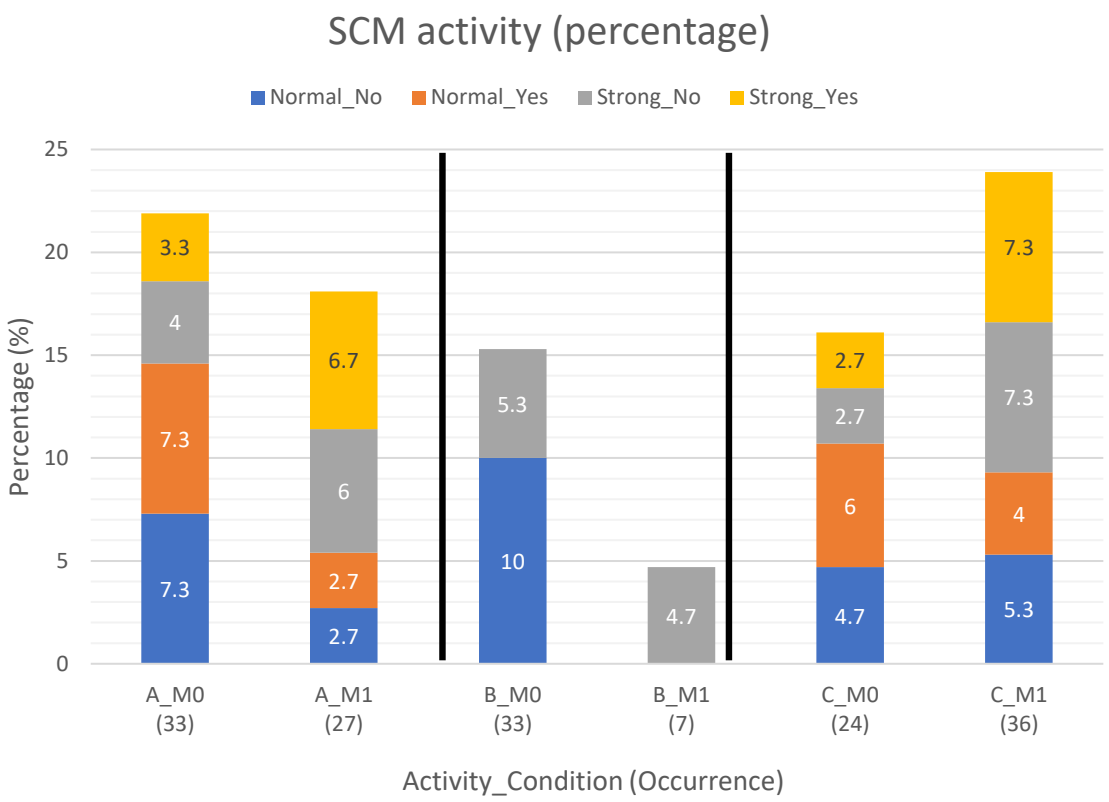

Figure 46: ***Proportion of Sternocleidomastoid (SCM) Muscle Activation Occurrences Categorized by Braking Intensity and Presence of Audible Alert.*** **The colors represent different braking intensities: Strong, and Normal. The presence ("yes") or absence ("no") of an audible alert is indicated by labels such as Strong_yes and Strong_No. On the x-axis, the first letter of each bar denotes the occupant's activity during the recorded event: (A) looking at the road; (B) using a device, such as a phone; (C) using devices before braking and then looking at the road when braking starts or when audible alert is activated. The combination of a letter and a number following the activity letter represents the observed physiological response: M0 indicates the absence of muscle activation, and M1 denotes muscle activation during or after braking. The number within parentheses indicates the frequency of occurrence for that specific condition represented by each bar.**

3.3.2. EMG of SC Muscle Activation

Table 26 systematically compares the occurrence rates of muscle activation across different braking scenarios and conditions, highlighting the relationship between occupant activity and muscle activation patterns observed through EMG recordings. On the first column, the first letter of each cell denotes the occupant's activity during the recorded event: (A) looking at the road; (B) using a device, such as a phone; (C) using a device before the event, then looking at the road when event begins or when audible alert is activated. The combination of a letter and a number following the activity letter represents the observed physiological response: M0 indicates the absence of muscle activation, and M1 denotes muscle activation during or after the event. Table 26 highlights the impact of alert presence on the occurrence rates during strong, and normal braking scenarios under various experimental conditions. Overall, muscle activation (M1) was more common during strong braking events, particularly for occupants who shifted from using a device to looking at the road (C_M1). These individuals exhibited

the highest occurrence of muscle activation, especially in strong braking events without an alert (12 occurrences) and with an alert (9 occurrences). In contrast, occupants who were looking at the road (A) showed a balanced distribution of muscle activation and non-activation across different braking intensities and alert conditions.

Figure 47 displays the percentage distribution of SC muscle activation occurrences across different braking intensities (Strong, Normal) and the presence or absence of an audible alert. The x-axis corresponds to the first column of Table 26, with each bar representing a specific combination of occupant activity and the associated muscle activation response. The most occurrent condition observed was A_M1, where occupant experienced a muscle activation during or after the event when looking at the road.

Table 26: ***Occupant activity and SC muscle response in relation to braking intensity (with and without an alert): occurrence distribution of muscle activation patterns across various braking scenarios and occupant activity*****. On the first column, the first letter of each cell denotes the occupant's activity during the recorded event: (A) looking at the road; (B) using a device, such as a phone; (C) using devices before braking and then looking at the road when braking starts or when audible alert is activated. The combination of a letter and a number following the activity letter represents the observed physiological response: M0 indicates the absence of muscle activation, M1 denotes muscle activation during or after the event.**

Occupant activity and SC Muscle Response over the total occurrence (150)	Occurrence	Normal braking without alert	Normal braking with alert	Strong braking without alert	Strong braking with alert
A_M0	40	12	13	8	7
A_M1	20	3	2	7	8
B_M0	25	14	Never Occurred	11	Never Occurred
B_M1	5	1	Never Occurred	4	Never Occurred
C_M0	18	3	6	3	6

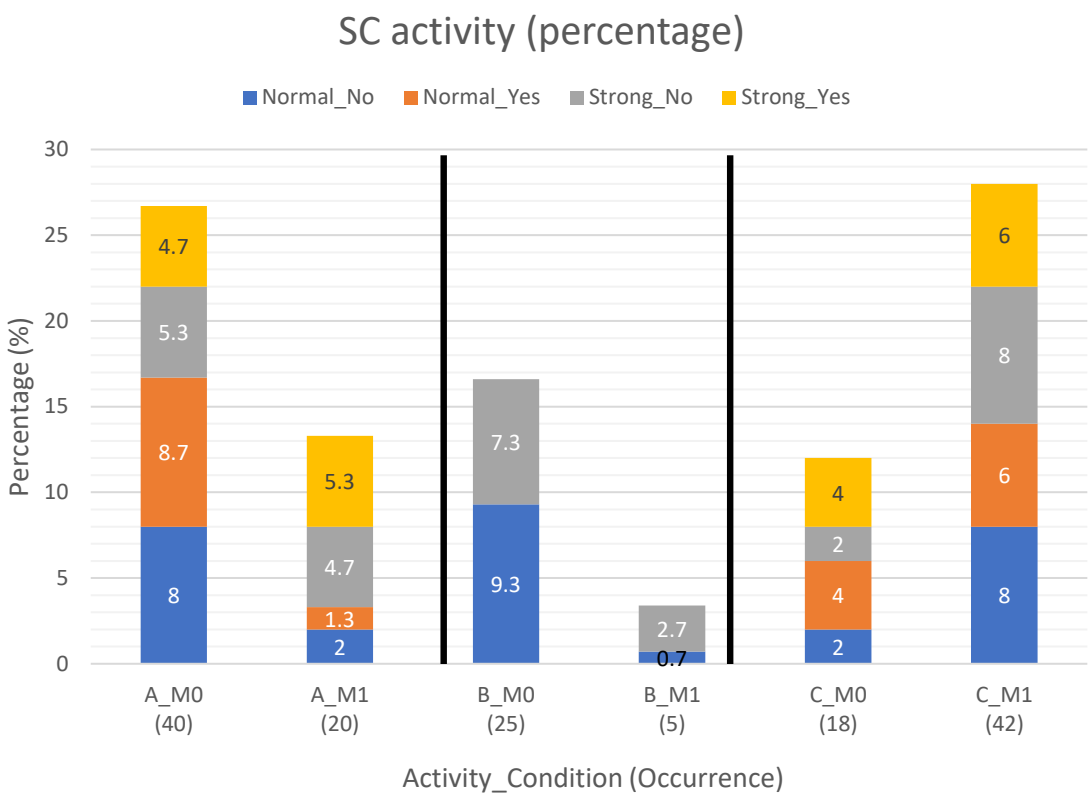

Figure 47: ***Proportion of splenius capitis (SC) Muscle Activation Occurrences Categorized by Braking Intensity and Presence of Audible Alert.*** **The colors represent different braking intensities: Strong, and Normal. The presence ("yes") or absence ("no") of an audible alert is indicated by labels such as Strong_yes and Strong_No. On the x-axis, the first letter of each bar denotes the occupant's activity during the recorded event: (A) looking at the road; (B) using a device, such as a phone; (C) using devices before braking and then looking at the road when braking starts or when audible alert is activated. The combination of a letter and a number following the activity letter represents the observed physiological response: M0 indicates the absence of muscle activation, M1 denotes muscle activation during or after the event, and M2 signifies muscle activation occurring twice: first, right after the audible alert, and again during or after the event. The number within parentheses indicates the frequency of occurrence for that specific condition represented by each bar.**

3.3.3. ANOVA test results for Muscle activity

A multivariate analysis of variance (N-way ANOVA) was conducted to assess the factors influencing **sternocleidomastoid (SCM)** and **splenius capitis (SC)** muscle activation, where the muscle activity was coded as binary data: **1** if one or both muscles were active and **0** if neither muscle was active. The grouping variables included participant number, audible alert activation, braking intensity, and occupant activity. The significance threshold was set to 0.05. The analysis revealed several significant effects on SCM and SC muscle activity:

- **Participant** had a highly significant effect on muscle activity ($p < 10^{-5}$), indicating that individual differences among participants strongly influenced muscle response.
- **Braking intensity** also had a highly significant effect on muscle activity ($p < 10^{-5}$), suggesting that the intensity of braking significantly impacted SCM and SC muscle responses.

- **Occupant activity** was found to have a significant effect on muscle activity ($p = 0.0007$), demonstrating that the type of task the occupant was engaged in influenced the level of muscle activation.
- There was a **significant interaction between participant and occupant activity** ($p = 0.0015$), indicating that the effect of occupant activity on muscle response varied across different participants.
- The **interaction between braking intensity and occupant activity** had a significant effect on muscle activity ($p = 0.0004$), suggesting that the combination of braking intensity and the occupant's activity had a measurable impact on the muscle response.

4. Discussion

In this study, we explored how different braking intensities and occupant activities influence head-neck kinematics and muscle responses in a simulated autonomous vehicle (AV) environment. Five participants, with varying levels of driving experience, engaged in three non-driving activities (looking at the road, using a device, and switching attention from a device to the road) while experiencing both normal (0.3 g) and strong (0.6 g) braking scenarios. The participants were seated in a dynamic SLED system synchronized with a virtual AV environment, allowing for the precise measurement of head acceleration, head pitch rotation, and muscle activation using inertial measurement units (IMUs) and electromyography (EMG) sensors. Additionally, the presence or absence of audible alerts was systematically manipulated to assess its impact on occupant response.

The study revealed that head acceleration and head pitch rotation significantly increased during strong braking in the absence of audible alerts, indicating that occupants were less prepared for sudden deceleration. Without warnings, occupants experienced exaggerated head movements, likely due to reduced awareness and delayed reflexive stabilization, which led to greater head displacement and higher acceleration forces. In contrast, the presence of audible alerts allowed occupants to anticipate the braking event, adjust their posture, and brace themselves by tightening muscles or shifting position. This not only reduced head acceleration but also minimized head pitch rotation, mitigating excessive forward movement—a primary contributor to whiplash injuries. These findings align with previous research showing that preemptive cues, such as audible alerts, enhance response times and reduce the severity of physical reactions during sudden braking (Di Loreto et al., 2019; Mackenzie et al., 2022). By preparing occupants for the deceleration, alert systems in autonomous vehicles (AVs) play a crucial role in reducing the potential physical impact and injury risk.

Head acceleration varied significantly based on the activities occupants were engaged in during braking events. The highest head accelerations were observed during Activity C, where participants were using a device and shifted their attention to the road only when braking or an alert occurred. This suggests that multitasking and cognitive distractions delay the physical response to sudden deceleration, resulting in greater head movement. In contrast, participants focused on the road (Activity A) consistently exhibited the lowest head accelerations, indicating that maintaining visual attention allows for better anticipation of braking events and minimizes excessive head movement. These findings are consistent

with previous research on driver distraction, which shows that engaging in secondary tasks impairs reaction time and reduces situational awareness (Li et al., 2019; Louw et al., 2015; Zangi et al., 2022). The higher head accelerations associated with device use in Activities B and device use then looking at the road in Activity C are likely due to increased cognitive load and delayed reflexes. Together, these results underscore the critical need to address cognitive distractions in the design of autonomous vehicle (AV) safety systems, as occupants may be less attentive to the driving environment. Effective alert systems are essential for mitigating the effects of occupant inattention and ensuring occupant safety during sudden braking events.

Additionally, electromyography (EMG) data revealed increased muscle activation in the sternocleidomastoid (SCM) and splenius capitis (SC) muscles during strong braking, particularly when an audible alert was present. This heightened muscle activity suggests that the alerts triggered a physiological response, prompting occupants to engage their neck muscles in anticipation of deceleration. The enhanced preparedness likely contributed to stabilizing the head and neck during braking. Previous research shows that anticipatory neck muscle activation plays a key role in injury prevention by absorbing forces that could otherwise cause excessive movement or strain (Eckner et al., 2014; Siegmund et al., 2003). In AVs, this anticipatory response may be crucial in reducing injury risk, as it allows for more controlled and stabilized movements during sudden braking. The increased muscle activation observed in this study highlights the dual importance of alert systems in both cognitive and physiological preparedness, enhancing safety in AV systems.

The study also revealed significant inter-participant variability in head acceleration, head pitch, and muscle activation during braking events, suggesting individual factors may influence responses to sudden deceleration. These differences imply that a one-size-fits-all approach to AV safety may not be sufficient. Tailored safety measures, such as adjustable alert systems that account for individual response times and customizable seat and restraint designs, could more effectively address the variability in occupant responses during braking events. Previous studies have emphasized the importance of personalized safety interventions in autonomous vehicles to accommodate individual differences in reaction times and physical responses (Ataya et al., 2021; Bellem et al., 2017; Manawadu et al., 2015). These insights highlight the importance of designing AV systems that adapt to occupant-specific needs to maximize safety outcomes.

The statistical analysis findings collectively demonstrate that head acceleration, head pitch rotation, and SCM/SC muscle activity are all significantly influenced by a combination of individual participant differences and external stimuli. Head acceleration is shaped by both occupant activity and braking intensity, along with complex interactions between participant characteristics and muscle activity. Similarly, head pitch rotation is affected by individual variability, as well as interactions between braking intensity, audible alerts, and occupant-specific factors such as activity and muscle response. In terms of muscle activity, SCM and SC muscle responses are modulated not only by individual differences and braking intensity, but also by the occupant's activity. The interactions between these factors, particularly between participants and their activities, as well as braking intensity and occupant activity, play a key

role in further influencing muscle response. Taken together, these results highlight the multifactorial nature of head and muscle dynamics in response to varying external stimuli and individual characteristics.

5. Limitations

Sample Size and Generalizability: The experiment had a small sample size (five participants), and all participants had no prior experience with the SLED system, which could limit the generalizability of the findings to a larger population. Further studies with a larger, more diverse population are needed to confirm these findings, especially given the significant variability between participants.

Lack of Real-World Scenarios: While the virtual environment mimicked urban settings, the absence of real-world variables (e.g., road conditions, other vehicles) could affect the ecological validity of the findings. Additionally, interior design of the AV could use a more interactive setting to improve immersion.

6. Conclusion

In conclusion, the present study aimed to investigate the effects of braking intensity and occupant activities on head and neck responses in a simulated autonomous vehicle (AV) environment. Our findings reveal that both braking intensity and the presence of audible alerts significantly influenced head acceleration, head pitch, and muscle activation in participants. Notably, strong braking without an audible alert resulted in the highest head acceleration and pitch rotation, particularly when participants shifted their attention from using a device to looking at the road during braking. These results highlight the crucial role of occupant preparedness, facilitated by audible alerts, in reducing sudden head movements and muscle activation during abrupt deceleration. This study contributes to the growing body of literature on occupant safety in AVs by emphasizing the need for enhanced alert systems to mitigate the risk of injury during braking events. Future AV designs should incorporate not only emergency braking systems but also sophisticated alert mechanisms, potentially integrating multisensory cues (e.g., auditory, haptic, or visual alerts) to enhance occupant awareness and preparedness. By providing advanced warning of deceleration events, AV systems can help reduce the physical impact of braking, particularly when occupants may be distracted. This approach aligns with optimizing safety in AVs, ensuring that occupants are not only passively protected but also actively prepared for emergency scenarios.

Future research could explore additional sensory alerts, such as haptic or visual cues, to further reduce head and neck movement during AV braking, building on the effectiveness of audible alerts. Moreover, while the current experiment was conducted over 30 trials, investigating the effects of repeated exposure to AV braking scenarios in longitudinal studies could provide insights into how occupant responses evolve over time. Understanding whether muscle activation and head movement patterns change with increased familiarity and adaptation to AV systems would offer valuable data for optimizing occupant safety and comfort in autonomous vehicles

CHAPTER 5: COMPARISON BETWEEN SAAM AND SLED EXPERIMENTS

Table 27 displays a comparison of the median head acceleration between the SAAM experiment and the SLED experiment. Before presenting the comparison, it is good to keep in mind that In the SAAM normal braking was between 0.2 and 0.4 g, Strong braking was between 0.4 and 0.6 g. on the other hand in the sled, normal braking was 0.3 g, and strong braking was 0.6 g. The analysis will focus exclusively on head acceleration because the comparative results for head acceleration and head pitch rotation were similar.

Table 27: Head acceleration comparison between the SAAM experiment and the SLED experiment: Median head pitch acceleration across different braking intensities and activities: Comparison between conditions with and without audible alert. Activity: (A) looking at the road; (B) using devices such as a phone; (C) using devices before braking and then looking at the road when braking starts or when audible alert is activated.

Braking intensity	Activity	With Alert (SAAM)	With Alert (SLED)	Without alert (SAAM)	Without alert (SLED)
		Median [1st; 3rd quartile] (g)	Median [1st; 3rd quartile] (g)	Median [1st; 3rd quartile] (g)	Median [1st; 3rd quartile] (g)
Strong	A	**0.68 [0.55 ; 0.74]**	**0.36 [0.32; 0.42]**	**0.43 [0.36 ; 0.52]**	**0.42 [0.31; 0.5]**
	B	**Never occurred**	**Never occurred**	**0.4 [0.32 ; 0.52]**	**0.5 [0.47; 0.61]**
	C	**Never occurred**	**0.41 [0.35; 0.59]**	**0.49 [0.42 ; 0.86]**	**1.11 [0.66; 1.25]**
Normal	A	**0.31 [0.27 ; 0.37]**	**0.18 [0.14; 0.19]**	**0.32 [0.25 ; 0.37]**	**0.17 [0.15; 0.22]**
	B	**Never occurred**	**Never occurred**	**0.32 [0.29 ; 0.42]**	**0.32 [0.27; 0.34]**
	C	**0.33 [0.26 ; 0.38]**	**0.19 [0.14; 0.22]**	**0.43 [0.29 ; 0.47]**	**0.73 [0.51; 1.25]**

1. Similarities between each activity

An analysis of the head acceleration data reveals several similarities between the SAAM and SLED experiments across different activities and braking conditions. Looking at Table 27, in **Activity A** (looking at the road), during strong braking without an alert, the head acceleration values were almost identical between the two experiments—0.43 g for SAAM and 0.42 g for SLED. This suggests a consistent response when participants were fully attentive to the road without any audible warnings.

In **Activity B** (using devices), the head acceleration values during strong braking without an alert were also very close between the two experiments, with SAAM recording 0.4 g and SLED 0.5 g. Additionally, during normal braking without alerts, both SAAM and SLED experiments showed identical head acceleration values of 0.32 g. These findings indicate that the act of using devices did not significantly

alter the head acceleration outcomes between the two experimental setups under these specific conditions.

For **Activity C** (using devices, then looking at the road during braking), the SLED experiment consistently yielded higher head acceleration values than the SAAM experiment across braking conditions without alert, however it was lower for the normal braking condition with an alert. This deviation suggests that the transition from device use to road observation during braking may have been influenced differently in the two experimental settings.

Overall, the observed similarities, particularly in Activities A and B without alerts, highlight a consistent head acceleration response between the SAAM and SLED experiments. The identical head acceleration of 0.32 g during normal braking without alerts in Activity B further underscores this consistency. These parallels reinforce the reliability of the findings across different experimental conditions and support the validity of the comparative analysis.

2. Similarities between patterns

An analysis of the head acceleration data reveals that both the SAAM and SLED experiments exhibit minimal differences between **Activity A** (participants looking at the road) and **Activity C** (participants using devices and then shifting their attention back to the road when braking begins or an alert is activated) during normal braking with an alert. In the SAAM experiment, head acceleration was 0.31 g for Activity A and 0.33 g for Activity C, a difference of only 0.02 g. Similarly, the SLED experiment showed head accelerations of 0.18 g for Activity A and 0.19 g for Activity C, differing by just 0.01 g. Although the absolute values differ between the two experiments, the relative differences between Activities A and C are consistently small. This suggests that during normal braking with an alert, whether a participant is continuously looking at the road or redirects their attention back to the road after using devices, the head acceleration remains nearly the same.

Furthermore, **Activity C** consistently yielded the highest head acceleration values across all conditions in both experiments. During strong braking without an alert, Activity C recorded head accelerations of 0.49 g in the SAAM experiment and 1.11 g in the SLED experiment—the highest values in their respective datasets. In normal braking without an alert, Activity C again resulted in the highest head accelerations, with values of 0.43 g for SAAM and 0.73 g for SLED. Even during normal braking with an alert, Activity C maintained the highest head acceleration values, registering 0.33 g in SAAM and 0.19 g in SLED. These consistent findings across both experiments and varying braking intensities indicate that the action of using devices followed by redirecting attention to the road during braking significantly increases head acceleration compared to Activities A and B, regardless of the presence of an alert.

2.1. Abnormality with strong barking with alert during Activity A

Upon examining head acceleration during strong braking with an audible alert in Chapter 3, we observed results that were contrary to our expectations. Specifically, head acceleration was higher when an alert was present compared to the condition without an alert. We hypothesized that this could be due to the use of the same audible alert for all braking intensities. Since the order of braking intensities with audible alerts in the SAAM experiment was normal, then strong, then normal, occupants may have anticipated the same braking intensity following the audible alert. As a result, they were less prepared when the braking intensity was stronger than expected, leading to increased head acceleration.

To investigate this hypothesis, we replicated the same order in the first batch of trials during the SLED experiment. Analysis of the overall median head acceleration for strong braking with an audible alert during Activity A in the SLED experiment showed results consistent with what we anticipated should have occurred in the SAAM experiment. However, when focusing on just the first batch of trials—where the order of audible alerts was similar to that in the SAAM experiment—we again found that head acceleration was higher with the presence of an audible alert. The median head acceleration was 0.4 g with an alert and 0.3 g without an alert, while the mean values were 0.5 g with an alert and 0.3 g without an alert.

These findings further confirm our initial hypothesis and highlight the need to investigate the effects of using different audible alerts for varying braking intensities. It is also noteworthy that in the second and third batches of trials during the SLED experiment for this condition, the head acceleration patterns for each participant were similar to those observed during normal braking under the same conditions.

CHAPTER 6: CONCLUSION AND PERSPECTIVES

1. Thesis Conclusion

The research presented in this manuscript aimed to address two primary research questions:

1. **How do the activities in which occupants are engaged prior to an emergency maneuver in an autonomous vehicle influence the body's physiological response under specific pre-maneuver conditions?**
2. **How can driving simulators and dynamic virtual environments help improve Human-Machine Interaction (HMI) in autonomous vehicles, especially sensory modalities?**

To answer these questions, the study was structured around two key experiments, each addressing one of the research axes: the impact of non-driving activities on occupant safety and the enhancement of HMI in AVs using sensory modalities. The findings of this research contribute to a more nuanced understanding of occupant safety and behaviour in autonomous driving contexts.

1.1. Impact of Occupant Activities on Head-Neck Dynamics in AVs

Our investigation into the impact of occupant activities prior to an emergency maneuver revealed that different non-driving tasks significantly affects head-neck kinematics during sudden braking events. Participants who were using their device before braking the looked at the road during the event or after hearing the audible alert experienced greater head accelerations and pitch rotations, indicating a delayed response to sudden deceleration. This result underscores the influence of cognitive load and attention on the body's dynamic response to AV maneuvers.

The study further demonstrated that the presence of auditory alerts plays a crucial role in preparing occupants for emergency braking, leading to anticipatory muscle activation and reduced head movement and acceleration. These findings highlight the importance of integrating multisensory alert systems in AV design to enhance occupant preparedness and minimize the risk of a potential injury. However, the significant variability observed among participants suggests that individual differences play a role in how occupants respond to sudden maneuvers. Therefore, the results indicate that AVs should be designed with these individual differences considered in the process, allowing for more personalized safety features. Nevertheless, these differences should be more thoroughly investigated in future studies to identify them and choose the appropriate adaptive safety mechanisms to mitigate associated risks.

While our study provides valuable insights into the relationship between occupant activities and physiological responses, the limitations, including the small sample size, suggest that further research is necessary. Future experiments should explore how a larger, more diverse population responds to various non-driving activities, potentially validating these findings in real-world AV scenarios.

1.2. Enhancing HMI in Virtual Environments for Realistic Occupant Behaviour

The second research question focused on how virtual environments and driving simulators can improve the HMI in AVs, particularly by replicating realistic occupant behaviours during emergency situations. Our findings demonstrated that the integration of auditory alerts within these environments effectively enhances occupant awareness and anticipatory responses. Specifically, participants responded more promptly to braking events when audible alerts were present, reducing the potential for excessive head movement and muscle strain. This suggests that the incorporation of sensory modalities, such as sound cues, is instrumental in achieving a more accurate representation of occupant behaviour and physiological responses in AV emergencies. It is also important to highlight the need to further investigate the effects of using different audible alerts for varying braking intensities.

The use of advanced simulation tools, including the SAAM driving simulator and the dynamic SLED system, allowed for a controlled investigation into the effects of emergency maneuvers on occupant responses. However, challenges related to the noise in electromyography (EMG) data acquisition were encountered during the SAAM experiment, indicating that future studies should incorporate more sophisticated sensors.

The insights gained from this research suggest that dynamic virtual environments are valuable tools for studying HMI and occupant safety in autonomous vehicles, offering a platform for understanding how sensory feedback mechanisms can be optimized. Further exploration into other sensory modalities, such as haptic or visual cues, could provide a more comprehensive understanding of how occupants interact with AV systems during emergency maneuvers.

1.3. Summary of the Work

The research reported in this manuscript was motivated by the growing need to understand occupant safety in SAE Level 3 autonomous vehicles, where occupants are going to be increasingly engaged in non-driving activities. The study is original in its approach to combining biomechanical sensors, virtual reality, and driving simulation technologies to explore head-neck dynamics under varying emergency maneuvers and across different conditions. This research contributes to the broader understanding of how occupant activities influence physiological responses and the potential for enhancing HMI using sensory modalities.

Our work demonstrates the critical role that multisensory alert systems play in preparing occupants for sudden maneuvers, thereby reducing the potential risk of injury. The significant variability in individual responses further highlights the necessity for adaptive AV safety systems that cater to diverse occupant profiles, rather than adopting a one-size-fits-all approach.

In conclusion, this study underscores the importance of considering both occupant activities and the integration of sensory modalities in AV design to improve occupant safety and comfort. By addressing the gaps in existing literature, our findings pave the way for more adaptable and responsive AV systems that can better accommodate the varied needs of occupants in autonomous transportation settings.

2. Perspective and Future work

The conclusions drawn from our work offer several promising perspectives for the continuation of this research. In the short term, refining the experimental protocols, particularly in the use of driving simulators and SLED systems, will enable us to build on the insights gained regarding occupant behaviour and physiological responses in autonomous vehicle scenarios. Enhancing data acquisition methods, incorporating advanced multisensory feedback, and increasing the realism of virtual environments will further our understanding of how non-driving activities and individual variability influence head-neck dynamics. These improvements will pave the way for more comprehensive studies, ultimately contributing to the development of adaptive and personalized safety systems for future autonomous vehicles.

2.1. Extending the SLED's Operational Duration for Longer Simulations

Extending the SLED's operational duration to simulate a full 10-minute or longer autonomous drive in urban environments with straight roads—such as those found in New York City—could broaden the scope of our experiments. Currently, the SLED is equipped with safety features that limit testing to braking events lasting up to 20 seconds, where the virtual vehicle accelerates, maintains a constant velocity, and then executes sudden braking. By leveraging the SLED's ability to move back and forth along its axis, it is feasible to simulate longer drives. This extension would enable us to test occupant behaviour, cognitive responses, human-machine interface (HMI) interactions, and safety in short-trip scenarios using the SLED—a methodology that, to our knowledge, has not been previously explored.

2.2. Incorporating Additional Degrees of Freedom into the SLED

Adding additional degrees of freedom to the SLED represents a significant enhancement to study other or combined AV emergency maneuvers. Currently constrained to linear motion along one axis, the sled's ability to simulate other maneuvers common in AVs—such as lane changing and turning—is limited. Incorporating a rotating base beneath the seat to simulate turning, along with a mechanism that allows lateral inclination to mimic lane changes, would enable the study of more complex head-neck responses during emergency maneuvers. This modification would provide a more comprehensive understanding of occupant biomechanics under a wider range of driving conditions using the SLED.

2.3. Transforming the SLED into an Immersive Cockpit Environment

Transforming the SLED into a cockpit-like environment equipped with screens and advanced HMIs would offer a more immersive and realistic experience for participants. By creating a virtual vehicle interior where subjects can interact with various devices, particularly their smartphones, we can better simulate real-world conditions. This setup would facilitate the study of occupant behaviour and interaction with in-vehicle systems, providing valuable insights into how distractions and engagement with technology affect safety and cognitive load during autonomous driving.

2.4. Enhancing the Driving Simulator's Interior Design and Alert Systems

Furthermore, improving the interior design of the driving simulator and incorporating multiple alert systems can offer a deeper understanding of the effects of different sensory alerts on the occupants HMI, behaviour, and safety. The simulator used in our experiments had an outdated interior and was limited to a single sensory alert system—audible alerts. In contrast, modern SAE Level 3 AVs are equipped with at least two sensory alert systems, typically audio-visual, along with dashboard screens and tablets that provide extensive information about the vehicle's surroundings and environmental conditions. Enhancing the simulator to include these features would allow us to test different alert configurations for varying braking intensities, thereby improving the ecological validity of our studies and aligning them more closely with current industry standards.

2.5. Implementing Vehicle-in-the-Loop (VIL) Playback Testing

Implementing Vehicle-in-the-Loop (VIL) or vehicle playback testing is proposed to further validate the findings from the SLED and driving simulator experiments. In this approach, we would use pre-recorded data from the virtual environment to guide a real vehicle operating in a controlled physical space, such as a large empty parking lot or an airport tarmac. The vehicle would drive as if it were in the virtual environment, with the surroundings projected onto the windshield and side windows to achieve a high level of immersion. Occupants inside the vehicle would be free to interact with the vehicle as they please or be instructed to perform specific activities, mirroring the protocols used in the SAAM and SLED experiments. This method would expose participants to real-life scenarios and physical forces, thereby potentially further validating the SAAM and SLED experiments.

2.6. Conclusion

In conclusion, these proposed enhancements aim to elevate the fidelity and scope of our experimental setups. By incorporating longer drive simulations, additional degrees of freedom, immersive cockpits with advanced HMIs, improved alert systems, and VIL testing, we can conduct more comprehensive investigations into occupant behaviour, safety, and human-machine interactions in autonomous vehicles. These advancements will contribute valuable knowledge to the field and support the development of safer and more user-centric AV technologies.

REFERENCES

Akamatsu, M., Green, P., Bengler, K., 2013. Automotive Technology and Human Factors Research: Past, Present, and Future. Int. J. Veh. Technol. 2013, 1–27. https://doi.org/10.1155/2013/526180

Ataya, A., Kim, W., Elsharkawy, A., Kim, S., 2021. How to Interact with a Fully Autonomous Vehicle: Naturalistic Ways for Drivers to Intervene in the Vehicle System While Performing Non-Driving Related Tasks. Sensors 21, 2206. https://doi.org/10.3390/s21062206

Beeman, S.M., Kemper, A.R., Madigan, M.L., Duma, S.M., 2011. Effects of Bracing on Human Kinematics in Low-Speed Frontal Sled Tests. Ann. Biomed. Eng. 39, 2998–3010. https://doi.org/10.1007/s10439-011-0379-1

Beeman, S.M., Kemper, A.R., Madigan, M.L., Franck, C.T., Loftus, S.C., 2012. Occupant kinematics in low-speed frontal sled tests: Human volunteers, Hybrid III ATD, and PMHS. Accid. Anal. Prev. 47, 128–139. https://doi.org/10.1016/j.aap.2012.01.016

Bellem, H., Klüver, M., Schrauf, M., Schöner, H.-P., Hecht, H., Krems, J.F., 2017. Can We Study Autonomous Driving Comfort in Moving-Base Driving Simulators? A Validation Study. Hum. Factors J. Hum. Factors Ergon. Soc. 59, 442–456. https://doi.org/10.1177/0018720816682647

Bertollini, G., Brainer, L., Chestnut, J.A., Oja, S., Szczerba, J., 2010. General Motors Driving Simulator and Applications to Human Machine Interface (HMI) Development. Presented at the SAE 2010 World Congress & Exhibition, pp. 2010-01–1037. https://doi.org/10.4271/2010-01-1037

Biondi, F., Rossi, R., Gastaldi, M., Mulatti, C., 2014. Beeping ADAS: Reflexive effect on drivers' behavior. Transp. Res. Part F Traffic Psychol. Behav. 25, 27–33. https://doi.org/10.1016/j.trf.2014.04.020

Boelhouwer, A., Van Dijk, J., Martens, M.H., 2019. Turmoil Behind the Automated Wheel: An Embodied Perspective on Current HMI Developments in Partially Automated Vehicles, in: Krömker, H. (Ed.), HCI in Mobility, Transport, and Automotive Systems, Lecture Notes in Computer Science. Springer International Publishing, Cham, pp. 3–25. https://doi.org/10.1007/978-3-030-22666-4_1

Bohrmann, D., Bengler, K., 2020. Reclined Posture for Enabling Autonomous Driving, in: Ahram, T., Karwowski, W., Pickl, S., Taiar, R. (Eds.), Human Systems Engineering and Design II, Advances in Intelligent Systems and Computing. Springer International Publishing, Cham, pp. 169–175. https://doi.org/10.1007/978-3-030-27928-8_26

Campbell, J.L., Brown, J.L., Graving, J.S., Richard, C.M., Lichty, M.G., Bacon, L.P., Morgan, J.F., Li, H., Williams, D.N., Sanquist, T., 2018. Human Factors Evaluation of Level 2 and Level 3 Automated Driving Concepts. https://doi.org/10.13140/RG.2.1.1874.7361

Carsten, O., Martens, M.H., 2019. How can humans understand their automated cars? HMI principles, problems and solutions. Cogn. Technol. Work 21, 3–20. https://doi.org/10.1007/s10111-018-0484-0

Chardonnet, J.-R., Mirzaei, M.A., Merienne, F., 2021. Influence of navigation parameters on cybersickness in virtual reality. Virtual Real. 25, 565–574. https://doi.org/10.1007/s10055-020-00474-2

Chardonnet, J.-R., Mirzaei, M.A., Mérienne, F., 2015. Visually Induced Motion Sickness Estimation and Prediction in Virtual Reality using Frequency Components Analysis of Postural Sway Signal. ICAT-EGVE 2015 - Int. Conf. Artif. Real. Telexistence Eurographics Symp. Virtual Environ. https://doi.org/10.2312/EGVE.20151304

Cohen-Lazry, G., Katzman, N., Borowsky, A., Oron-Gilad, T., 2019. Directional tactile alerts for take-over requests in highly-automated driving. Transp. Res. Part F Traffic Psychol. Behav. 65, 217–226. https://doi.org/10.1016/j.trf.2019.07.025

Corrales, M.A., 2021. Development of Elderly Posture Male and Female Finite Element Neck Models and Assessment of Tissue-Level Response Under Impact Loading. https://doi.org/10.13140/RG.2.2.10359.75682

Cunningham, M.L., Regan, M.A., 2018. Driver distraction and inattention in the realm of automated driving. IET Intell. Transp. Syst. 12, 407–413. https://doi.org/10.1049/iet-its.2017.0232

Di Loreto, C., 2019. Apport des simulations immersives pour l'étude du comportement dynamique des occupants d'un véhicule.

Di Loreto, C., Dutschke, J., Forrest, M., Van Den Berg, A., Chardonnet, J., Mérienne, F., Mackenzie, J., Sandoz, B., 2019. Head dynamics during emergency braking events. Comput. Methods Biomech. Biomed. Engin. 22, S224–S226. https://doi.org/10.1080/10255842.2020.1714249

Diels, C., Bos, J.E., Hottelart, K., Reilhac, P., 2016. Motion Sickness in Automated Vehicles: The Elephant in the Room, in: Meyer, G., Beiker, S. (Eds.), Road Vehicle Automation 3, Lecture Notes in Mobility. Springer International Publishing, Cham, pp. 121–129. https://doi.org/10.1007/978-3-319-40503-2_10

Dijksterhuis, C., Stuiver, A., Mulder, B., Brookhuis, K.A., De Waard, D., 2012. An Adaptive Driver Support System: User Experiences and Driving Performance in a Simulator. Hum. Factors J. Hum. Factors Ergon. Soc. 54, 772–785. https://doi.org/10.1177/0018720811430502

Dosovitskiy, A., Ros, G., Codevilla, F., Lopez, A., Koltun, V., 2017. CARLA: An Open Urban Driving Simulator. 1st Annu. Conf. Robot Learn. 16. https://doi.org/PMLR 78:1-16, 2017

Doubek, F., Loosveld, E., Happee, R., De Winter, J., 2020. Takeover Quality: Assessing the Effects of Time Budget and Traffic Density with the Help of a Trajectory-Planning Method. J. Adv. Transp. 2020, 1–12. https://doi.org/10.1155/2020/6173150

Dunn, N., Dingus, T., Soccolich, S., 2019. Understanding the Impact of Technology: Do Advanced Driver Assistance and SemiAutomated Vehicle Systems Lead to Improper Driving Behavior?

Dutia, M.B., 1991. The muscles and joints of the neck: Their specialisation and role in head movement. Prog. Neurobiol. 37, 165–178. https://doi.org/10.1016/0301-0082(91)90026-W

Eckner, J.T., Oh, Y.K., Joshi, M.S., Richardson, J.K., Ashton-Miller, J.A., 2014. Effect of Neck Muscle Strength and Anticipatory Cervical Muscle Activation on the Kinematic Response of the Head to Impulsive Loads. Am. J. Sports Med. 42, 566–576. https://doi.org/10.1177/0363546513517869

Ejima, S., Zama, Y., Ono, K., Kaneoka, K., Shiina, I., Asada, H., 2009. PREDICTION OF PRE-IMPACT OCCUPANT KINEMATIC BEHAVIOR BASED ON THE MUSCLE ACTIVITY DURING FRONTAL COLLISION.

Ewing, C.L., Thomas, D.J., Lustik, L., Muzzy, W.H., Willems, G.C., Majewski, P., 1977. Dynamic response of the human head and neck to +Gy impact acceleration. SAE Tech. Pap. Ser. https://doi.org/10.4271/770928

Fagnant, D.J., Kockelman, K., 2015. Preparing a nation for autonomous vehicles: opportunities, barriers and policy recommendations. Transp. Res. Part Policy Pract. 77, 167–181. https://doi.org/10.1016/j.tra.2015.04.003

Feipel, V., Rondelet, B., Le Pallec, J.-P., Rooze, M., 1999. Normal global motion of the cervical spine: an electrogoniometric study. Clin. Biomech. https://doi.org/10.1016/S0268-0033(98)90098-5

Filatov, A., Scanlon, J.M., Bruno, A., Danthurthi, S.S.K., Fisher, J., 2019. Effects of Innovation in Automated Vehicles on Occupant Compartment Designs, Evaluation, and Safety: A Review of Public Marketing, Literature, and Standards. Presented at the WCX SAE World Congress Experience, pp. 2019-01–1223. https://doi.org/10.4271/2019-01-1223

Fuchs, P., Moreau, G., Berthoz, A., 2003. Le traité de la réalité virtuelle, vol 2. Les Presses de l'École des Mines, Paris.

Fuentes Del Toro, S., Santos-Cuadros, S., Olmeda, E., San Román, J.L., 2020. Study of the Emergency Braking Test with an Autonomous Bus and the sEMG Neck Response by Means of a Low-Cost System. Micromachines 11, 931. https://doi.org/10.3390/mi11100931

Gastaldi, M., Rossi, R., Gecchele, G., 2014. Effects of Driver Task-related Fatigue on Driving Performance. Procedia - Soc. Behav. Sci. 111, 955–964. https://doi.org/10.1016/j.sbspro.2014.01.130

Gold, C., Damböck, D., Lorenz, L., Bengler, K., 2013. “Take over!” How long does it take to get the driver back into the loop? Proc. Hum. Factors Ergon. Soc. Annu. Meet. 57, 1938–1942. https://doi.org/10.1177/1541931213571433

Gold, C., Naujoks, F., Radlmayr, J., Bellem, H., Jarosch, O., 2018. Testing Scenarios for Human Factors Research in Level 3 Automated Vehicles, in: Stanton, N.A. (Ed.), Advances in Human Aspects of Transportation, Advances in Intelligent Systems and Computing. Springer International Publishing, Cham, pp. 551–559. https://doi.org/10.1007/978-3-319-60441-1_54

Grébonval, C., Beillas, P., Wang, X., 2021a. Experimental investigation of preferred seating positions and postures in reclined seating configurations 7.

Grébonval, C., Trosseille, X., Petit, P., Wang, X., Beillas, P., 2021b. Effects of seat pan and pelvis angles on the occupant response in a reclined position during a frontal crash. PLOS ONE 16, e0257292. https://doi.org/10.1371/journal.pone.0257292

Green, M., 2000. “How Long Does It Take to Stop?” Methodological Analysis of Driver Perception-Brake Times. Transp. Hum. Factors 2, 195–216. https://doi.org/10.1207/STHF0203_1

Harbluk, J.L., Burns, P.C., El-Hage, Y., 2018. Caroll P. Lau, M.Sc. Transport Canada 15.

Harm, D.L., 2002. Motion Sickness Neurophysiology, Physiological Correlates, and Treatment, in: Handbook of Virtual Environments. CRC Press, pp. 677–702.

Hoff, K.A., Bashir, M., 2015. Trust in Automation: Integrating Empirical Evidence on Factors That Influence Trust. Hum. Factors J. Hum. Factors Ergon. Soc. 57, 407–434. https://doi.org/10.1177/0018720814547570

Holländer, K., Wintersberger, P., Butz, A., 2019. Overtrust in External Cues of Automated Vehicles: An Experimental Investigation, in: Proceedings of the 11th International Conference on Automotive User Interfaces and Interactive Vehicular Applications. Presented at the AutomotiveUI ’19: 11th International Conference on Automotive User Interfaces and Interactive Vehicular Applications, ACM, Utrecht Netherlands, pp. 211–221. https://doi.org/10.1145/3342197.3344528

Holmes, D.A., Gabler, H., Sherony, R., 2018. Estimating Benefits of LDW Systems Applied to Cross-Centerline Crashes. https://doi.org/10.4271/2018-01-0512

Huang, A., Derakhshan, S., Madrid-Carvajal, J., Nosrat Nezami, F., Wächter, M.A., Pipa, G., König, P., 2024. Enhancing Safety in Autonomous Vehicles: The Impact of Auditory and Visual Warning Signals on Driver Behavior and Situational Awareness. Vehicles 6, 1613–1636. https://doi.org/10.3390/vehicles6030076

Iskander, J., Hossny, M., Nahavandi, S., 2018. A Review on Ocular Biomechanic Models for Assessing Visual Fatigue in Virtual Reality. IEEE Access 6, 19345–19361. https://doi.org/10.1109/ACCESS.2018.2815663

Kalra, N., Paddock, S.M., 2016. Driving to Safety: How Many Miles of Driving Would It Take to Demonstrate Autonomous Vehicle Reliability? 15.

Kemeny, A., Chardonnet, J.-R., Colombet, F., 2020. Getting Rid of Cybersickness: In Virtual Reality, Augmented Reality, and Simulators. Springer International Publishing, Cham. https://doi.org/10.1007/978-3-030-59342-1

Kemeny, A., Panerai, F., 2003. Evaluating perception in driving simulation experiments. Trends Cogn. Sci. 7, 31–37. https://doi.org/10.1016/S1364-6613(02)00011-6

Kennedy, R.S., Frank, L., 1985. Review of Motion Sickness with Special Reference to Simulator Sickness.

Kennedy, R.S., Lane, N.E., Berbaum, K.S., Lilienthal, M.G., 1993. Simulator Sickness Questionnaire: An Enhanced Method for Quantifying Simulator Sickness. Int. J. Aviat. Psychol. 3, 203–220. https://doi.org/10.1207/s15327108ijap0303_3

Kern, D., Schmidt, A., 2009. Design space for driver-based automotive user interfaces, in: Proceedings of the 1st International Conference on Automotive User Interfaces and Interactive Vehicular Applications. Presented at the AutomotiveUI ’09: International Conference on Automotive User Interfaces and Interactive Vehicular Applications, ACM, Essen Germany, pp. 3–10. https://doi.org/10.1145/1620509.1620511

Kirschbichler, S., Huber, P., Prüggler, A., Steidl, T., Sinz, W., Mayer, C., DAddetta, G.A., 2014. Factors Influencing Occupant Kinematics during Braking and Lane Change Maneuvers in a Passenger Vehicle.

Krašna, S., Đorđević, S., 2020. Estimating the Effects of Awareness on Neck-Muscle Loading in Frontal Impacts with EMG and MC Sensors. Sensors 20, 3942. https://doi.org/10.3390/s20143942

Kumar, S., Narayan, Y., Amell, T., 2003. Analysis of low velocity frontal impacts. Clin. Biomech. 18, 694–703. https://doi.org/10.1016/S0268-0033(03)00137-2

Kumar, S., Narayan, Y., Amell, T., 2000. Role of awareness in head-neck acceleration in low velocity rear-end impacts. Accid. Anal. Prev. 32, 233–241. https://doi.org/10.1016/S0001-4575(99)00114-1

Langlois, S., 2013. ADAS HMI using peripheral vision, in: Proceedings of the 5th International Conference on Automotive User Interfaces and Interactive Vehicular Applications. Presented at the AutomotiveUI '13: Automotive User Interfaces and Interactive Vehicular Applications, ACM, Eindhoven Netherlands, pp. 74–81. https://doi.org/10.1145/2516540.2516558

Larsson, E., 2023. Passenger kinematics in evasive maneuvers.

Li, F., Liu, N., Li, H., Zhang, B., Tian, S., Tan, M., Sandoz, B., 2019. A review of neck injury and protection in vehicle accidents. Transp. Saf. Environ. 1, 89–105. https://doi.org/10.1093/tse/tdz012

Liang, H., Kaewmanee, T., Aruin, A.S., 2020. The role of an auditory cue in generating anticipatory postural adjustments in response to an external perturbation. Exp. Brain Res. 238, 631–641. https://doi.org/10.1007/s00221-020-05738-6

Litman, T., 2023. Autonomous Vehicle Implementation Predictions: Implications for Transport Planning.

Litman, T., 2014. A New Transit Safety Narrative. J. Public Transp. 17, 114–135. https://doi.org/10.5038/2375-0901.17.4.7

Louw, T., Merat, N., Jamson, H., 2015. Engaging With Highly Automated Driving: To Be Or Not To Be In The Loop? https://doi.org/10.13140/RG.2.1.2788.9760

Lucas, G., Kemeny, A., Paillot, D., Colombet, F., 2020. A simulation sickness study on a driving simulator equipped with a vibration platform. Transp. Res. Part F Traffic Psychol. Behav. 68, 15–22. https://doi.org/10.1016/j.trf.2019.11.011

Mackenzie, J., Dutschke, J., Di Loreto, C., Forrest, M., Van Den Berg, A., Merienne, F., Chardonnet, J.-R., Sandoz, B., 2022. Human Head and Neck Kinematics during Autonomous and Human Braking in Three Initial Head Positions. SAE Int. J. Transp. Saf. 10, 09-10-02–0007. https://doi.org/10.4271/09-10-02-0007

Magnusson, M.L., Pope, M.H., Hasselquist, L., Bolte, K.M., Ross, M., Goel, V.K., Lee, J.S., Spratt, K., Clark, C.R., Wilder, D.G., 1999. Cervical electromyographic activity during low-speed rear impact. Eur. Spine J. 8, 118–125. https://doi.org/10.1007/s005860050140

Manawadu, U.E., Ishikawa, M., Kamezaki, M., Sugano, S., Department of Modern Mechanical Engineering, School of Creative Science and Engineering, Waseda University, Research Institute for Science and Engineering (RISE), Waseda University, 2015. Analysis of Preference for Autonomous Driving Under Different Traffic Conditions Using a Driving Simulator. J. Robot. Mechatron. 27, 660–670. https://doi.org/10.20965/jrm.2015.p0660

Mazloumi Gavgani, A., Walker, F.R., Hodgson, D.M., Nalivaiko, E., 2018. A comparative study of cybersickness during exposure to virtual reality and "classic" motion sickness: are they different? J. Appl. Physiol. 125, 1670–1680. https://doi.org/10.1152/japplphysiol.00338.2018

Mehrotra, S., Wang, M., Wong, N., Parker, J., Roberts, S.C., Kim, W., Romo, A., Horrey, W.J., 2022. Human-Machine Interfaces and Vehicle Automation: A Review of the Literature and Recommendations for System Design, Feedback, and Alerts.

Melnicuk, V., Thompson, S., Jennings, P., Birrell, S., 2021. Effect of cognitive load on drivers' State and task performance during automated driving: Introducing a novel method for determining stabilisation time following take-over of control. Accid. Anal. Prev. 151, 105967. https://doi.org/10.1016/j.aap.2020.105967

Morgan, P.L., Williams, C., Flower, J., Alford, C., Parkin, J., 2019. Trust in an Autonomously Driven Simulator and Vehicle Performing Maneuvers at a T-Junction with and Without Other Vehicles, in: Stanton, N. (Ed.), Advances in Human Aspects of Transportation, Advances in Intelligent Systems and Computing. Springer International Publishing, Cham, pp. 363–375. https://doi.org/10.1007/978-3-319-93885-1_33

Morris, R., Cross, G., 2005. Improved Understanding of Passenger Behaviour During Pre-Impact Events to Aid Smart Restraint Development.

Mueller, A.S., Cicchino, J.B., Calvanelli, J.V., 2024. Habits, attitudes, and expectations of regular users of partial driving automation systems. J. Safety Res. 88, 125–134. https://doi.org/10.1016/j.jsr.2023.10.015

Muggenthaler, H., Adamec, J., Praxl, N., Schönpflug, M., 2005. The Influence of Muscle Activity on Occupant Kinematics.

Müller, A.L., Fernandes-Estrela, N., Hetfleisch, R., Zecha, L., Abendroth, B., 2021. Effects of non-driving related tasks on mental workload and take-over times during conditional automated driving. Eur. Transp. Res. Rev. 13, 16. https://doi.org/10.1186/s12544-021-00475-5

NHTSA, 2022. National Roadway Safety Strategy.

Oliver, J., 2018. Virtual and Augmented Reality: from Promise to Productivity.

Östling, M., Larsson, A., 2019. OCCUPANT ACTIVITIES AND SITTING POSITIONS IN AUTOMATED VEHICLES IN CHINA AND SWEDEN 10.

Östling, M., Sunnevång, C., Svensson, C., Kock, H.-O., 2017. Potential future seating positions and the impact on injury risks in a Learning Intelligent Vehicle (LIV) 16.

Paxion, J., Galy, E., Berthelon, C., 2014. Mental workload and driving. Front. Psychol. 5. https://doi.org/10.3389/fpsyg.2014.01344

Peng, C., Merat, N., Romano, R., Hajiseyedjavadi, F., Paschalidis, E., Wei, C., Radhakrishnan, V., Solernou, A., Forster, D., Boer, E., 2022. Drivers' Evaluation of Different Automated Driving Styles: Is It Both Comfortable and Natural? Hum. Factors J. Hum. Factors Ergon. Soc. 001872082211134. https://doi.org/10.1177/00187208221113448

Petermeijer, S., Doubek, F., De Winter, J., 2017. Driver response times to auditory, visual, and tactile take-over requests: A simulator study with 101 participants, in: 2017 IEEE International Conference on Systems, Man, and Cybernetics (SMC). Presented at the 2017 IEEE International Conference on Systems, Man and Cybernetics (SMC), IEEE, Banff, AB, pp. 1505–1510. https://doi.org/10.1109/SMC.2017.8122827

Petermeijer, S.M., De Winter, J.C.F., Bengler, K.J., 2016. Vibrotactile Displays: A Survey With a View on Highly Automated Driving. IEEE Trans. Intell. Transp. Syst. 17, 897–907. https://doi.org/10.1109/TITS.2015.2494873

Pfleging, B., Rang, M., Broy, N., 2016. Investigating user needs for non-driving-related activities during automated driving, in: Proceedings of the 15th International Conference on Mobile and Ubiquitous Multimedia. Presented at the MUM '16: 15th International Conference on Mobile and Ubiquitous Multimedia, ACM, Rovaniemi Finland, pp. 91–99. https://doi.org/10.1145/3012709.3012735

Radlmayr, J., Fischer, F.M., Bengler, K., 2019. The Influence of Non-driving Related Tasks on Driver Availability in the Context of Conditionally Automated Driving, in: Bagnara, S., Tartaglia, R., Albolino, S., Alexander, T., Fujita, Y. (Eds.), Proceedings of the 20th Congress of the International Ergonomics Association (IEA 2018), Advances in Intelligent Systems and Computing. Springer International Publishing, Cham, pp. 295–304. https://doi.org/10.1007/978-3-319-96074-6_32

Rangelova, S., Andre, E., 2018. A Survey on Simulation Sickness in Driving Applications with Virtual Reality Head-Mounted Displays. Presence Teleoperators Virtual Environ. 27, 15–31. https://doi.org/10.1162/pres_a_00318

Reason, J.T., Brand, J.J., 1975. Motion Sickness. Academic Press.

Reed, M.P., Ebert, S.M., Jones, M.L.H., Park, B.-K.D., Hallman, J.J., Sherony, R., 2018. Passenger head kinematics in abrupt braking and lane change events. Traffic Inj. Prev. 19, S70–S77. https://doi.org/10.1080/15389588.2018.1481957

Reymond, G., Kemeny, A., 2000. Motion Cueing in the Renault Driving Simulator. Veh. Syst. Dyn. 34, 249–259. https://doi.org/10.1076/vesd.34.4.249.2059

Riccio, G.E., Stoffregen, T.A., 1991. An ecological Theory of Motion Sickness and Postural Instability. Ecol. Psychol. 3, 195–240. https://doi.org/10.1207/s15326969eco0303_2

Riegler, A., Riener, A., Holzmann, C., 2021. A Systematic Review of Virtual Reality Applications for Automated Driving: 2009–2020. Front. Hum. Dyn. 3, 689856. https://doi.org/10.3389/fhumd.2021.689856

Ruscio, D., Ciceri, M.R., Biassoni, F., 2015. How does a collision warning system shape driver's brake response time? The influence of expectancy and automation complacency on real-life emergency braking. Accid. Anal. Prev. 77, 72–81. https://doi.org/10.1016/j.aap.2015.01.018

Sandoz, B., Persohn, S., González-García, M., Weber, J., 2023. Société de Biomécanique Young Investigator Award 2019: Upper body behaviour of seated humans in vivo under controlled lateral accelerations. Clin. Biomech. 105, 105952. https://doi.org/10.1016/j.clinbiomech.2023.105952

Santos-Cuadros, S., Fuentes Del Toro, S., Olmeda, E., San Román, J.L., 2021. Surface Electromyography Study Using a Low-Cost System: Are There Neck Muscles Differences When the Passenger Is Warned during an Emergency Braking Inside an Autonomous Vehicle? Sensors 21, 5378. https://doi.org/10.3390/s21165378

Sawabe, T., Kanbara, M., Hagita, N., 2016. Diminished Reality for Acceleration — Motion Sickness Reduction with Vection for Autonomous Driving, in: 2016 IEEE International Symposium on Mixed and Augmented Reality (ISMAR-Adjunct). Presented at the 2016 IEEE International Symposium on Mixed and Augmented Reality (ISMAR-Adjunct), IEEE, Merida, Yucatan, Mexico, pp. 297–299. https://doi.org/10.1109/ISMAR-Adjunct.2016.0100

Saxby, D.J., Matthews, G., Warm, J.S., Hitchcock, E.M., Neubauer, C., 2013. Active and passive fatigue in simulated driving: Discriminating styles of workload regulation and their safety impacts. J. Exp. Psychol. Appl. 19, 287–300. https://doi.org/10.1037/a0034386

Schaap, N., Van Der Horst, R., Van Arem, B., Brookhuis, K., 2017. The Relationship between Driver Distraction and Mental Workload, in: Regan, M.A. (Ed.), Driver Distraction and Inattention. CRC Press, pp. 63–80. https://doi.org/10.1201/9781315578156-5

Schoettle, B., Sivak, M., 2014. Public opinion about self-driving vehicles in China, India, Japan, the US, the UK, and Australia. https://doi.org/doi: UMTRI-2014-30.

Schöner, H.-P., Morys, B., 2016. Dynamic Driving Simulators, in: Winner, H., Hakuli, S., Lotz, F., Singer, C. (Eds.), Handbook of Driver Assistance Systems. Springer International Publishing, Cham, pp. 177–198. https://doi.org/10.1007/978-3-319-12352-3_9

Sherman, W.R., Craig, A.B., 2003. Understanding Virtual Reality: Interface, Application, and Design. Morgan Kaufmann Publishers. https://doi.org/10.1016/B978-1-55860-353-0.50019-7

Siegmund, G.P., Sanderson, D.J., Myers, B.S., Timothy Inglis, J., 2003. Rapid neck muscle adaptation alters the head kinematics of aware and unaware subjects undergoing multiple whiplash-like perturbations. J. Biomech. 36, 473–482. https://doi.org/10.1016/S0021-9290(02)00458-X

Sivak, M., Schoettle, B., 2015. Motion sickness in self-driving vehicles.

Slater, M., Usoh, M., 1993. Presence in immersive virtual environments, in: Proceedings of IEEE Virtual Reality Annual International Symposium. Presented at the IEEE Virtual Reality Annual International Symposium, IEEE, Seattle, WA, USA, pp. 90–96. https://doi.org/10.1109/VRAIS.1993.380793

Sovani, S., 2017. Simulation Accelerates Development of Autonomous Driving. ATZ Worldw. 119, 24–29. https://doi.org/10.1007/s38311-017-0088-y

Sportillo, D., Paljic, A., Ojeda, L., 2018. Get ready for automated driving using Virtual Reality. Accid. Anal. Prev. 118, 102–113. https://doi.org/10.1016/j.aap.2018.06.003

Standring, S., Gray, H., Anand, N., Tunstall, R., 2021. Gray's anatomy: The anatomical basis of Clinical Practice. Elsevier, Amsterdam.

Stewart, D., 1965. A Platform with Six Degrees of Freedom. Proc. Inst. Mech. Eng. 180, 371–386. https://doi.org/10.1243/PIME_PROC_1965_180_029_02

Subit, D., Vézin, P., Laporte, S., Sandoz, B., 2017. Will Automated Driving Technologies Make Today's Effective Restraint Systems Obsolete? Am. J. Public Health Ajph.

Treisman, M., 1977. Motion Sickness: An Evolutionary Hypothesis. Science 197, 493–495. https://doi.org/10.1126/science.301659

Walker, F., 2021. To trust or not to trust? : assessment and calibration of driver trust in automated vehicles (PhD). University of Twente, Enschede, The Netherlands. https://doi.org/10.3990/1.9789055842766

Walker, F., Forster, Y., Hergeth, S., Kraus, J., Payre, W., Wintersberger, P., Martens, M., 2023. Trust in automated vehicles: constructs, psychological processes, and assessment. Front. Psychol. 14, 1279271. https://doi.org/10.3389/fpsyg.2023.1279271

Williams, B., Garton, A.E., Headleand, C.J., 2020. Exploring Visuo-haptic Feedback Congruency in Virtual Reality, in: 2020 International Conference on Cyberworlds (CW). Presented at the 2020 International Conference on Cyberworlds (CW), IEEE, Caen, France, pp. 102–109. https://doi.org/10.1109/CW49994.2020.00022

Wintersberger, P., Frison, A.-K., Riener, A., Sawitzky, T.V., 2018. Fostering User Acceptance and Trust in Fully Automated Vehicles: Evaluating the Potential of Augmented Reality. Presence Teleoperators Virtual Environ. 27, 46–62. https://doi.org/10.1162/pres_a_00320

Wood, M., Wittmann, D., Liu, S., Knobel, C., Syguda, S., Wiltschko, T., Garbacik, N., O'Brien, M., Dannebaum, U., Weast, J., Dornieden, B., 2019. Safety First for Automated Driving.

Yoganandan, N., Haffner, M., Maiman, D.J., Nichols, H., Pintar, F.A., Jentzen, J., Weinshel, S.S., Larson, S.J., Sances, A., 1989. Epidemiology and Injury Biomechanics of Motor Vehicle Related Trauma to the Human Spine. Presented at the 33rd Stapp Car Crash Conference, p. 892438. https://doi.org/10.4271/892438

Yun, H., Lee, J.W., Yang, H.D., Yang, J.H., 2018. Experimental Design for Multi-modal Take-over Request for Automated Driving, in: Stephanidis, C. (Ed.), HCI International 2018 – Posters' Extended Abstracts, Communications in Computer and Information Science. Springer International Publishing, Cham, pp. 418–425. https://doi.org/10.1007/978-3-319-92285-0_57

Zangi, N., Srour-Zreik, R., Ridel, D., Chassidim, H., Borowsky, A., 2022. Driver distraction and its effects on partially automated driving performance: A driving simulator study among young-experienced drivers. Accid. Anal. Prev. 166, 106565. https://doi.org/10.1016/j.aap.2022.106565

Zhang, B., de Winter, J., Varotto, S., Happee, R., Martens, M., 2019. Determinants of take-over time from automated driving: A meta-analysis of 129 studies. Transp. Res. Part F Traffic Psychol. Behav. 64, 285–307. https://doi.org/10.1016/j.trf.2019.04.020

Zhang, Z., Tian, R., Duffy, V.G., 2023. Trust in Automated Vehicle: A Meta-Analysis, in: Duffy, V.G., Landry, S.J., Lee, J.D., Stanton, N. (Eds.), Human-Automation Interaction, Automation, Collaboration, & E-Services. Springer International Publishing, Cham, pp. 221–234. https://doi.org/10.1007/978-3-031-10784-9_13

Zou, X., O'Hern, S., Ens, B., Coxon, S., Mater, P., Chow, R., Neylan, M., Vu, H.L., 2021. On-road virtual reality autonomous vehicle (VRAV) simulator: An empirical study on user experience. Transp. Res. Part C Emerg. Technol. 126, 103090. https://doi.org/10.1016/j.trc.2021.103090

APPENDIX

1. Processing the IMU data

1.1. IMU mode of function

The Xsens MTx Inertial Measurement Unit (IMU) serves as the reference for the inertial measurements used in this study. Operating at a frequency of 100 Hz, each unit is equipped with multiple sensors, including accelerometers, gyroscopes, and magnetometers, allowing for the measurement of key parameters such as acceleration, rotational velocities, and orientation, which can be represented in quaternions. The Xsens system enables synchronization across multiple units and facilitates data export for analysis.

Each unit operates with its own sensor reference frame (denoted as C) and can be compared against a global reference frame (denoted as G). The global reference frame (G) is predefined with:

- The positive x-axis aligned toward magnetic north,
- The y-axis oriented to maintain a right-handed coordinate system,
- The positive z-axis directed opposite to the force of gravity.

The orientation of each sensor unit is thus defined by its reference frame (C) relative to the global frame (G). The acceleration and magnetic data are also represented within the sensor's reference frame (C). The Xsens utility offers alignment procedures to adjust and align the reference frames (C) and (G) as needed.

1.2. IMU placement

In this study, two inertial measurement units (IMUs) were utilized for each subject: one was positioned on the head using a rigid plastic helmet, and the other was placed at the level of the T1 vertebra (as illustrated in Figure 48).

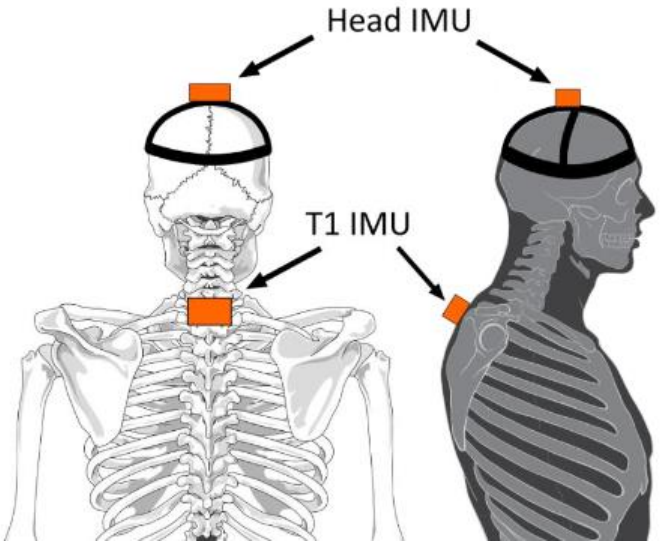

Figure 48: IMU Placement, adapted from Patrick J. Lynch & C. Carl Jaffe

1.3. Alignment Process

The Xsens utility enables modification of the sensor (C) and global (G) reference frames, allowing the acceleration and orientation data to be expressed in the desired coordinate system. Several methods are available for adjusting these frames:

- **"Heading reset":** This procedure redefines the x-axis of the global frame (G) while keeping the z-axis vertical. The x-axis of the global frame is included in the plane formed by the vertical axis and the x-axis of the IMU frame.
- **"Object reset":** This method aligns the IMU axes (S) with the object frame (O) to which the IMU is attached. The sensor frame (C) is transformed into a new frame (C'), where:
    - The z'-axis is vertical and positive in the anti-gravity direction.
    - The x'-axis corresponds to the x-axis of the original (C) frame, projected onto the new horizontal plane.
    - The y'-axis is chosen to maintain a right-handed coordinate system.
- **"Alignment reset":** This procedure combines both the "heading reset" and "object reset," aligning the IMU and global reference points. After this alignment, the reference point remains fixed relative to the IMU and can rotate again as needed.

For the purposes of this study, the primary data of interest include the accelerations from the head and T1 IMUs, as well as the relative orientations between the two units, specifically focusing on the evolution of the head/T1 angle. The placement of the IMUs was conducted as previously described.

An arbitrary reference point is established to define the different orientations, with the following characteristics:

- A vertical z-axis in the anti-gravity direction,
- A x-axis aligned with the movement of the dynamic system, maintaining a right-handed coordinate system,
- A lateral y-axis such that head extension is recorded as positive.

It is assumed that the subjects' bodies are symmetrical along their sagittal plane, and the IMUs are placed such that the IMU and the subject's medial planes coincide. Due to the lack of a quantification method for potential placement discrepancies, this assumption is essential for the analysis.

In the experiments conducted for this study, the "alignment reset" method was systematically applied. The inertial units were positioned such that the x-axis of their native reference frame (C) lay within the frontal plane, effectively dividing the body into anterior and posterior sections. This ensured that the x-axes of the inertial units remained within the subject's frontal plane and parallel to the horizontal plane, with the z-axis oriented upwards and the y-axis adjusted to maintain a right-handed orthogonal reference frame.

The alignment procedure was performed before each measurement session, enabling the resetting of all angle values to 0, as the inertial sensors measure only changes in angle. Figure 49 provides a summary of the effects of this alignment procedure within the context of the conducted tests.

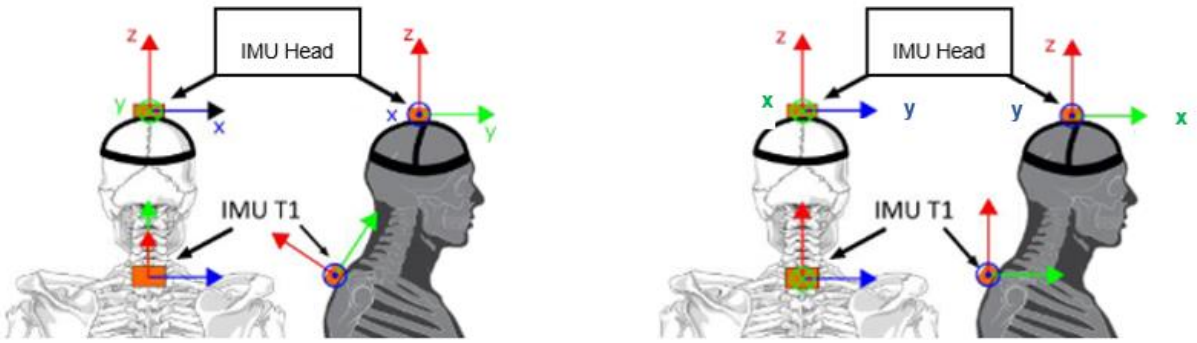

Figure 49: Alignment of IMU reference frames, Before Alignment (Left); After Alignment (Right), adapted from Patrick J. Lynch & C. Carl Jaffe

1.4. Calculating Euler's Angles

Th The orientation data provided by the sensors are expressed in the form of quaternions, which are hypercomplex numbers that extend the arithmetic of complex numbers. Quaternions are widely used for representing rotations because they uniquely define the orientation, except for a sign ambiguity. In practical terms, a quaternion is represented by a set of four real numbers $\mathrm{q_{GC}} = (\mathrm{q_0}, \mathrm{q_1}, \mathrm{q_2}, \mathrm{q_3})$, where $\mathrm{q_{GC}}$ specifically represents the quaternion that describes the rotation of a vector from the inertial unit's reference frame (C) to the global frame (G). Relations between quaternions and rotation matrix exist and by denoting RGC the rotation matrix between the G and C frames, we have:

$$R_{GC} = \begin{bmatrix} q_0^2 + q_1^2 - q_2^2 - {q_3}^2 & 2(q_1q_2 - q_0q_3) & 2(q_0q_2 + q_1q_3) \\ 2(q_0q_3 + q_1q_2) & q_0^2 - q_1^2 + q_2^2 - {q_3}^2 & 2(q_2q_3 - q_0q_1) \\ 2(q_1q_3 - q_0q_2) & 2(q_0q_1 + q_2q_3) & q_0^2 - q_1^2 - q_2^2 + {q_3}^2 \end{bmatrix}$$

To determine the relative angles between different IMU units, Euler angles are employed to describe a rotation as a sequence of three sub-rotations around specific axes of a coordinate frame.

The process involves starting from an initial frame $\mathrm{R_0(x_0, y_0, z_0)}$. A first rotation by an angle φ is performed around one of the frame's axes, resulting in a new frame $\mathrm{R_1(x_1, y_1, z_1)}$. Subsequently, a second rotation by an angle θ is applied around one of the axes of the updated frame, producing frame $\mathrm{R_2(x_2, y_2, z_2)}$. Finally, a third rotation by an angle ψ is executed around one of the axes of this latest frame, yielding the final frame $\mathrm{R_3(x_3, y_3, z_3)}$. The rotation $\mathrm{R_{GC}}$ can then be broken down into three rotations as follows:

$$R_{GC} = R_{\psi}^{Z} R_{\theta}^{Y} R_{\varphi}^{X}$$

The sequence of axes chosen for these rotations is termed the "rotation sequence," and it directly affects the values of the Euler angles obtained. There are 12 possible rotation sequences (e.g., (x, y, x), (x, y, z), (y, z, y)). In this study, the Cardan sequence (x, y, z) is adopted, corresponding to the yaw, pitch, and roll system commonly used in aeronautics.

Thus, we get:

$$R_{GC} = \begin{bmatrix} \cos\psi & -\sin\psi & 0 \\ \sin\psi & \cos\psi & 0 \\ 0 & 0 & 1 \end{bmatrix} \begin{bmatrix} \cos\theta & 0 & \sin\theta \\ 0 & 1 & 0 \\ -\sin\theta & 0 & \cos\theta \end{bmatrix} \begin{bmatrix} 1 & 0 & 0 \\ 0 & \cos\varphi & -\sin\varphi \\ 0 & \sin\varphi & \cos\varphi \end{bmatrix}$$

$$R_{GC} = \begin{bmatrix} \cos\theta\cos\psi & \sin\varphi\sin\theta\cos\psi - \cos\varphi\sin\psi & \cos\varphi\sin\theta\cos\psi + \sin\varphi\sin\psi \\ \cos\theta\sin\psi & \sin\varphi\sin\theta\sin\psi + \cos\varphi\cos\psi & \cos\varphi\sin\theta\sin\psi - \sin\varphi\cos\psi \\ -\sin\theta & \sin\varphi\cos\theta & \cos\varphi\cos\theta \end{bmatrix}$$

Knowing the rotation matrix $\mathrm{R_{GC}}$, we can therefore calculate the Euler angles as follows:

$$\theta = -\arcsin(R_{GS}[3,1])$$

$$\varphi = arctan(\frac{R_{GS}[3,2]}{R_{GS}[3,3]})$$

$$\psi = arctan(\frac{R_{GS}[2,1]}{R_{GS}[2,0]})$$

To determine the relative angles between the head, and T1, we utilize the quaternion output data from their respective IMUs: $\mathrm{q_{G-Head}}$, and $\mathrm{q_{G-T1}}$. From these quaternions, we calculate the corresponding rotation matrices $\mathrm{R_{G-Head}}$, and $\mathrm{R_{G-T1}}$.

By matrix multiplication, we derive the relative rotation matrices $\mathrm{R_{Head-T1}} = R_{G-Head}^{T} R_{G-T1}$, noting that for orthogonal matrices, the inverse is equivalent to their transpose. Finally, the Euler angles corresponding to these relative rotation matrices can be calculated. The primary angle of interest for this study is the one representing movement in the head's flexion/extension plane, which corresponds to rotation around the x-axis (as depicted in Figure 49).

2. Motion Cueing Algorithm

2.1. Development of a Classical Motion Cueing Algorithm

To enhance the fidelity of driving simulations, we developed a classical motion cueing algorithm (MCA) that transforms pre-recorded horizontal acceleration data from a virtual vehicle into vertical acceleration cues through rotational movements. This transformation is critical for replicating the inertial sensations experienced by drivers, utilizing a six degrees of freedom (6 DOF) motion platform.

The core challenge addressed was the limitation of the motion platform's translational range, which is insufficient for replicating prolonged horizontal accelerations experienced during driving. To overcome this, we employed tilt coordination—a technique where slow rotation (pitch and roll) of the simulator induces perceived horizontal acceleration due to gravity's effect on the vestibular system.

Our MCA operates by decomposing the horizontal acceleration inputs into high-frequency and low-frequency components using a split filtering approach:

1. High-Pass Filtering: Captures rapid changes in acceleration, allowing for direct translational movements within the platform's physical limits. This preserves the onset cues essential for driver perception during quick maneuvers like sudden braking or sharp turns.

2. Low-Pass Filtering: Isolates slow-changing acceleration components, which are then converted into rotational commands. By tilting the platform, we create a sustained gravitational force vector that simulates continuous acceleration without exceeding translational constraints.

The transformation from horizontal to vertical acceleration involves calculating the required tilt angles. The tilt angles for pitch (θ) and roll (φ) are determined using the equations:

- $\theta = \arcsin\left(\frac{a_x}{g}\right)$

- $\varphi = \arcsin\left(\frac{a_y}{g}\right)$

where ax and ay are the low-pass filtered longitudinal and lateral accelerations, respectively, and g is the acceleration due to gravity.

We integrated the algorithm into the simulator's control system, ensuring real-time processing of the acceleration data. Key considerations included:

- Filter Design: Selection of appropriate cutoff frequencies to balance responsiveness and smoothness. The high-pass filter cutoff was set to retain critical motion cues, while the low-pass filter cutoff ensured gradual tilt motions to prevent motion sickness.

- Tilt Rate Limiting: Imposed constraints on the rate of change of tilt angles to remain within human perceptual thresholds, avoiding disorientation or discomfort for the driver.

- Washout Algorithms: Implemented to gradually return the platform to a neutral position without noticeable cues to the driver, preparing the system for subsequent maneuvers.

An essential aspect of the implementation is the inclusion of scaling factors, which adjust the sensitivity for each degree of freedom. These factors ensure that the motion platform's output matches the driver's perception of movement while respecting the physical limitations of the simulator. The scaling factors S_x, S_y, S_z for translational movements and $S_\theta, S_\varphi, S_\psi$ for rotational movements were applied to adjust the motion cues' intensity. These factors were determined through iterative testing and ensure that the acceleration data processed by the algorithm is adjusted to align with human sensitivity and platform capabilities.

Testing involved simulating various driving scenarios, such as acceleration, deceleration, and cornering. The algorithm effectively translated horizontal accelerations into combined translational and rotational motions, enhancing the realism of inertial cues. Drivers reported improved perception of sustained accelerations and a more immersive experience.

Quantitative analysis showed that the platform's motions closely matched the desired acceleration profiles. The tilt coordination successfully simulated prolonged accelerations without exceeding the physical limits of the motion system.

The development of this classical motion cueing algorithm significantly improved the driving simulator's capability to replicate real-world inertial sensations. By transforming horizontal acceleration data into

vertical acceleration through controlled rotations, we addressed the limitations of the motion platform's translational range. This advancement contributes to more effective driver training and research by providing a heightened sense of realism and immersion in simulated environments.

2.2. Equations for the Classical Motion Cueing Algorithm with Scaling Factors

The motion cueing algorithm transforms horizontal acceleration data from a virtual vehicle into commands for a 6 DOF driving simulator. The key steps involve filtering the acceleration signals, applying scaling factors, and converting them into translational and rotational motions

1. Input Accelerations

- **Longitudinal acceleration:** $a_x(t)$
- **Lateral acceleration:** $a_y(t)$

2. Filtering Acceleration Components with Scaling Factors

The acceleration signals are decomposed into high-frequency (HF) and low-frequency (LF) components using high-pass (HPF) and low-pass filters (LPF). Scaling factors are then applied to adjust for motion sensitivity, ensuring the cues are realistic and comfortable for the driver.

- **High-Pass Filtered Accelerations (for translational motion):**

$$a_{x_{\text{HF, scaled}}}(t) = S_x \cdot \text{HPF}\left[a_x(t)\right]$$

$$a_{y_{\text{HF, scaled}}}(t) = S_y \cdot \text{HPF}\left[a_y(t)\right]$$

- **Low-Pass Filtered Accelerations (for tilt coordination):**

$$a_{x_{\text{LF, scaled}}}(t) = S_\theta \cdot \text{LPF}\left[a_x(t)\right]$$

$$a_{y_{\text{LF, scaled}}}(t) = S_\phi \cdot \text{LPF}\left[a_y(t)\right]$$

3. Translational Motion Commands with Scaling Factors

The scaled high-pass filtered accelerations are integrated to produce velocity and displacement signals.

- **Integrate to obtain scaled velocities:**

$$v_{x_{\text{scaled}}}(t) = \int (S_x \cdot a_{x_{\text{HF}}}(t))\ dt$$

$$v_{y_{\text{scaled}}}(t) = \int (S_y \cdot a_{y_{\text{HF}}}(t))\ dt$$

- **Integrate velocities to obtain scaled displacements:**

$$x_{\text{scaled}}(t) = \int v_{x_{\text{scaled}}}(t)\, dt$$

$$y_{\text{scaled}}(t) = \int v_{y_{\text{scaled}}}(t)\, dt$$

- **Apply washout filters to return to the neutral position:**

$$x_{\text{wash, scaled}}(t) = \text{HPF}_{\text{wash}}\left[x_{\text{scaled}}(t)\right]$$

$$y_{\text{wash, scaled}}(t) = \text{HPF}_{\text{wash}}\left[y_{\text{scaled}}(t)\right]$$

- **4. Rotational Motion Commands (Tilt Coordination) with Scaling Factors**

The low-frequency filtered signals are used to calculate tilt angles that simulate sustained acceleration through platform rotation.

- **Calculate scaled tilt angles:**

$$\theta_{\text{scaled}}(t) = \arcsin\left(\frac{S_\theta \cdot a_{x_{\text{LF}}}(t)}{g}\right)$$

$$\phi_{\text{scaled}}(t) = \arcsin\left(\frac{S_\phi \cdot a_{y_{\text{LF}}}(t)}{g}\right)$$

- **Limit tilt angles and rates to prevent discomfort:**

$$|\theta_{\text{scaled}}(t)| \leq \theta_{\max}$$

$$|\phi_{\text{scaled}}(t)| \leq \phi_{\max}$$

$$|\dot{\theta}_{\text{scaled}}(t)| \leq \dot{\theta}_{\max}$$

$$|\dot{\phi}_{\text{scaled}}(t)| \leq \dot{\phi}_{\max}$$

- **5. Washout Algorithms for Rotational Motion with Scaling**

The washout filters help return the simulator to a neutral orientation without noticeable cues to the driver.

- **Apply high-pass filters to the tilt angles:**

$$\theta_{\text{wash, scaled}}(t) = \text{HPF}_{\text{wash}}\left[\theta_{\text{scaled}}(t)\right]$$

$$\phi_{\text{wash, scaled}}(t) = \text{HPF}_{\text{wash}}\left[\phi_{\text{scaled}}(t)\right]$$

- **6. Vertical Motion Commands with Scaling Factors**

If vertical acceleration $a_z(t)$ is present, it is processed as follows:

- **Apply scaling and high-pass filtering:**

$$\mathrm{a_{z_{HF,scaled}}(t) = S_z \cdot HPF[\, a_z(t)\,]}$$

- **Integrate to obtain scaled vertical displacement:**

$$z_{\text{scaled}}(t) = \iint a_{z_{\text{HF, scaled}}}(t)\, dt^2$$

- **Apply washout filter:**

$$z_{\text{wash, scaled}}(t) = \text{HPF}_{\text{wash}}\left[z_{\text{scaled}}(t)\right]$$

- **7. Yaw Motion Commands with Scaling Factors**

For yaw rate $\omega_z(t)$:

- **Apply scaling and high-pass filtering:**

$$\omega_{z_{\text{HF, scaled}}}(t) = S_\psi \cdot \text{HPF}\left[\omega_z(t)\right]$$

- **Integrate to obtain scaled yaw angle:**

$$\psi_{\text{scaled}}(t) = \int \omega_{z_{\text{HF, scaled}}}(t)\, dt$$

- **Apply washout filter:**

$$\psi_{\text{wash, scaled}}(t) = \text{HPF}_{\text{wash}}\left[\psi_{\text{scaled}}(t)\right]$$

- **8. Final Platform Commands with Scaling**

The final motion commands sent to the simulator are based on the scaled and filtered signals:

- **Translational Commands:**

$$\text{Platform Displacement in X-axis} = x_{\text{wash, scaled}}(t)$$

$$\text{Platform Displacement in Y-axis} = y_{\text{wash, scaled}}(t)$$

$$\text{Platform Displacement in Z-axis} = z_{\text{wash, scaled}}(t)$$

- **Rotational Commands:**

$$\text{Platform Pitch Angle} = \theta_{\text{wash, scaled}}(t)$$

$$\text{Platform Roll Angle} = \phi_{\text{wash, scaled}}(t)$$

$$\text{Platform Yaw Angle} = \psi_{\text{wash, scaled}}(t)$$

3. Acceleration, Velocity, and Position profiles of the SLED during Normal and Strong braking

Below are the two figures representing the Acceleration, Velocity, and Position profiles of the SLED during Normal braking (Figure 50) and Strong braking (Figure 51).

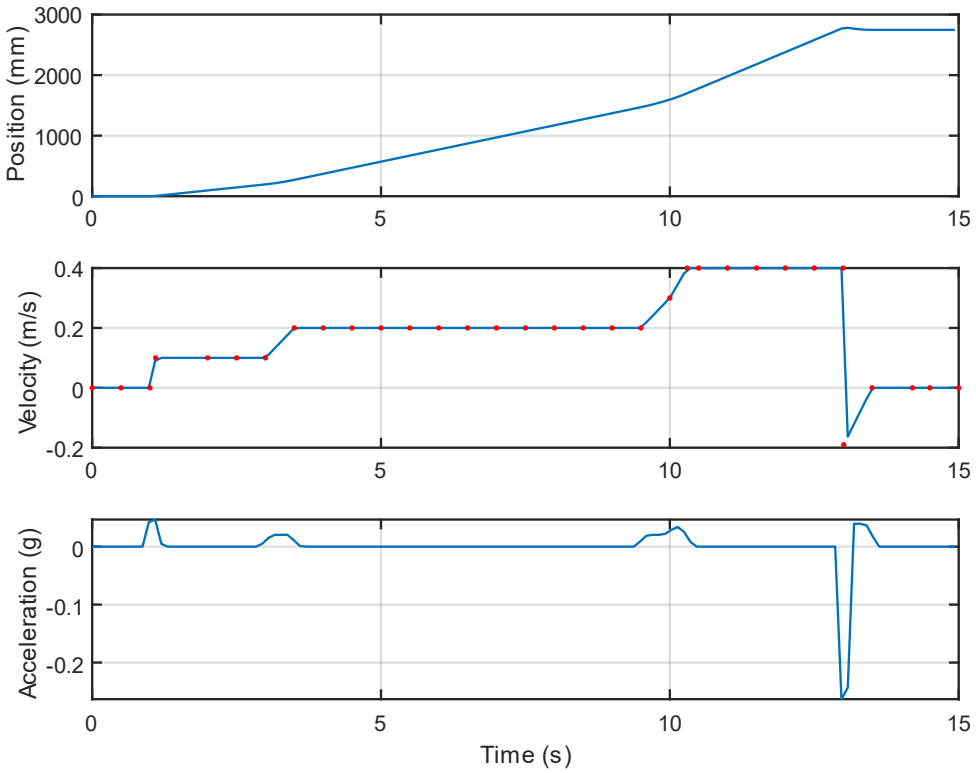

Figure 50: Position, Velocity, and Acceleration profiles respectively for Normal braking intensity

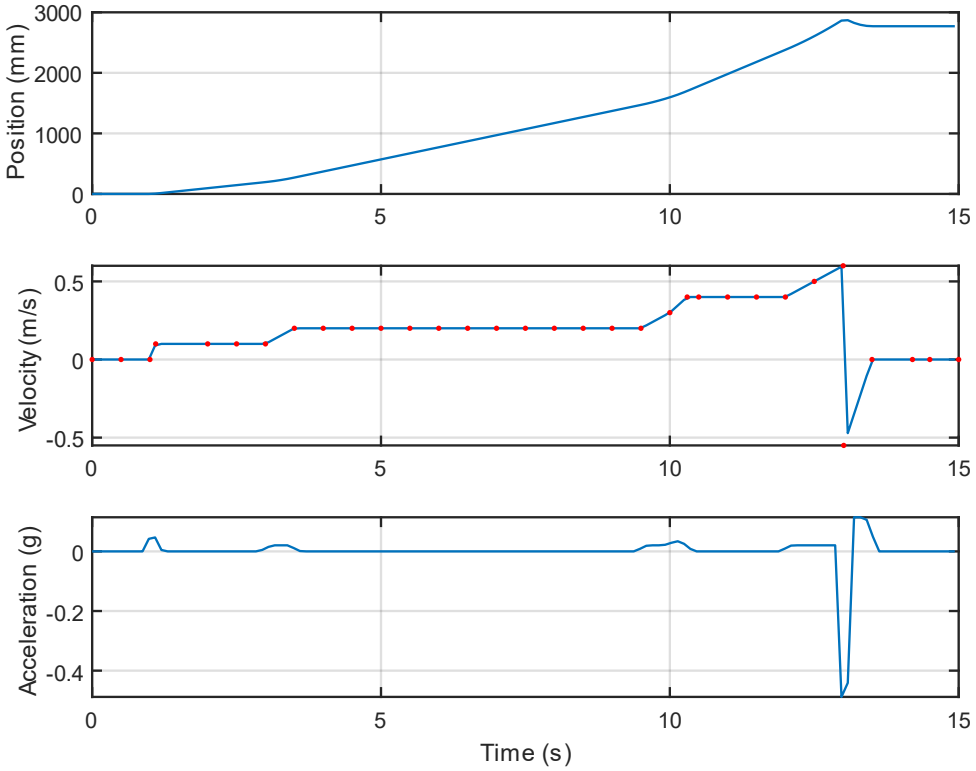

Figure 51: Position, Velocity, and Acceleration profiles respectively for Strong braking intensity

4. Influence of HMD on head stabilization strategies during linear accelerations

At the end of the first year, and in preparation for the SLED experiment we had an M2 master's intern from the BME Paris master program to help us investigate the effect of the HMD of the head-neck response.

Purpose and Methods: The study aimed to investigate whether the kinematics of the head-neck during linear accelerations are influenced by wearing a virtual reality (VR) headset and exposure to different 3D virtual environments. Additionally, it sought to determine whether increased immersion in VR results in greater head stability during sudden acceleration.

Three distinct virtual environments were created: (1) a virtual dark environment, (2) an environment composed of cubes, planes, and horizontal surfaces, and (3) a scaled-down virtual sled room. Dynamic trials were conducted using a SLED system with a controlled acceleration profile. Subjects wore the VR headset, and physiological responses, including variations in EMG signals and head-trunk motion, were measured using sensors and inertial measurement units (IMUs). After the trials, participants completed questionnaires to assess their level of immersion in VR.

Results: The study observed significant differences in head/trunk angle amplitudes across the different virtual environments. Wearing the VR headset resulted in stronger EMG signals in the sternocleidomastoid muscle compared to conditions without the headset. Participants 063 and 064 exhibited smaller head/trunk angles when wearing the headset, indicating more stable head movements, while participant 062 showed a different response. The results validated the hypothesis that both the VR headset and the different virtual environments could influence head-trunk behaviour and movement. Moreover, participants 063 and 064 reported higher immersion levels, suggesting that greater VR immersion corresponds to more stable head movements.

Conclusion: Overall, the virtual dark and plane environments led to more stable head movements than the virtual sled room. The observed decrease in movement and increased neck muscle contraction suggested a "freezing" response triggered by the VR headset and different virtual scenes, resulting in restricted and tenser motion. These findings indicate that subjecting individuals to virtual environments that differ significantly from real-life or mimic real-life traffic conditions could be essential for in-vivo whiplash testing, as it may significantly alter test outcomes.

Arts Sciences et Technologies et Métiers

Ali OLAYAN

Human-Machine Interaction Studies of Occupants in Level 3 Autonomous

Résumé :

La sécurité des occupants dans les véhicules autonomes (VA) représente un enjeu crucial à mesure que ces véhicules progressent vers le niveau 3 d'autonomie selon la classification SAE, où les activités non liées à la conduite deviennent plus courantes. Malgré les avancées dans ce domaine, l'impact des activités des occupants et de leur engagement cognitif sur la dynamique tête-cou lors de manœuvres d'urgence reste insuffisamment compris. Cette recherche émet l'hypothèse que les activités non liées à la conduite et les modalités sensorielles influencent de manière significative les réponses physiologiques des occupants, en particulier lors des freinages brusques. Afin d'étudier cette hypothèse, nous avons mené des expériences en utilisant deux outils avancés de simulation de conduite, à savoir un simulateur de conduite et un système SLED dynamique, pour reproduire des scénarios de freinage d'urgence et évaluer les réponses des occupants dans des conditions cognitives et physiques variées.

La première expérience a utilisé le simulateur SAAM de l'Institut de Chalon-sur-Saône pour étudier l'influence des activités des occupants et des alertes auditives sur la cinématique tête-cou et l'activation musculaire lors des freinages d'urgence. Les résultats ont montré que les alertes auditives jouaient un rôle essentiel dans la préparation des occupants à la décélération, facilitant les ajustements posturaux anticipatoires et réduisant l'accélération de la tête. La deuxième expérience, réalisée à l'aide du système SLED de l'Institut de Biomécanique Humaine Georges Charpak, synchronisé avec un environnement virtuel AV à 360°, a confirmé ces résultats, démontrant que les distractions cognitives liées à des tâches non conduites augmentaient l'accélération de la tête et retardaient les réponses musculaires, notamment dans les scénarios de freinage intense.

Cette étude souligne l'importance d'intégrer des alertes sensorielles, telles que des signaux auditifs, pour améliorer la préparation et la sécurité des occupants dans les VA. En outre, les résultats mettent en évidence la nécessité de systèmes VA adaptatifs qui tiennent compte de la variabilité individuelle des réponses des occupants afin d'assurer une protection optimale. En utilisant des technologies de simulation immersive, cette recherche apporte des informations précieuses sur l'interaction entre les activités non liées à la conduite, l'engagement cognitif et la sécurité des occupants, ouvrant la voie à des stratégies de conception de VA plus efficaces et personnalisées qui peuvent réduire le risque de blessure dans les futurs systèmes de transport autonomes.

Mots clés : Réalité virtuelle, Biomécanique, Interaction Homme-Machine, Véhicules Autonomes

Abstract :

Occupant safety in autonomous vehicles (AVs) represents a critical concern as these vehicles progress toward SAE Level 3 autonomy, where non-driving activities become more prevalent. Despite advancements in this field, the impact of occupant activities and cognitive engagement on head-neck dynamics during emergency maneuvers remains insufficiently understood. This research hypothesizes that non-driving activities and sensory modalities significantly influence occupant physiological responses, especially in sudden braking events. To investigate this, we conducted experiments using two advanced driving simulation tools, including first a driving simulator and then a dynamic SLED system, to replicate emergency braking scenarios and evaluate occupant responses under varying cognitive and physical conditions.

The first experiment utilized the Institute of Chalon-sur-Saône SAAM simulator to investigate the influence of occupant activities and auditory alerts on head-neck kinematics and muscle activation during emergency braking events. Results indicated that auditory alerts played a pivotal role in preparing occupants for deceleration, facilitating anticipatory postural adjustments and reducing head acceleration. The second experiment, using the Institut de Biomécanique Humaine Georges Charpak SLED system synchronized with a 360° virtual AV environment, confirmed these findings, demonstrating that cognitive distractions from non-driving tasks increased head acceleration and delayed muscular responses, particularly in strong braking scenarios.

This study underscores the importance of integrating sensory alerts, such as auditory cues, to enhance occupant preparedness and safety in AVs. Moreover, the results highlight the necessity for adaptive AV systems that account for individual variability in occupant responses to ensure optimal protection. By employing immersive simulation technologies, this research provides valuable insights into the interaction between non-driving activities, cognitive engagement, and occupant safety, paving the way for more effective and personalized AV design strategies that can mitigate injury risk in future autonomous transportation.

Keywords : Virtual Reality, Biomechanics, Human-Machine Interaction, Autonomous Vehicles